Chapter (III)

3. Results and Discussion

3.1. The spectral characterization for $Co_xMg_{1-x}Al_2O_4$ systems

3.1.1. Fourier Transform Infrared Spectra (FTIR)

Infrared Spectra are an important tool for identification and characterization branching and functional for organic groups as -OH, -NH2, -NO3, C=O, C-O in range 1000-4000 cm-1. In this work, it used for identification of metal-oxides such as in range 400-1000 cm-1 as Al-O, Mg-O, Co-O, Ni-O and other functions. Infrared spectra are used also for studying the phase transformation under testing of different structures as spinel, perovskite and other structures.

3.1.1.1. Fourier Transform Infrared Spectra (FTIR) for cobalt system using urea as fuel.

The FTIR spectra for A, F and M systems of 0.01, 0.05, 0.10 mole of Co^{2+}, respectively using urea as fuel are given in Figure (2).These results for the samples after ignition temperature equal to 500ºC contain a broad absorption band at 34٠٠ cm^{-1} for A system and 3500 cm^{-1} for F and M systems, respectively. This broad band is due to the stretching vibration of free (-OH) group of water molecules. The absorption bands at 2920 cm^{-1} for A, F and M systems dues to the stretching vibration of C-H aliphatic in organic molecules residual. The three absorption band at 1800, 1650 and 1400 cm^{-1} for A system, 1650 and 1450 cm^{-1} for F system and at 1750, 1650 and 1400 cm^{-1} for M system are related to the stretching vibration of C=O, C-O groups of residual organic fuel [84] and carbonate groups. The absorption bands at 1658, 1383 and 825 cm^{-1} for A system, 1150 and 850 cm^{-1} for F system and also 1170 and 850 cm^{-1} for M system are corresponding to undecomposed [85] nitrate ions.

The weak absorption bands in the region 400-800 cm^{-1} for all systems appear due to the formation of trace amounts of metal oxides. After calcinations at different temperatures in range 500 -1200 ºC, the intensity of observed absorption bands in the region 800-4000 cm^{-1} are decreased gradually until disappeared at 1100ºC. On the other hand, the strong absorption bands at 3434 cm^{-1} for A system, 3440 for F system and 3450 for M system correspond to the stretching vibration of adsorption water molecules [86]. The strong absorption bands below 800 cm^{-1} corresponds to metal oxides. The absorption bands at 695 and 530 cm^{-1} for A system, 690 and 530 cm^{-1} for F system and at 700 and 535 cm^{-1} for M system are related to $AlO_٦$ groups of the building up the magnesium aluminates spinel. These bands appeared for vibration of Al^{3+} ions in octahedral positions [87-89] comparing with 700, 530 and 425 cm^{-1} for $MgAl_2O_4$ as blank. Other bands at 695, 530 and 425cm^{-1} for A, F and M systems are related to CoO_4 /MgO_4 groups in crystal for the cobalt and magnesium aluminates spinel. These bands appeared for the vibration of Co^{2+}/Mg^{2+} ions [90-92] in the tetrahedral sites comparing with the absorption bands in range 700 and 425 cm^{-1} for $CoAl_2O_4$ as blank that shown in Figure (3).The assignment of the important bands in the IR spectra for 0.01, 0.05 and 0.10 mole of Co^{2+} systems at different calcination temperatures using urea as fuel are given in Table (1).

3.1.1.2. Fourier Transform Infrared Spectra (FTIR) for cobalt system using oxalyl dihydrazide as fuel.

FTIR spectra of 0.01(A), 0.05 (F) and 0.10 (M) mole of Co^{2+} systems using oxalyl dihydrazide as fuel are studied after ignition and calcination at different temperatures. The broad absorption bands around 3490 cm^{-1} for A, F and M systems, respectively correspond to the stretching vibration of free (–OH) group of water molecules. The absorption bands at 2920 cm^{-1} for A and F systems, 2950 cm^{-1} for M system are related to the stretching vibration of

C-H aliphatic in organic molecules. The absorption bands at 1650 and 1100 cm^{-1} are related to the stretching vibration of C= O and C–O groups of residual organic fuel [84]. The absorption bands at 1658, 1383 and 825 cm^{-1}, respectively correspond to undecomposed [85] nitrate ions.

Figure (4) shows the absorption bands in the region 400–1000 cm^{-1} due to the formation of spinel structure after calcination at different temperatures in the range 500°C-1200°C. These bands in the region 800–4000 cm^{-1} are disappeared at 1100 ◦C except, the strong absorption band at 3480 cm^{-1} for A, F and M systems, respectively, correspond to the stretching vibration of adsorption water molecules [86]. The two absorption bands in range 700 and 535 cm^{-1} for A system and the vibrational bands at 690,530 and 520 cm^{-1} for F and M systems, respectively are corresponding to AlO_6 groups building up the spinel as a result of vibration of Al^{3+} ions in octahedral positions [87-89] comparing with the bands at 700, 530 and 420 cm^{-1} which related to $MgAl_2O_4$ spinel. The other vibrational bands 700, 535 and 420 cm^{-1} for A system, 690, 530, 520 and 422 cm^{-1} for F system and 690, 530, 520 and 418 cm^{-1} for M system are corresponding to CoO_4/MgO_4 groups for the cobalt and magnesium aluminates spinel as a result of vibration of its ions (Co^{2+} and Mg^{2+}) in the tetrahedral sites comparing with that in the range 700 and 530 cm^{-1} for $CoAl_2O_4$ spinel as blank [90-92]. The assignment of an important bands in the IR spectra for 0.01, 0.05 and 0.10 mole of Co^{2+} systems at different calcination temperatures using oxalyl dihydrazide as fuel are given in Table (2).

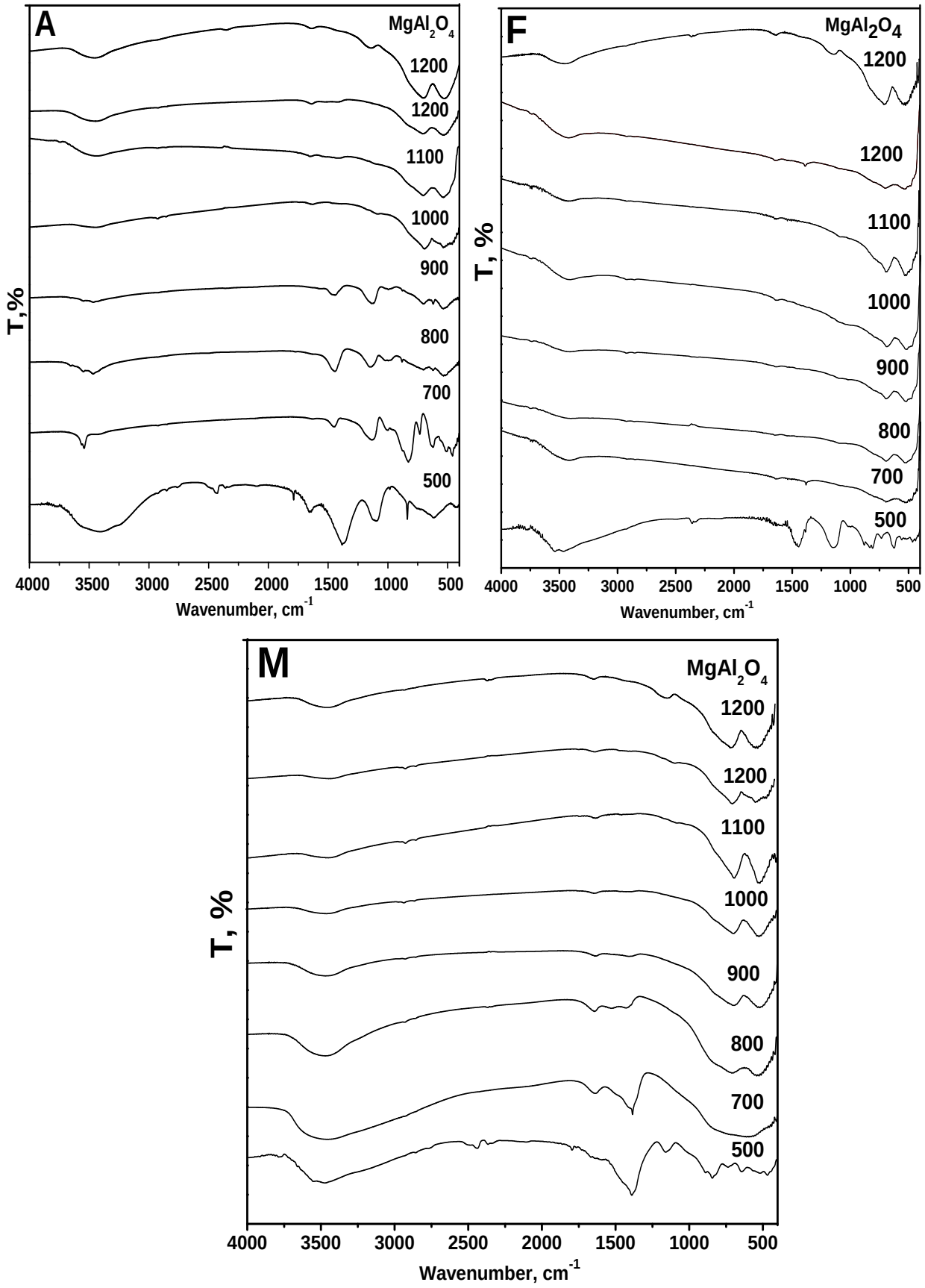

Figure (2): Infrared spectra for 0.01(A), 0.05 (F) and 0.10 (M) mole of Co^{2+} systems using urea as fuel at different calcination temperatures.

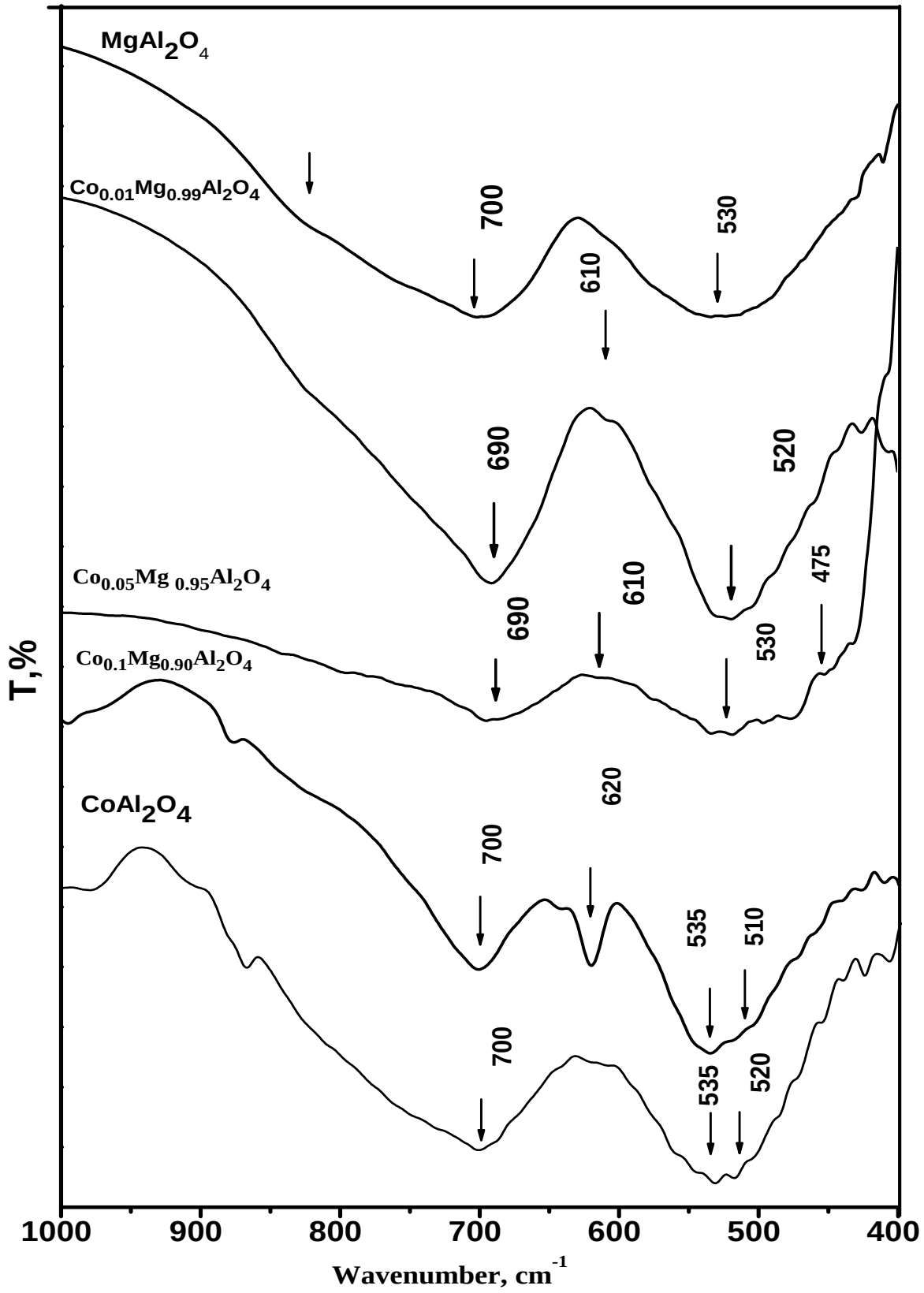

Figure(3): Infrared spectra for 0.01, 0.05, 0.10 mole of Co^{2+} systems, $CoAl_2O_4$ and $MgAl_2O_4$ by using urea as fuel in range 400-1000 cm^{-1} at 1200 ^{o} C.

Table(١): Assignment of the important bands in the IR spectra for 0.01,0.05 and 0.10 mole of Co^{2+} systems at different calcination temperatures using urea as fuel.

Temperature, °C	system 0.01 mole of Co^{2+}						
	υ-OH	υ-CH	υC=O	υC-O	υC-N	υ N=O	υ M-O
٥٠٠	٣٤٠٠	٢٩٢٠	١٦٥٠	١١٠٠	-	٨٥٠	٦٠٠
٧٠٠	٣٤٦٠	-	-	١١٥٠	١٤٥٠	٨٥٠	610,505,450
٨٠٠	٣٤٥٠	-	-	١١٥٠	١٤٥٠	-	700,620,٥٢٠
٩٠٠	٣٤٥٠	-	-	-	١٤٥٠	-	700,610,٥٣٠
١٠٠٠	٣٤٤٠	-	-	-	-	-	700,600,٥٣٠
١١٠٠	٣٤٢٥	-	-	-	-	-	700,620,٥٣٠,425
١٢٠٠	٣٤٢٥	-	-	-	-	-	700,620,٥٣٠,425
	0.05 mole of Co^{2+}						
٥٠٠	٣٥٠٠	٢٩١٠	١٦٥٠	١١٥٠	١٤٥٠	٨٥٠	٦١٠
٧٠٠	٣٤٥٠	-	١٦٥٠	-	-	-	700,٥٠٠
٨٠٠	٣٤٥٠	-	-	-	-	-	700,٥٢٠
٩٠٠	٣٤٠٠	-	-	-	-	-	700,٥٣٠
١٠٠٠	٣٤٠٠	-	-	-	-	-	700,٥٣٠,425
١١٠٠	٣٤١٠	-	-	-	-	-	700,٥٣٠,425
١٢٠٠	٣٤٢٠	-	-	-	-	-	700,٥٣٠,425
	0.10 mole of Co^{2+}						
٥٠٠	٣٥٠٠	٢٨٥٠	١٦٥٠	١١٥٠	١٤٥٠	٨٥٠	٦٥٠
٧٠٠	٣٥٠٠	-	١٦٥٠	-	١٤٠٠	-	٦٠٠
٨٠٠	٣٤٥٠	-	١٦٥٠	-	١٤٠٠	-	700,٥٣٠
٩٠٠	٣٤٥٠	-	١٦٥٠	-	١٤٠٠	-	700,530
١٠٠٠	٣٤٥٠	-	-	-	-	-	700,٥٣٠,425
١١٠٠	٣٤٥٠	-	-	-	-	-	700,٥٣٠,425
١٢٠٠	٣٤٨٠	-	-	-	-	-	700,٥٣٠,425

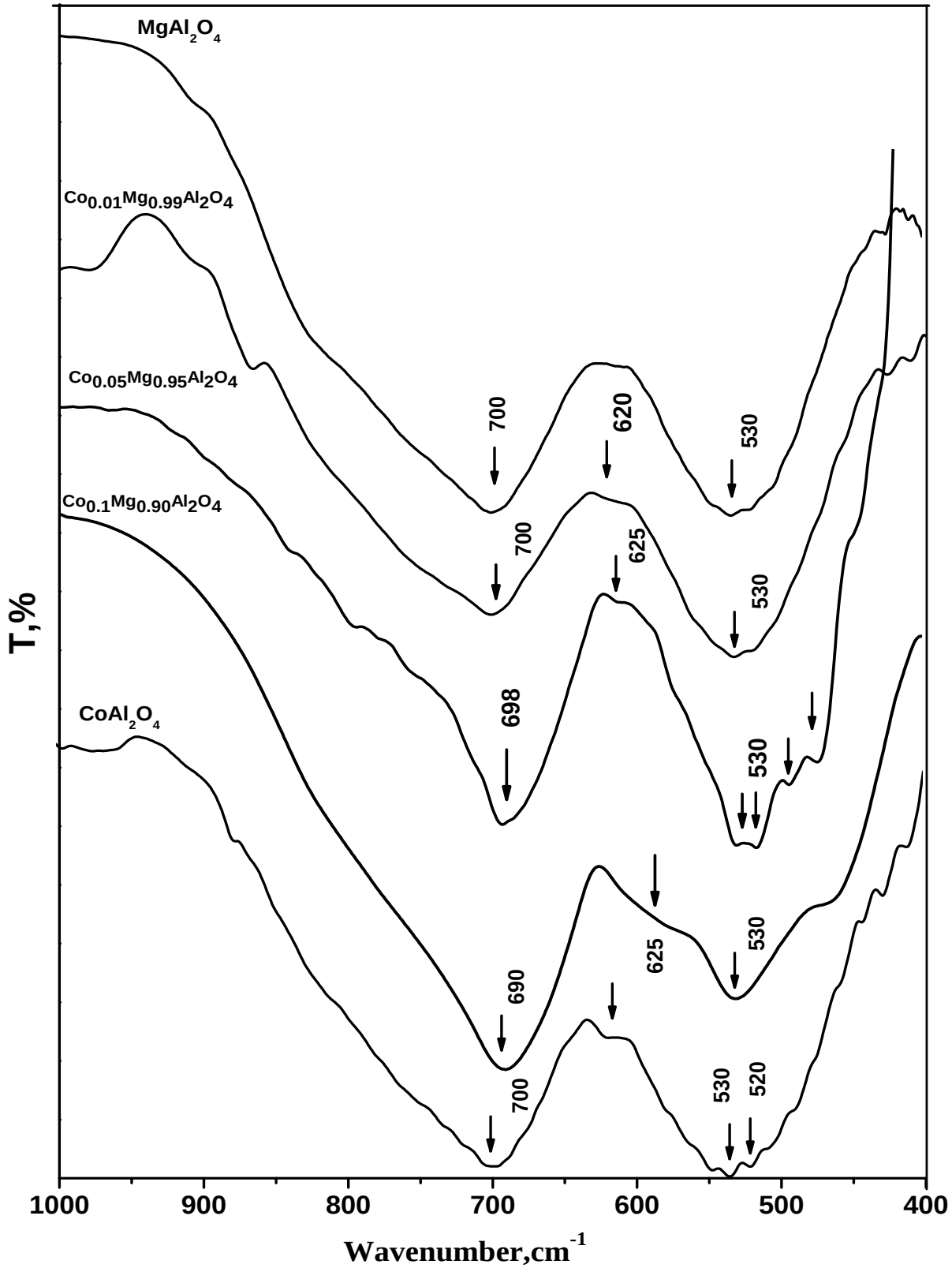
MgAl2O4
Co0.01Mg0.99Al2O4
Co0.05Mg0.95Al2O4
Co0.1Mg0.90Al2O4
CoAl2O4
700
620
530
700
625
530
698
530
690
625
530
700
530
520
T,%
1000
900
800
700
600
500
400
Wavenumber,cm-1

Figure(4): Infrared spectra for 0.01, 0.05, 0.10 mole of Co^{2+} systems, $CoAl_2O_4$ and $MgAl_2O_4$ by using oxalyl dihydrazide as fuel in range 400- 1000 cm^{-1} at 1200 ^{o} C.

Table(2): Assignment of the important bands in the IR spectra for 0.01,0.05 and 0.10 mole of Co^{2+} systems at different calcination temperatures using oxalyl dihydrazide as fuel.

Temperature, ^{o}C	system 0.01 mole of Co^{2+}							
	υ-OH	υN-H	υ-CH	υC=O	υ C-O	υ C-N	υ N=O	υ M-O
٥٠٠	٣٤٩٠	-	٢٩٢٠	١٦٥٠	١١٠٠	١٤٠٠	٨00	٦٠٠
٧٠٠	٣٤٦٠	-	-	١٦٥٠	١١٥٠	١٤٥٠	٨00	695,500,425
٩٠٠	٣٤٥٠	-	-	-	-	١٤٥٠	-	700,610,٥١٥
١١٠٠	٣٤٠٠	-	-	-	-	-	-	698, 610, 510, 410
١٢٠٠	٣٤٠٠	-	-	-	-	-	-	٦٩٨, 521,٤٢٨
	0.05 mole of Co^{2+}							
٥٠٠	٣٤٩٠	-	٢٩50	١٦٥٠	١١00	١٤0٠	٨٠٠	-
٧٠٠	٣٤٩٠	-	-	١٦٥٠	١١١٠	1390	-	700,٥٠٠
٩٠٠	٣٤٠٠	-	-	١٦٥٠	1110	-	-	700,٥١٥,422
١١٠٠	٣٤١٠	-	-	-	-	-	-	691,٥٢٠,422
١٢٠٠	٣٤٢٠	-	-	-	-	-	-	685,٥٢٢,422
	0.10 mole of Co^{2+}							
٥٠٠	٣٤٩٠	-	٢٨٥٠	١٦٨٠	١١١٠	١٣٩٠	٨٠٠	٧٠٠,500
٧٠٠	٣45٠	-	-	١٦20	1110	-	-	700,530
٩٠٠	٣٤٥٠	-	-	١٦٥٠	1110	١٤٠٠	-	697,530,420
١١٠٠	٣٤٩٠	-	-	-	-	-	-	690,٥٣٠,425
١٢٠٠	٣٥٠٠	-	-	-	-	-	-	690,٦١٠,٥٣٠,425

3.1.1.3. Fourier Transform Infrared Spectra (FTIR) for cobalt system using 3-methyl pyrozole-5-one (3MP5O) as fuel.

The spectra of 3-methyl pyrozole-5-one (3MP5O) system 0.01 (A), 0.05 (F) and 0.10 (M) mole of Co^{2+} systems after ignition at 400°C and calcinations at different temperatures are shown in Figures (5). The samples at ignition temperature 500°C contain a broad absorption band around 3450 cm^{-1} for A system, 3450 cm^{-1} for F and M systems. These later bands are related to the stretching vibration of free (–OH) group of water molecules. The absorption bands at 2920 cm^{-1} for A, F and M systems are related to the stretching vibration of C-H aliphatic in organic molecules. The absorption bands at 1650 and 1400 cm^{-1} for A system, 1650 and 1450 cm^{-1} for F system, 1650 and 1190 cm^{-1} for M system are related to the stretching vibration of C=O and C–O groups of residual organic molecules . The absorption bands at 1380, 1268, 1100 and 850 cm^{-1}, 1400, 1150, 1050 and 850 cm^{-1} and also 1400, 1190 and 800 cm^{-1} for A, F and M systems, respectively are corresponding to undecomposed nitrate ions.

The weak absorption bands in the region 400–800 cm^{-1} appear due to the formation of trace amounts of metal oxides and its intensity increase with calcinations at different temperatures in range 500-1200 °C. The observed absorption bands in the region 800–4000 cm^{-1} are decreased gradually until disappeared at 1000 °C. The strong absorption band at 3460 cm^{-1}, 3400 cm^{-1} and 3450 cm^{-1} for A, F and M systems, respectively. These bands are corresponding to the stretching vibration of adsorptions water molecules. The appearance of strong absorption bands below 800 cm^{-1} corresponds to metal

oxides. The absorption bands in range 690, 520 cm^{-1}, 690, 530 cm^{-1} and 700, 520 cm^{-1} for A, F and M systems, respectively are related to AlO_6 groups building up the spinel as a result of vibration of ions of valence Al^{3+} in octahedral positions compare with the bands in range 700, 425 cm^{-1} for $MgAl_2O_4$ [93-95] as blank. The bands in range 690, 420 cm^{-1}, 690, 475 cm^{-1} and 700, 425 cm^{-1} for A, F and M systems, respectively are related to CoO_4 /MgO_4 groups for the cobalt and magnesium spinel as a result of vibration of its ions in the tetrahedral sites compare with that in range 700, 520 cm^{-1} for $CoAl_2O_4$ [96-97] as blank that shown in Figure (6). The assignment of an important bands in the IR spectra for A, F and M systems at different calcination temperatures using 3-methyl pyrozole-5-one (3MP5O) as fuel are given in Table(3).

3.1.1.4. Fourier Transform Infrared Spectra (FTIR) for cobalt system using N, N-bis-(3-amino-propyl) oxalamide as fuel.

FT-IR spectra of 0.01 (A), 0.05(F) and 0.10(M) mole of Co^{2+} systems using N, N-bis-(3-amino-propyl) oxalamide as fuel are studied. The samples after ignition at 500 ˚C give a broad absorption band around 3450 cm^{-1} for A, F and M systems which due to the stretching vibration of free (–OH) group of water molecules. The absorption bands at 2990 cm^{-1} for A, F and M systems are corresponding to the stretching vibration of C-H aliphatic in organic molecules. The absorption bands at 1650, 1410 and 1190 cm^{-1}, 1640, 1390 and 1190 cm^{-1} and 1640, 1380 and 1180 cm^{-1} for A, F and M systems, respectively are related to the stretching vibration of carbonyl C=O and C–O groups of residual organic molecules. The absorption bands at 1380, 1120 and 825 cm^{-1}, 1390, 1120 and 800 cm^{-1} and 13980, 1120 and 800 cm^{-1} for A, F and M systems, respectively are related to undecomposed nitrate ions.

The intensity absorption bands in the region 400–1000 cm^{-1} are corresponding to metal oxides after calcination at different temperatures in range 500-1200˚C as shown in Figure (7). The observed absorption bands in the region 800–4000 cm^{-1} are decreased gradually until disappeared at 1100 ◦C. The strong absorption band at 3500 cm^{-1} for A system, 3450 cm^{-1} for F and M systems are corresponding to the stretching vibration of adsorption water molecules. The two absorption bands in ranges 700, 530 cm^{-1}, 700, 525 cm^{-1} and 695, 525 cm^{-1} for A, F and M systems, respectively are corresponding to AlO_6 [93-95] groups for the cobalt magnesium aluminates systems under investigation as a result of vibration of ions of valence Al^{3+} in octahedral sites compare with 700, 525 and 420cm^{-1} for pure $MgAl_2O_4$. The other bands in ranges 700, 520 and 420 cm^{-1} for A and F systems, 695, 525 and 420 cm^{-1} for M system are corresponding to CoO_4 /MgO_4 groups for the cobalt magnesium aluminates spinel as a result of vibration in the tetrahedral sites compare with 700, 535 and 520 cm^{-1} for pure $CoAl_2O_4$ [96-97]. The assignment of an important bands in the IR spectra for A, F and M systems at different calcinations temperatures using N, N-bis-(3-amino-propyl) oxalamide as fuel are given in Table (4).

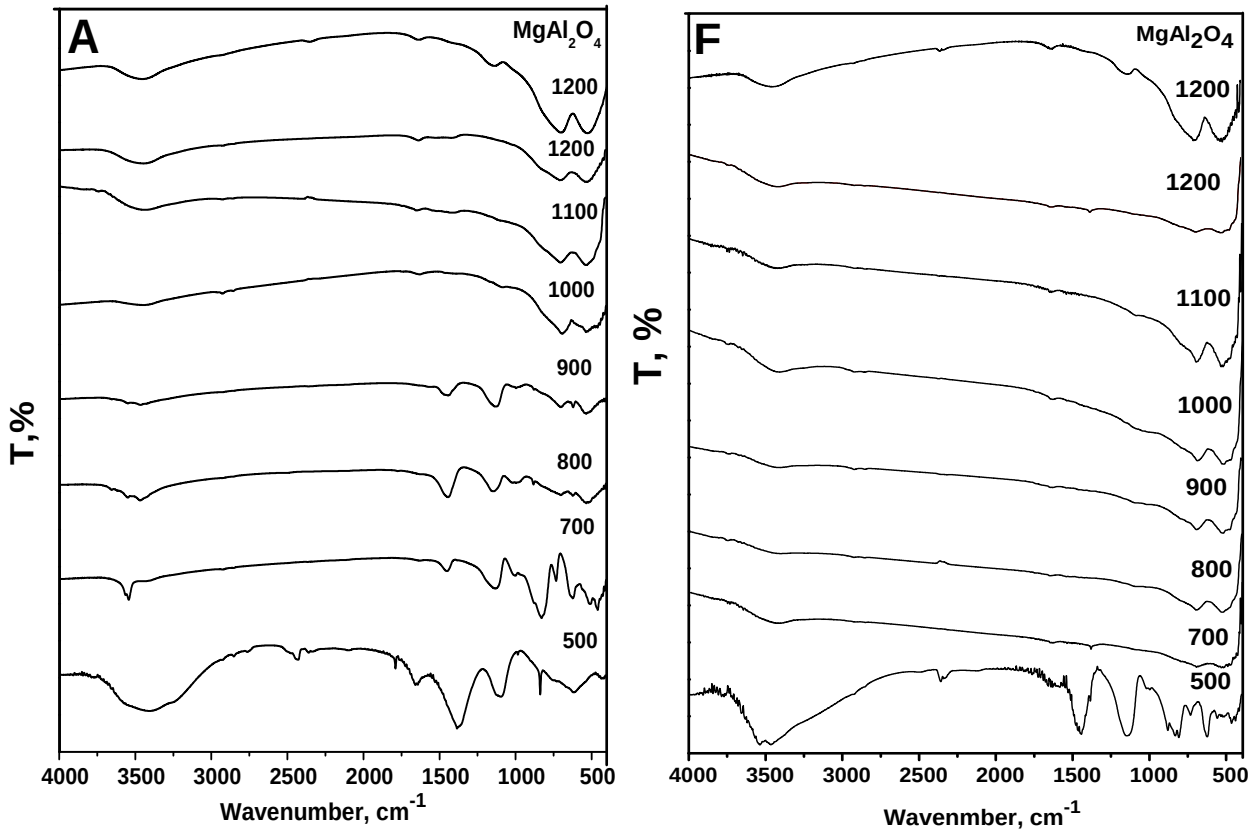
A
MgAl2O4
1200
1200
1100
1000
900
800
700
500
T,%
4000 3500 3000 2500 2000 1500 1000 500
Wavenumber, cm-1
F
MgAl2O4
1200
1200
1100
1000
900
800
700
500
T, %
4000 3500 3000 2500 2000 1500 1000 500
Wavenmber, cm-1

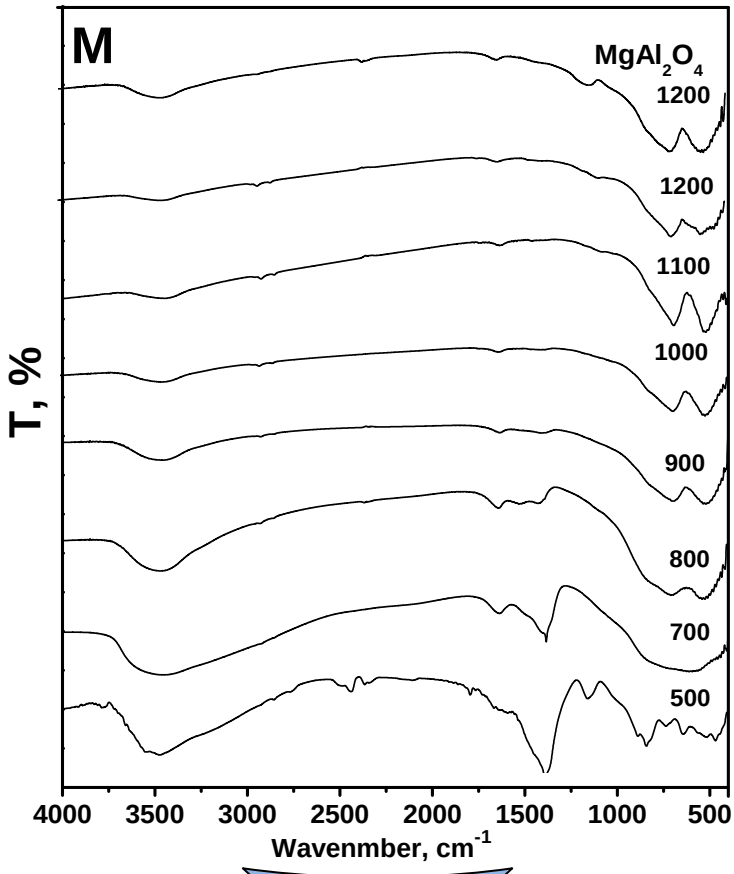
M
MgAl2O4
1200
1200
1100
1000
900
800
700
500
T, %
4000 3500 3000 2500 2000 1500 1000 500
Wavenmber, cm-1

Figure(5): Infrared spectra 0.01 (A), 0.05 (F) and 0.10 (M) mole of Co^{2+} system using 3-methyl pyrozole-5-one as fuel at different calcination t

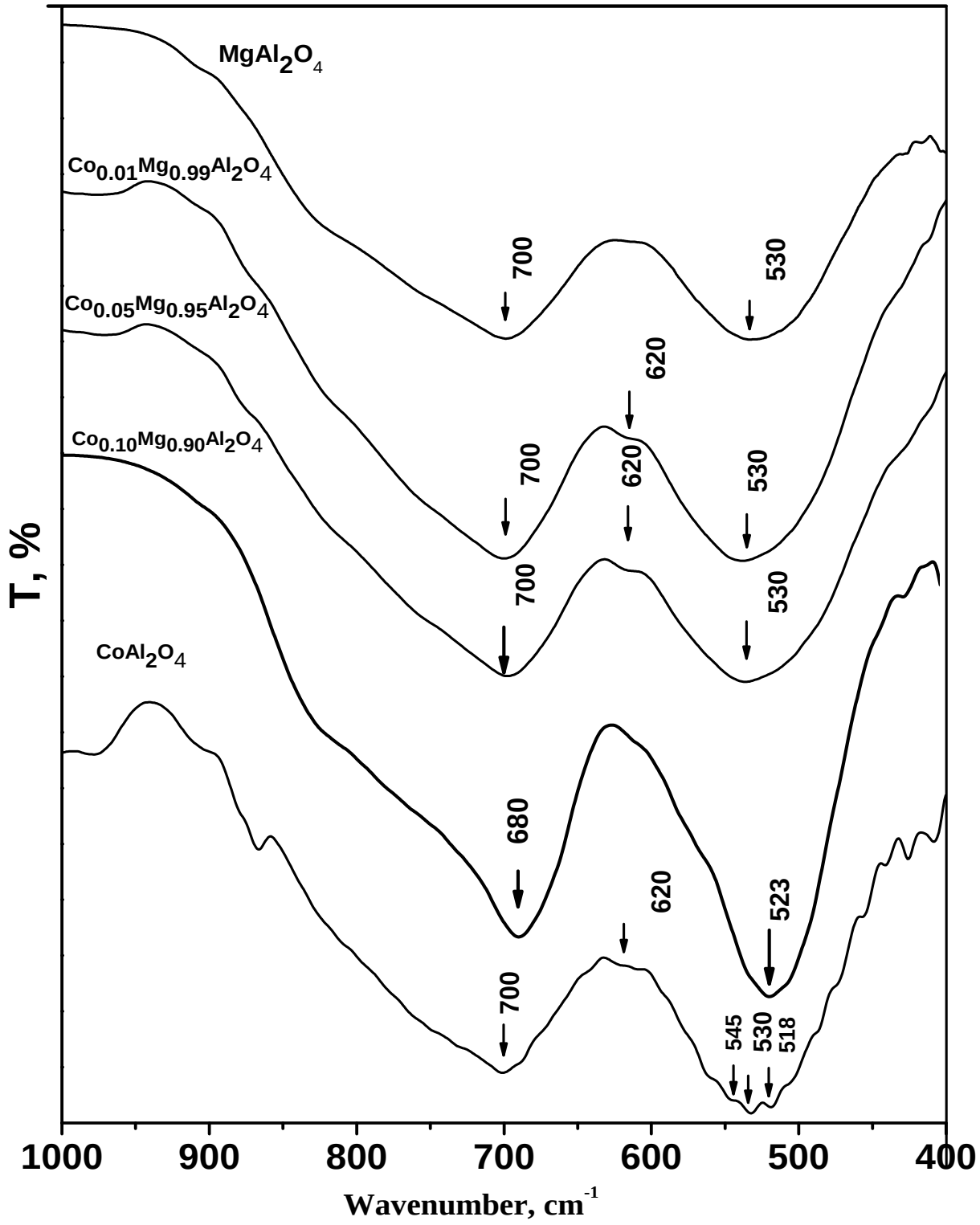

Figure(6): Infrared spectra for 0.10, 0.50, 0.80 mole of Co^{2+} systems, $CoAl_2O_4$ and $MgAl_2O_4$ by using 3-methyl pyrozole-5-one as fuel in range 400-1000 cm^{-1}.

Temperature, °C	system 0.01 mole of Co^{2+}						
	υ -OH	υ-CH	υ C=O	υC-O	υC-N	υ N=O	υ M-O
٥٠٠	٣٤٥٠	٢٩٢٠	١٦٥٠	١١٠٠	١٤٠٠	850	٦٠٠
٧٠٠	٣51٠	-	-	١١1٠	١٤٥٠	٨25	720,610,450
٨٠٠	٣٤٥٠	-	-	١١٥٠	١٤٥٠	-	700,610,٥٢٠
٩٠٠	٣٤٥٠	-	-	١١٥٠	١٤٥٠	-	700,610,٥٢٠
١٠٠٠	٣٤50	-	-	-	-	-	700,٥٢٠
١١٠٠	٣٤50	-	-	-	-	-	700,٥٣٠,425
١٢٠٠	٣٤50	-	-	-	-	-	700,٥٣٠,425
	0.05 mole of Co^{2+}						
٥٠٠	٣٤٥٠	٢٩٢٠	١٦٥٠	١١٥٠	١٤٥٠	٨٥٠	٦١٠
٧٠٠	٣٤٠٠	-	١٦٥٠	-	١٤٠٠	-	700,٥٠٠
٨٠٠	٣٤٥٠	-	-	-	-	-	700,٥٢٠
٩٠٠	٣٤٥٠	-	-	-	-	-	700,٥٣٠
١٠٠٠	٣٤٥٠	-	-	-	-	-	700,٥٢٠,420
١١٠٠	٣٤٥٠	-	-	-	-	-	700,٥٢٥,420
١٢٠٠	٣٤٥٠	-	-	-	-	-	700,٥٢٥,475
	0.10 mole of Co^{2+}						
٥٠٠	٣٤٥٠	٢٩٢٠	١٦٥٠	١١٩٠	١٤٠٠	٨٥٠	٦٥٠,500
٧٠٠	٣٥٠٠	-	١٦٥٠	-	١٤٠٠	-	٦٠٠
٨٠٠	٣٤٥٠	-	١٦٥٠	-	١٤٠٠	-	700,٥٣٠
٩٠٠	٣٤٥٠	-	١٦٥٠	-	١٤٠	-	700,530

					٠		
١٠٠٠	٣٤٥٠	-	-	-	-	-	700,٥٣٠,425
١١٠٠	٣٤٥٠	-	-	-	-	-	700,٥٢٠,425
١٢٠٠	٣٤٨٠	-	-	-	-	-	700,٦١٠,520,425

Table(3): Assignment of the important bands in the IR spectra for 0.01,0.05 and 0.10 mole of Co^{2+} systems at different calcination temperatures using 3-methyl pyrozole-5-one as fuel.

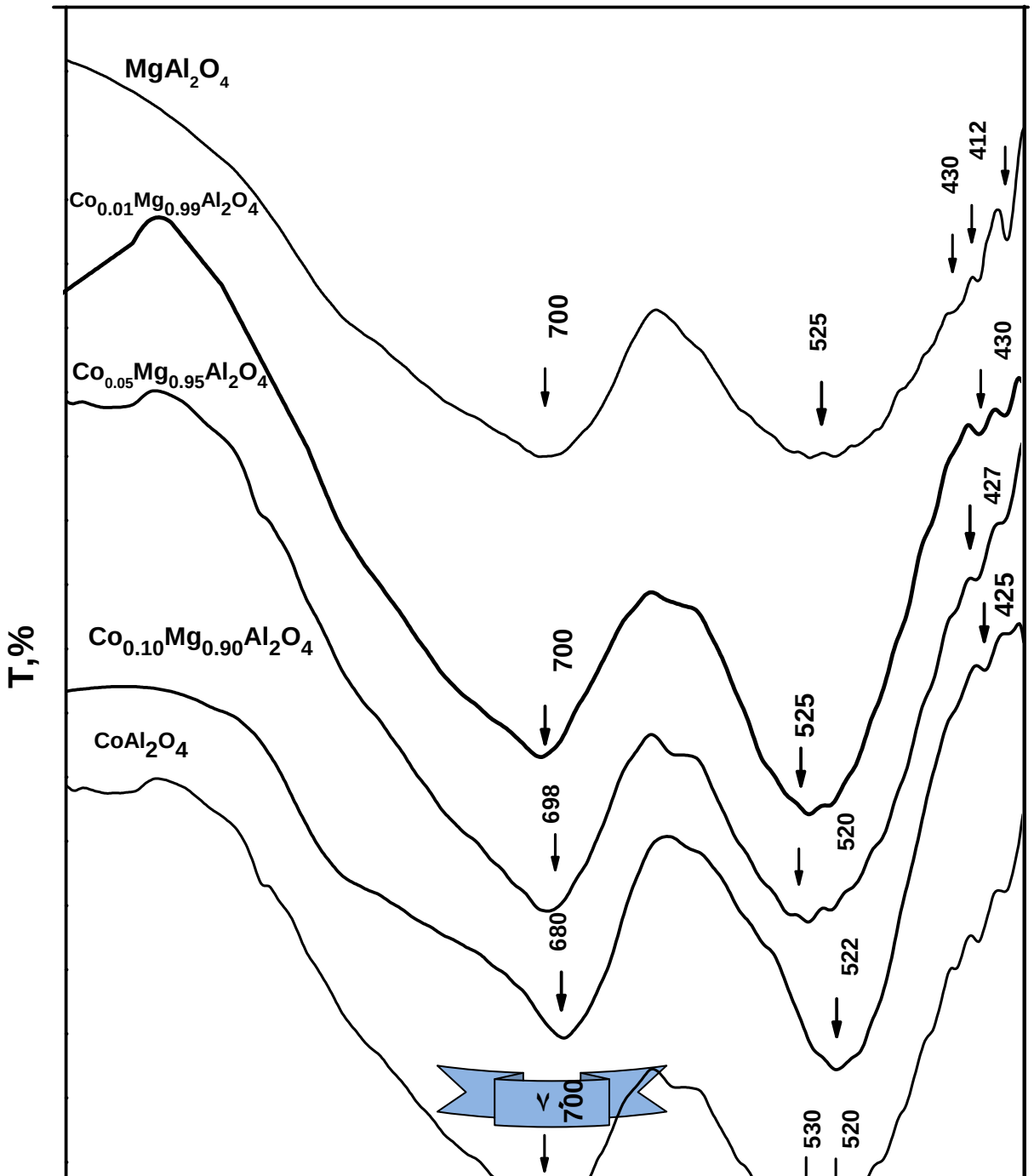

Figure (7): Infrared spectra for 0.01, 0.05, .010 mole of Co^{2+} systems, $CoAl_2O_4$ and $MgAl_2O_4$ by using N, N-bis-(3-amino-propyl) oxalamide as fuel in range 400-1000 cm^{-1}.

Table(4): Assignment of the important bands in the IR spectra for 0.01,0.05 and 0.10 mole of Co^{2+} systems at different calcination temperatures using N, N-bis-(3-amino-propyl) oxalamide as fuel.

Temperature, °C	system 0.01 mole of Co^{2+}						
	υ-OH	υ-CH	υC=O	υC-O	υC-N	υ N=O	υ M-O
٥٠٠	٣٤٥٠	٢٩٩٠	١٦٥٠	١١٢٠	١٤١٠	٨٥٠	700,٥٠٠
٧٠٠	٣٤9٠	-	1620	١١1٠	١39٠	-	700,515,415
٩٠٠	٣٤8٠	-	1625	1115	١39٠	-	700,٥٣٠,410
١١٠٠	٣٤90	-	1650	1110	1390	-	700,610,٥٢٥,420
١٢٠٠	٣٤50	-	-	-	-	-	700,٥٢٠,420
	0.05 mole of Co^{2+}						
٥٠٠	٣٤٥٠	٢٩٨٠	١٦٤٠	١١٩٠	١٣٩٠	٨٠٠	700,500
٧٠٠	٣٤٥٠	-	١٦٣٠	١١١٠	١٣٩٠	-	700,610,520,420
٩٠٠	٣٤9٠	-	١٦٢٠	١١١٠	١٣٩٠	-	700,610,520,420
١١٠٠	٣٤5٠	-	١٦٢٠	١١١٠	-	-	700,٥٢٠,420
١٢٠٠	٣٤5٠	-	-	١١١٠	-	-	700,610,٥٣٥,420

	0.10 mole of Co^{2+}						
٥٠٠	٣٤٥٠	٢٩٩٠	١٦٤٠	١١٢٠	١٣٨٠	٨٠٠	70٠,٥٠٠
٧٠٠	٣٤٥٠	-	١٦٢٠	١١١٠	١٣٩٠	-	700,٥٢٠,420
٩٠٠	٣٤٨٠	-	١٦١٠	١١١٠	١٣٩٠	-	699,525,420
١١٠٠	٣٤٥٠	-	-	-	-	-	700,٥٢٥,425
١٢٠٠	٣٤٩٠	-	-	-	-	-	700,٥30,425

3.1.2. Diffuse reflectance spectra

Diffuse Reflectance Spectroscopy (DRS) is a technique that collects and analyzes scattered light as energy. It is used for measurement of fine particles and powders, as well as rough surface (e.g., the interaction of a surfactant with the inner particle, the adsorption of molecules on the particle surface or color of material under investigation). Sampling is fast and easy because little or no sample preparation is required. Diffuse reflectance spectra are the relations between reflectance and wavelength. The color of different material can not differentiate using your eyes, but we can use the diffuse reflectance spectra with program [98] for differentiation between the colors of material when the difference is much neared. The CIE- L*a*b* colormetric method, recommended by the Commission Internationale de l'Eclairage (CIE) [83] was followed. In this method, L* is lightness axis: black (0) ---- white (100), b* is the blue (-) ---- yellow (+), a* is the green (-) --- red (+) axis as

shown in Figure (8) and ΔE [99] is the hue variation $\Delta E^2 = (L^*)^2 + (a^*)^2 + (b^*)^2$. The delta E or color difference measures the difference in luminosity chromaticity with standards.

3.1.2.1. Diffuse reflectance spectra for cobalt systems using urea as fuel.

Diffuse reflectance spectra for A, F and M systems of 0.01, 0.05 and 0.10 mole of Co^{2+} respectively using urea as fuel present in Figure (9). Figures show the appearance bands around 490 nm for A system, 462 nm for F system and 510 nm for M system at 700º C that tends to pale blue color of pigment powders and this band shift to blue side as calcinated temperatures increase until reaching around 445 nm for A system, 450-490 nm for F system and 500-460 nm for M system at 900ºC. These bands also shift to blue side at 425 and 490 nm for A system and 425, 455 and 480 nm for F and M systems at 1200ºC [100-101] that show the bluest color pigment.

The colorimetric data are present in Table (5). The values of a* are random while L* values decrease and b* values increase in negative direction as a result of increasing calcination temperatures. The increasing in negative values of b* means the higher intensity of blue color. The decreasing in L* parameter tends to reduce the lightness of sample. In the same time, the increasing of amount cobalt percent, the values of b* increase as present in Figure (10). This leads to the depth of blue color as result of calcinations temperatures. The lower value of hue variation ΔE tends to a good color matching [102] on glaze. Colorimetric data show the high value of b* and lower value of hue variation ΔE at 1200ºC for all cobalt systems using urea as fuel as well as demonstrated in Table (5). This means that the appearance of good pigment powder color and a good color matching occur in temperature range

1200ºC.The color of ceramic pigment powders with different doping and change calcination temperatures is shown in Figure (11).

3.1.2.2. Diffuse reflectance spectra for cobalt systems using oxalyl dihydrazide as fuel.

Figure (12) show diffuse reflectance spectra for A, F and M systems of 0.01, 0.05 and 0.10 mole of Co^{2+} respectively using oxalyl dihydrazide as fuel. It is clear from these observed figures that the appearance of bands in range 495 and 450 nm for A system, 450 nm for F system and 440 nm for M system at 700º C that tends to pale blue color of samples. These bands shift to blue side as calcinated temperatures increase until reaching around 435 and 490 nm for A system, 435 and 495 nm for F system and 430 and 390 nm for M system at 900ºC for blue color. These bands shift to blue side at 480, 460 and 425 nm for A and M systems and 480, 425nm for F system at 1200ºC that show the bluest [100-101] color pigment.

From colorimetric data present in Table (6), the values of a* are random while L* values decrease and b* values increases in negative direction as a result of increasing calcination temperatures. The increasing in negative values of b* means the higher intensity of blue color. The decreasing in L* parameter tends to reduce the lightness of sample. Figure (13) shows the correlation between calcination temperatures with b* values depending on amount cobalt percent, the value of b* increases leading to the depth of blue color. The lower value of hue variation ΔE tends to a good color matching [102]. Colorimetric data show the high negative value of b* and lower value of hue variation ΔE at 1200ºC for A and F doping cobalt. This means the appearance of good pigment powder color and a good color matching occur at 1200ºC for A and F systems. But, the high value of b* for M system presents at 1100 ºC and lower value of hue variation ΔE at 1200ºC. This means that

the appearance of good pigment powder color at 1100 ºC and a good color matching occur at 1200ºC for M doping cobalt as show in Table (6). The color of ceramic pigment powders of different doping with change calcinations temperatures is shown in Figure (14).

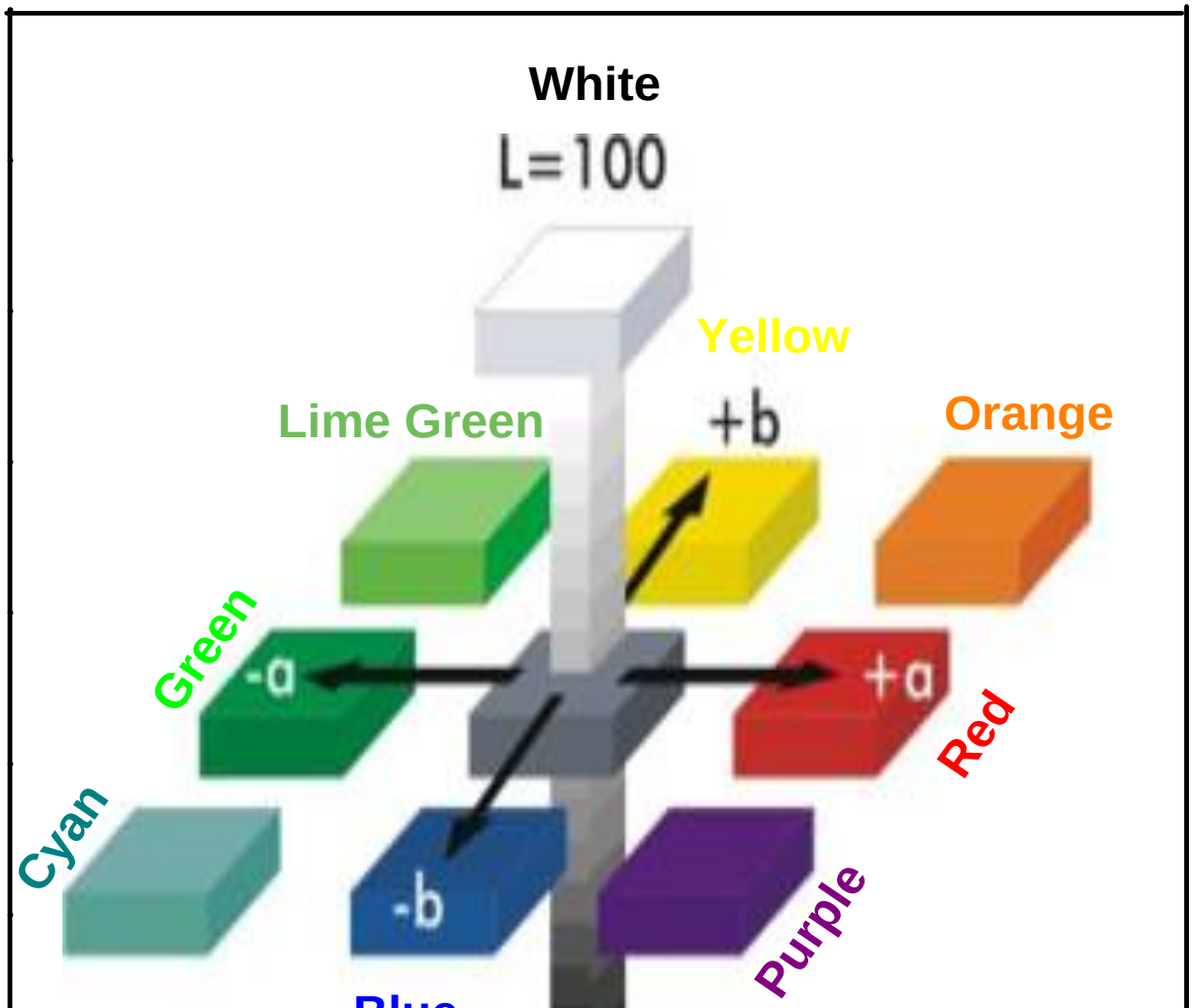

Figure (8):L*a*b* colormetric axis for L* is lightness axis:black(0)→ white (100), b* is the blue (-)⟶ yellow(+), a* is the green (-)→ red (+) axis and color between them.

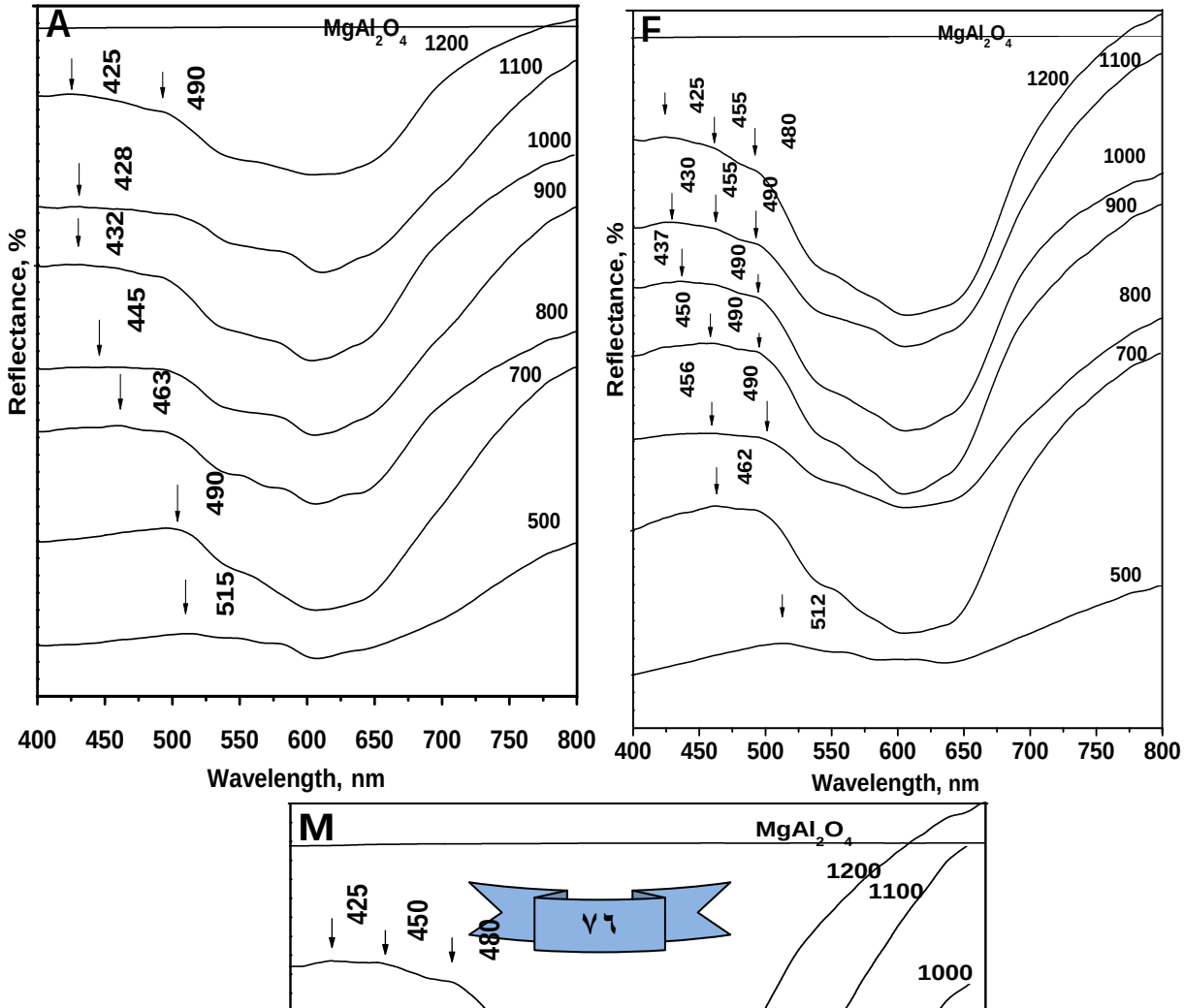

Figure (9): Diffuse reflectance spectra of A system (0.01 mole of Co^{2+}), F system (0.05 mole of Co^{2+}) and M system (0.10 mole of Co^{2+}) at different calcination temperatures by using urea as fuel.

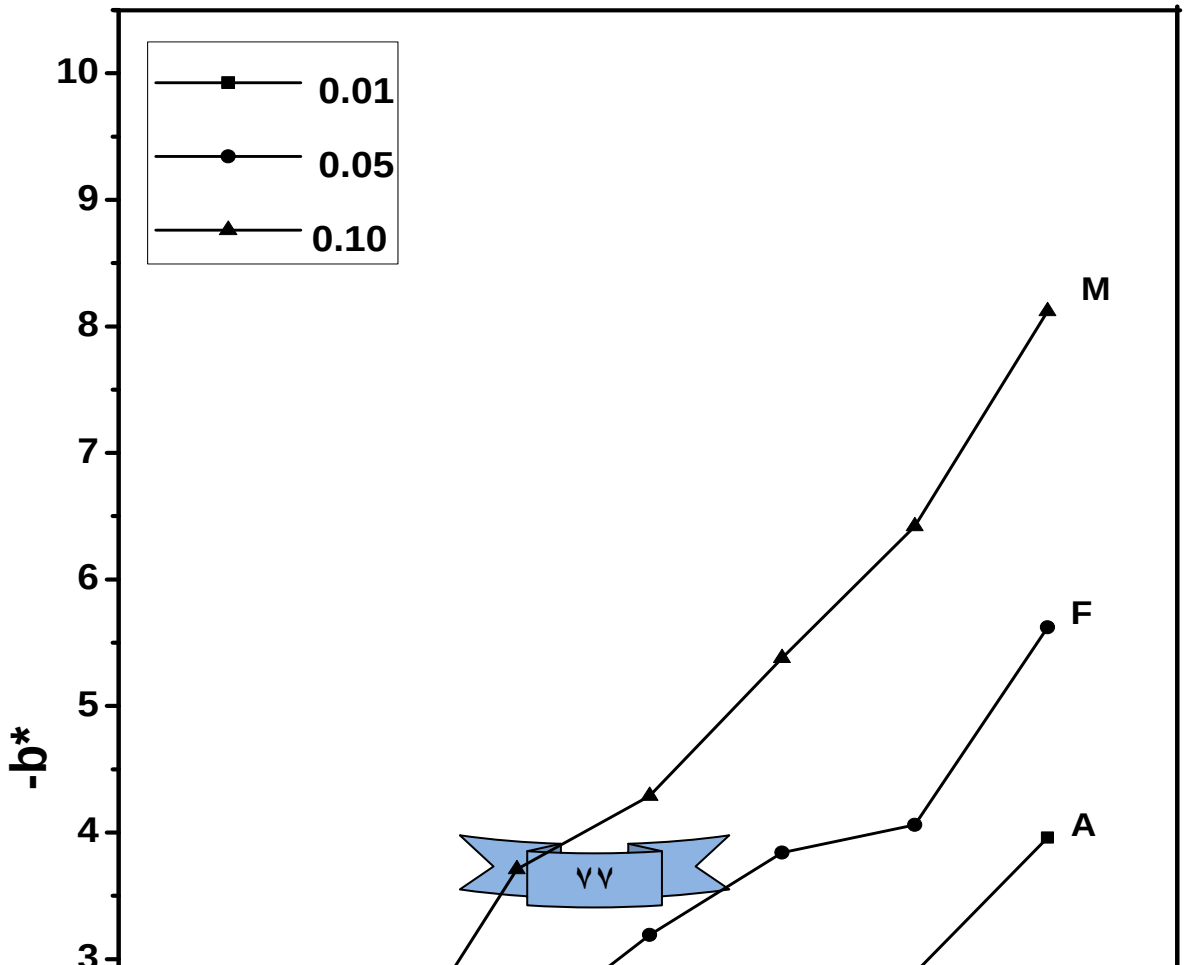

Figure (10): Colorimetric data for 0.01, 0.05 and 0.1 mole of Co^{2+} system at different calcination temperatures by using urea as fuel.

System	temperature	L*	a*	b*	ΔE
0.01	٥٠٠	93.58	-1.55	0.90	94.10
	٧٠٠	97.09	-0.96	-0.53	97.10
	٨٠٠	96.64	-1.40	-1.09	96.60
	٩٠٠	95.77	-1.01	-1.48	95.80
	١٠٠٠	94.50	-0.91	-2.33	94.50
	١١٠٠	94.00	-0.67	-2.89	94.10
	١٢٠٠	93.04	-0.85	-3.96	93.00

0.05	٥٠٠	92.70	-1.05	0.08	92.71
	٧٠٠	95.19	-1.70	-1.07	95.21
	٨٠٠	95.00	-0.54	-2.38	95.03
	٩٠٠	94.69	-0.76	-3.19	94.75
	١٠٠٠	93.65	-0.58	-3.84	93.73
	١١٠٠	92.29	-0.76	-4.06	92.38
	١٢٠٠	91.77	-0.72	-5.62	92.00
0.10	٥٠٠	91.11	-1.61	٠.73	91.13
	٧٠٠	93.06	-1.38	-2.06	93.01
	٨٠٠	92.39	-1.26	-3.71	92.47
	٩٠٠	92.24	-0.96	-4.29	92.34
	١٠٠٠	91.87	-1.11	-5.38	92.00
	١١٠٠	91.26	-1.00	-6.42	91.50
	١٢٠٠	90.29	-0.74	-8.12	90.64

Table (٥): Colorimetric data for different doping of 0.01, 0.05 and 0.1 mole of Co^{2+} systems at different calcination temperatures using urea as fuel.

Temperature, °C	0.01 mole of Co^{2+}	٠,٠٥ mole of Co^{2+}	٠,١0 mole of Co^{2+}
٥٠٠			
٧٠٠		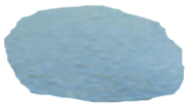	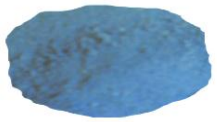
٨٠٠			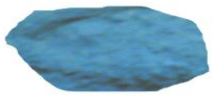
٩٠٠	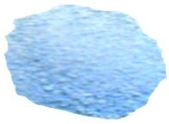	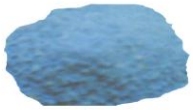	
١٠٠٠	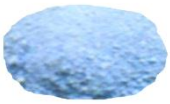	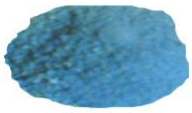	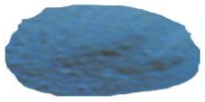
١١٠٠			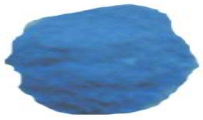
١٢٠٠			
Blank	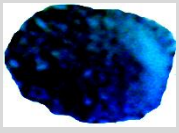 **$CoAl_2O_4$**		**$MgAl_2O_4$**

Figure (11): The color of ceramic powder for 0.01, 0.05 and 0.010 mole of Co^{2+} systems using urea as fuel at different calcination temperatures.

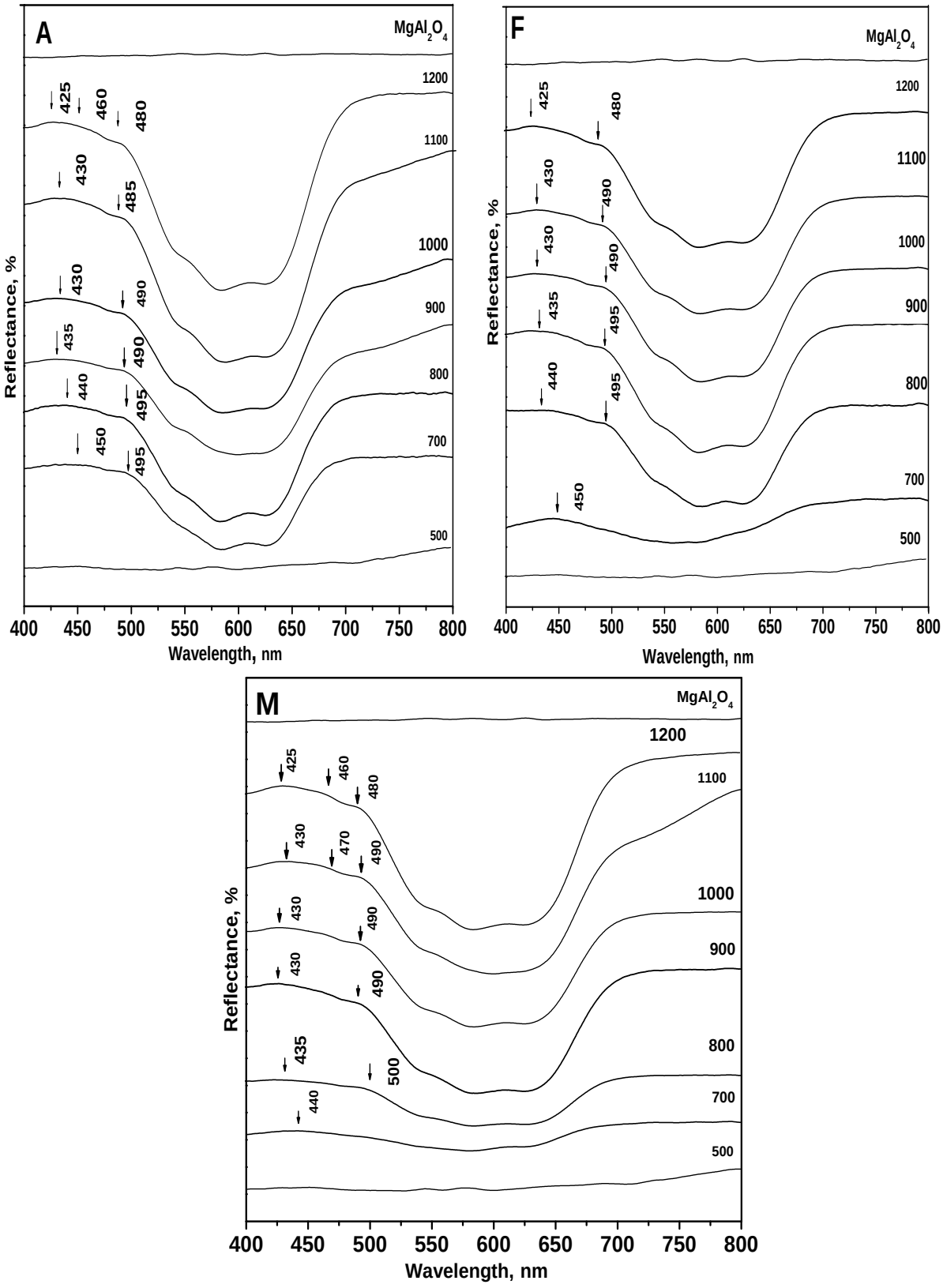

Figure (12): Diffuse reflectance spectra of A system (0.01 mole of Co^{2+}), F system (0.05 mole of Co^{2+}) and M system (0.10 mole of Co^{2+}) at different calcination temperatures by using oxalyl dihydrazide as fuel.

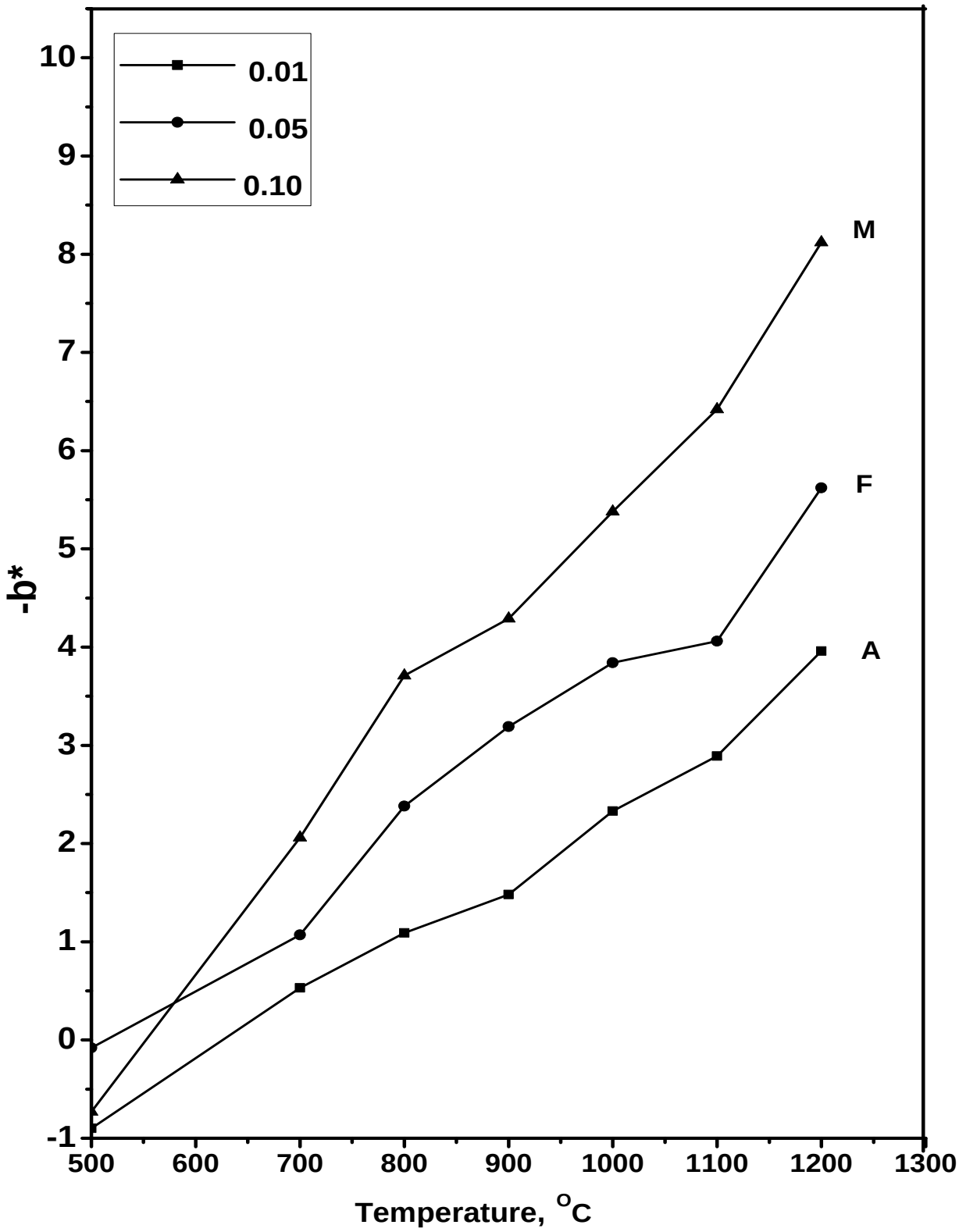

Figure (13): Colorimetric data for 0.01, 0.05 and 0.1 mole of Co^{2+} systems at different calcination temperatures by using oxalyl dihydrazide as fuel.

Table (6): Colorimetric data for 0.01, 0.05 and 0.1 mole of Co^{2+} systems at different calcinations temperatures using oxalyl dihydrazide as fuel.

system	Temperature, ^{O}C	L*	a*	b*	ΔE
٠,٠١	٥٠٠	٩٩,٧٤	-٠,٠٢	-٠,١٠	٩٩,٧٤
	٧٠٠	٩٧,٩	-٠,٩١	-٢,٢٠	٩٧,٩٣
	٨٠٠	٩٥,٢٥	-٠,٧٥	-٣,١٤	٩٥,٣١
	٩٠٠	٩٤,٢٠	-١,٦٠	-٦,٤٣	٩٤,٤٣
	١٠٠٠	٩٢,٥١	-٠,٨١	-٦,٦١	٩٢,٧٥
	١١٠٠	٩١,٣٢	-١,٦٨	-٦,٩٨	٩١,٦٠
	١٢٠٠	٩٠,٦٠	-١,٣٦	-٨,٠٤	٩٠,٩٧
٠,٠٥	٥٠٠	٩٨,٧٧	**-0.13**	**3.81**	٩٨,٨٤
	٧٠٠	**97.3**	**-1.16**	**-3.52**	٩٧,٣٧
	٨٠٠	**96.53**	**-0.71**	**-4.65**	٩٦,٦٥
	٩٠٠	**96.07**	-١,٦٩	-٥,٣٨	٩٦,٢٤
	١٠٠٠	٩٤,٤١	-١,٧٩	-٧,٣٨	٩٤,٧٢
	١١٠٠	٩٢,٧٦	-١,١٥	**-9.12**	٩٣,٢١
	١٢٠٠	٩١,٤١	-١,٣١	-١٠,٥	٩٢,٠٢
٠,١٠	٥٠٠	٩٧,٣٧	**--0.07**	٠,٠٢	٩٧,٣٧
	٧٠٠	٩٥,٤٣	**-0.80**	**-4.20**	٩٥,٥٣
	٨٠٠	٩٣,٢٩	**-1.78**	**-7.05**	٩٣,٥٧
	٩٠٠	٩٢,٢٨	**-1.24**	**-9.17**	٩٢,٧٤
	١٠٠٠	**90.97**	**-2.35**	**-11.79**	٩١,٧٦
	١١٠٠	**89.19**	**-1.66**	**-13.43**	٩٠,٢١
	١٢٠٠	٨٤,٧٧	**-2.32**	**-12.34**	٨٥,٧٠

Temperature, °C	mole of Co^{2+} ٠,٠١	٠,٠٥ mole of Co^{2+}	٠,١0 mole of Co^{2+}
٥٠٠			
٧٠٠			
٨٠٠			
٩٠٠		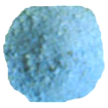	
١٠٠٠	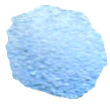	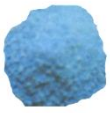	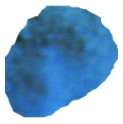
١١٠٠		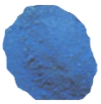	
١٢٠٠		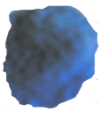	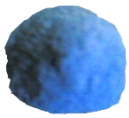
Blank	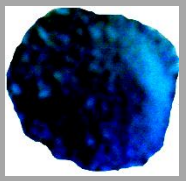 $CoAl_2O_4$		 $MgAl_2O_4$

Figure (14): The color of ceramic powder for 0.01, 0.05 and 0.010 mole of Co^{2+} systems using oxalyl dihydrazide as fuel at different calcination temperatures.

3.1.2.3. Diffuse reflectance spectra for cobalt systems using3-methyl pyrozole-5-one (3MP5O) as fuel.

The ceramic pigment of cobalt systems A, F and M systems of 0.01, 0.05 and 0.10 mole of Co^{2+} respectively are studied by diffuse reflectance spectra after firing with 3-methyl pyrozole-5-one (3MP5O) as fuel and the results are present in Figure (15). The data show the appearance of bands around 500 nm for A system, 495 nm for F system and 512 nm for M system at 700º C that tends to pale blue color of samples. These bands of the systems shift to lower wavelength as the calcination temperatures increase until reaching around 460 nm for A system, 465 nm for F system and 495 nm for M at 900ºC to become clear blue color. These bands shift to blue side at 388, 425 and 490 nm for A system and 489, 425 and 487 and 386, 423 and 488 nm for F and M system at 1200ºC show the bluest color pigment.

Diffuse reflectance data are given in Table (7) that show the values of a* are random while L* values decrease and b* values increases in the negative direction as result of increasing calcination temperatures. The values of b* are increasing in negative direction, with the higher intensity of blue color. The decreasing in L* parameter tends to reduce the lightness of sample with increasing the amount cobalt percent. The values of b* increase as shown in Figure (16), leading to the depth of blue color as result of calcination temperatures. The lower value of hue variation ΔE tends to a good color matching. Diffuse reflectance spectra data show the high negative values of b* at 1100ºC and lower value of hue variation ΔE at 1200ºC for all cobalt systems as shown in Table (7). The colors of ceramic powder of different doping with change temperature are shown in Figure (17). This

means that the appearance of good pigment powder color occurs at calcination temperatures in range1100-1200ºC.

3.1.2.4. Diffuse reflectance spectra for cobalt systems using N, N-bis-(3-amino-propyl) oxalamide as fuel.

Diffuse reflectance spectra for A, F and M systems of 0.01, 0.05 and 0.10 mole of Co^{2+} respectively using N, N-bis-(3-amino-propyl) oxalamide as fuel present in Figures (18).The pale blue color of sample show the appearance of band around 500, 445 nm for system A, 490, 455 nm for F system and 490,430 nm for M system at 700º C. This band shift to lower wavelength as calcination temperatures increases to reach to 500,435 nm for A system, 490, 430 nm for F system and 490, 425 nm for M system at 900ºC. These bands also shift to 480, 465 and 430 nm for A system, 480,430 nm for F system and 480, 460 and 425 nm for M system at 1200ºC.

The diffuse reflectance spectra data show the bluest color pigment as given in Table (8), the data reveal that the values of a* increase while L* values decrease and b* values increases in the negative direction as a result of increasing calcination temperatures. The values of b* are increasing in negative direction, this mean that the higher intensity of blue color. The decreasing in L* parameter tends to reduce the lightness of sample. In the same time, the increasing of the amount of cobalt percent reveals the increasing of defect in crystal structure of spinel. These defects lead to the distorted tetrahedral and octahedral sites in spinel structure, changing the ligand-field around the chromophore and hence changing the observed color [(103)].The value of b* increases as observed in Figure (19), leading to the depth of blue color as result of calcination temperatures. The lower value of hue variation ΔE tends to a good color matching. Diffuse reflectance data show the high value of b* and lower value of hue variation ΔE at 1200ºC for all doping cobalt percents as shown in Table (8). The color ceramic powder of

different doping with change the calcination temperatures shows in Figure (20). This means that the appearance of good pigment powder color and a good color matching at 1200ºC.

From Figures (21-23), we find that the color of powder for 0.01, 0.05 and 0.10 mole of cobalt systems is better in case of N, N-bis-(3-amino-propyl) oxalamide as fuel than the other fuel and urea systems is the less color. Oxalyl dihydrazide fuel gives good color than 3-methyl pyrozole-5-one (3MP5O) fuel for 0.01 mole of cobalt systems as shown in Figure (21). For 0.05 mole of cobalt systems, the color of pigment for oxalyl dihydrazide fuel system better than 3-methyl pyrozole-5-one (3MP5O) fuel except at 1100 ºC as shown in figure (22). In Figure (23), the color of pigment powder for 0.10 mole of cobalt system using oxalyl dihydrazide also is better than 3-methyl pyrozole-5-one (3MP5O) except at 1100 and 1200ºC.

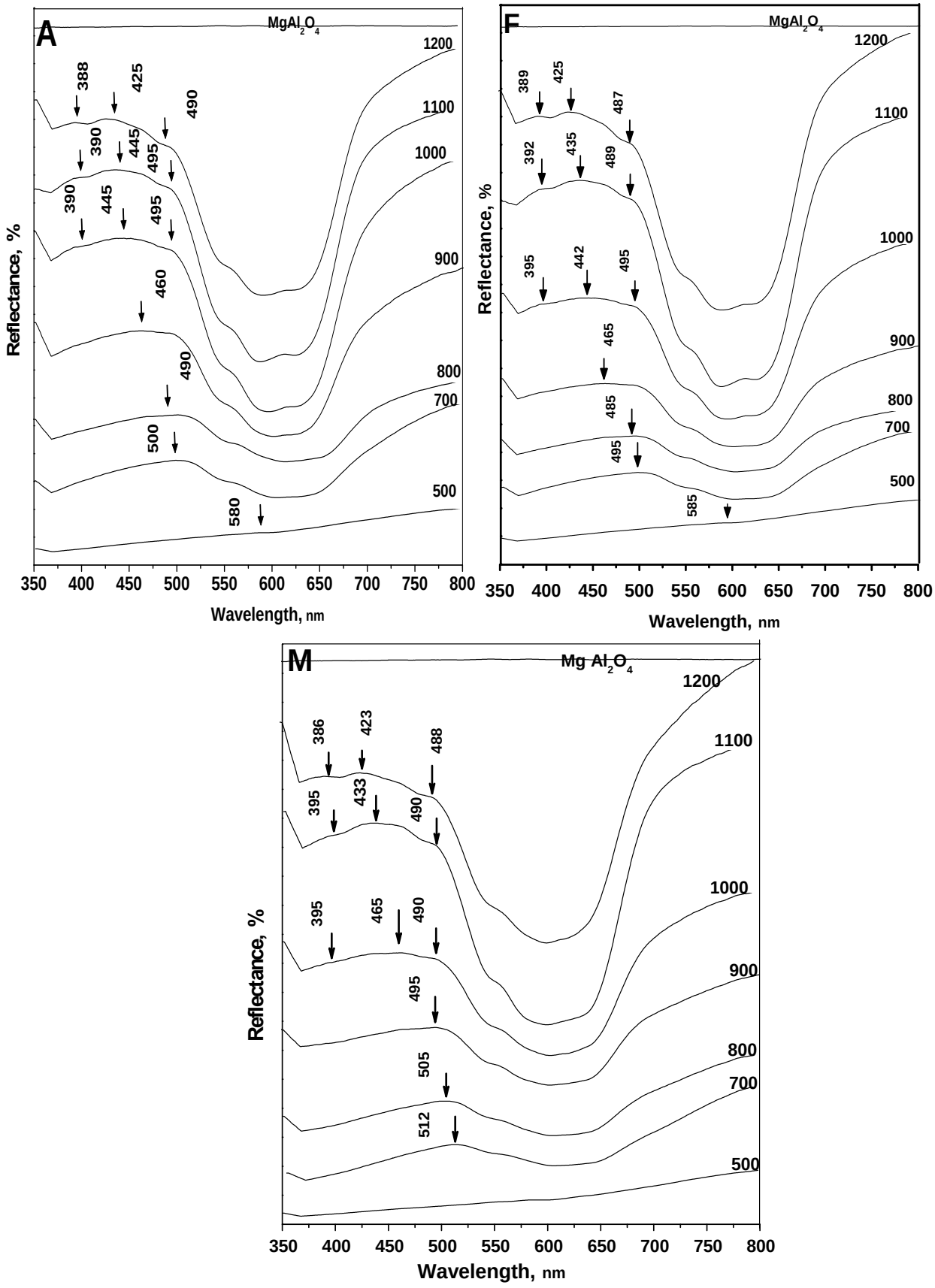
A
MgAl2O4
1200
1100
1000
900
800
700
500
388
425
490
390
445
495
460
500
580
Reflectance, %
Wavelength, nm
F
MgAl2O4
389
425
487
392
435
489
395
442
495
465
485
585
M
Mg Al2O4
386
423
488
433
505
512

Figure(15): Diffuse reflectance spectra for 0.01(A), 0.05 (F) and 0.10 (M) of Co^{2+} system at different calcination temperatures by using 3-methyl pyrozole-5-one as fuel.

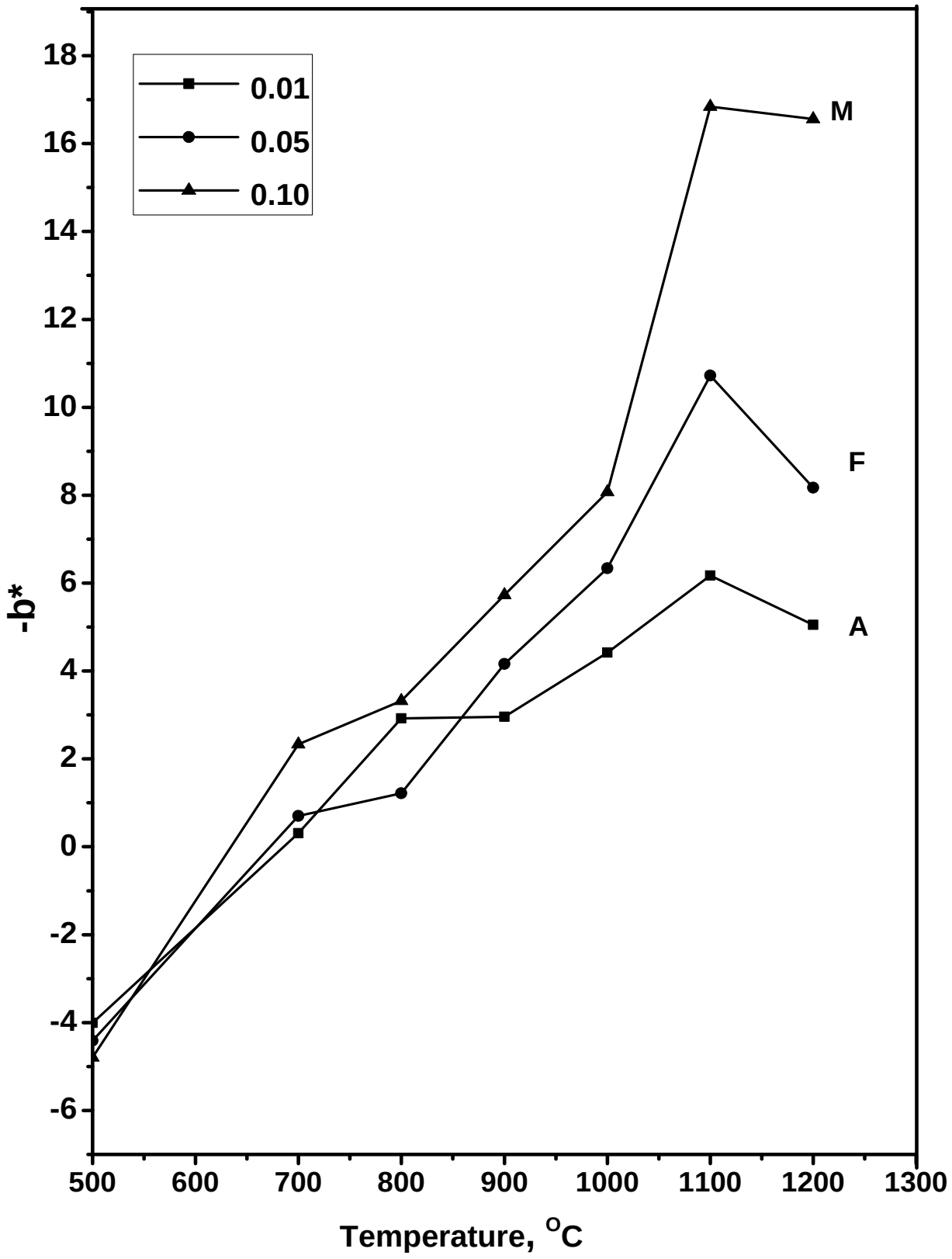

Figure(16): Colorimetric data for 0.01, 0.05 and 0.1 mole of Co^{2+} systems at different calcination temperatures by using 3-methyl pyrozole-5-one as fuel.

system	Temperature	L*	a*	b*	ΔE
٠,٠١	٥٠٠	95.58	0.60	4.01	95.67
	٧٠٠	95.09	-0.84	-0.31	95.09
	٨٠٠	96.64	-1.49	-2.92	96.69
	٩٠٠	95.77	-1.30	-2.96	95.83
	١٠٠٠	95.50	-1.85	-4.42	95.62
	١١٠٠	95.02	-2.35	-6.17	95.18
	١٢٠٠	93.04	-1.86	-5.05	93.26
٠,٠٥	٥٠٠	94.70	1.18	4.41	94.81
	٧٠٠	93.29	-3.08	-0.70	93.34
	٨٠٠	95.19	-2.48	-1.22	95.23
	٩٠٠	93.65	-2.71	-4.16	93.78
	١٠٠٠	92.69	-2.18	-6.34	92.93
	١١٠٠	92.00	-2.56	-10.72	92.66
	١٢٠٠	91.77	-1.72	-8.17	92.15
٠,١٠	٥٠٠	94.11	1.02	4.79	91.9
	٧٠٠	93.06	-2.79	-2.33	92.34
	٨٠٠	95.39	-2.41	-3.32	94.94
	٩٠٠	95.24	-2.57	-5.73	93.36
	١٠٠٠	94.87	-2.52	-8.07	92.4
	١١٠٠	93.26	-4.01	-16.84	87.44

	١٢٠٠	92.29	-2.82	-16.56	86.1

Table(7): Colorimetric data for 0.01, 0.05 and 0.10 mole of Co^{2+} systems at different calcination temperatures using 3-methyl pyrozole-5-one as fuel.

Temperature, °C	٠,٠١ mole of Co^{2+}	٠,٠٥ mole of Co^{2+}	0 mole of ٠,١Co^{2+}
٥٠٠			
٧٠٠			
٨٠٠			
٩٠٠			
١٠٠٠			
١١٠٠٠			
١٢٠٠		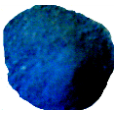	
Blank	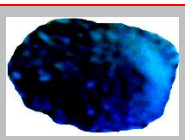 **$CoAl_2O_4$**		 **$MgAl_2O_4$**

Figure (17): The color of ceramic powder for 0.01, 0.05 and 0.010 mole of Co^{2+} systems using 3-methyl pyrozole-5-one as fuel at different calcination temperatures.

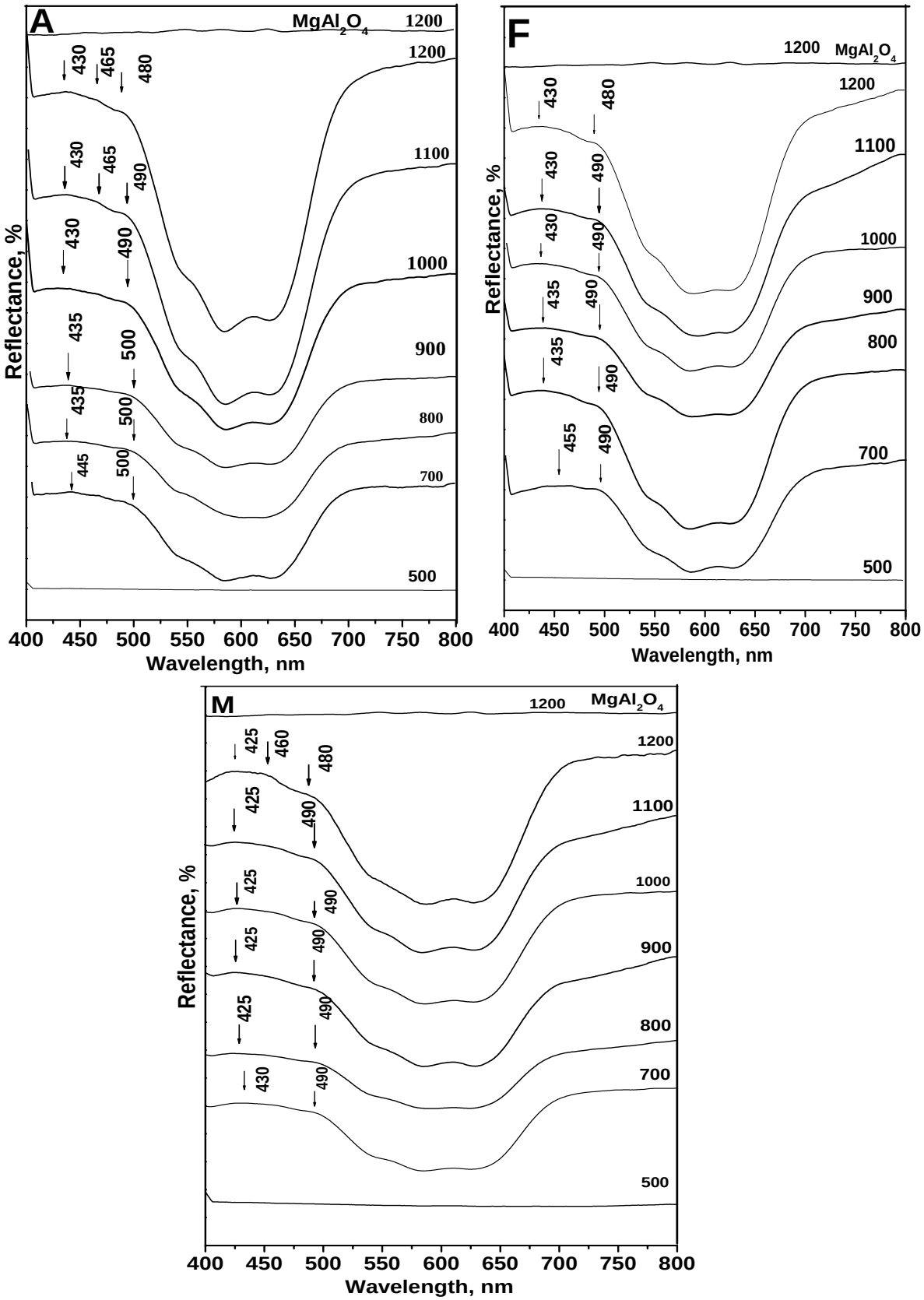
A
MgAl2O4
1200
1100
1000
900
800
700
500
430
465
480
490
435
500
445
Reflectance, %
Wavelength, nm
400 450 500 550 600 650 700 750 800
F
MgAl2O4
1200
1100
1000
900
800
700
500
430
480
490
435
455
Reflectance, %
Wavelength, nm
400 450 500 550 600 650 700 750 800
M
MgAl2O4
1200
1100
1000
900
800
700
500
425
460
480
490
430
Reflectance, %
Wavelength, nm
400 450 500 550 600 650 700 750 800

Figure(18): Diffuse reflectance spectra for 0.01 (A), 0.01 (F) and 0.01 (M) mole of Co^{2+} systems at different calcination temperatures by using N, N-bis-(3-amino-propyl) oxalamide as fuel.

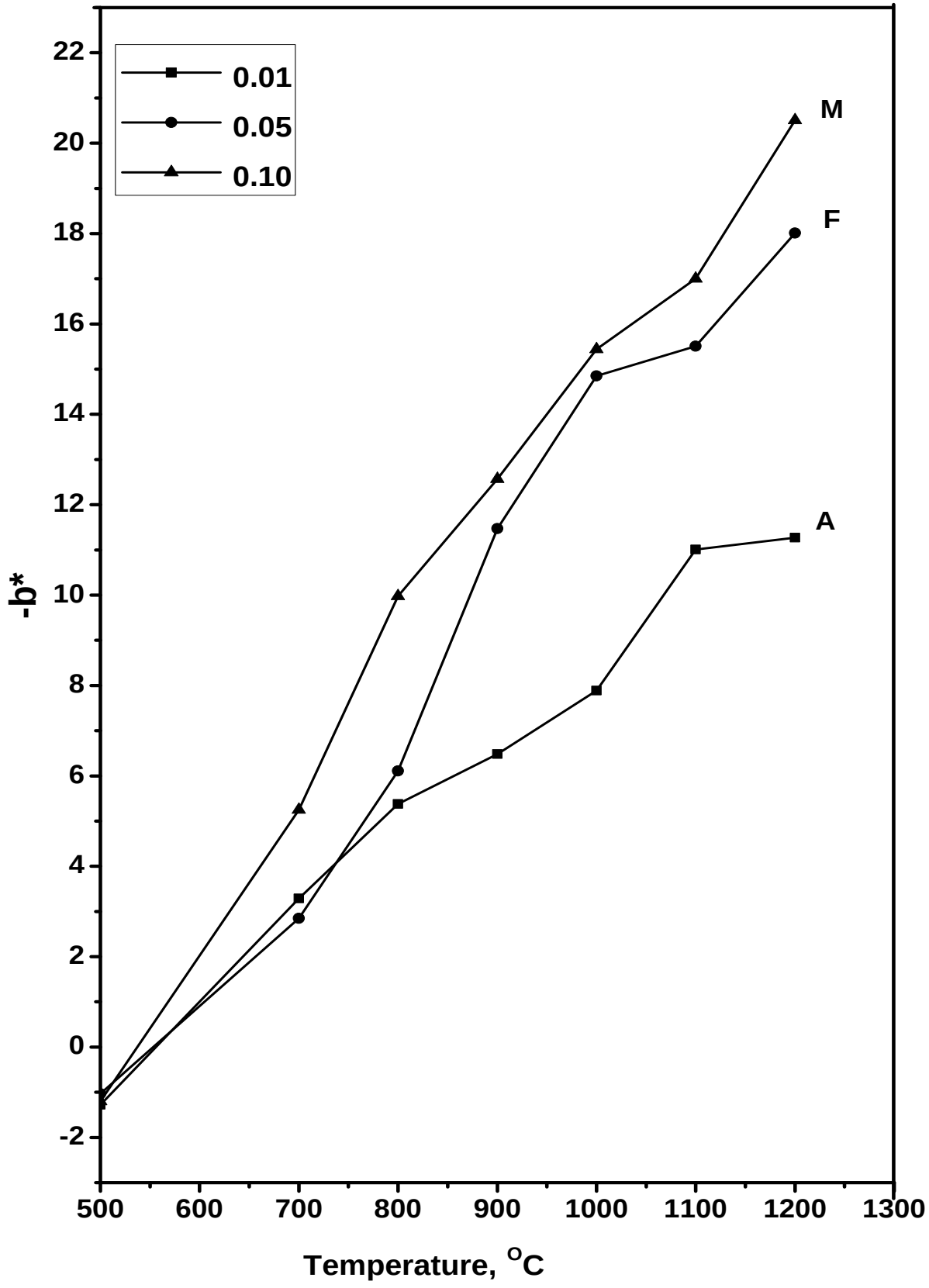

Figure(19): Colorimetric data for 0.01, 0.05 and 0.1 mole of Co^{2+} systems at different calcination temperatures by using N, N-bis-(3-amino-propyl) oxalamide as fuel.

Table (8): Colorimetric data for 0.01, 0.05 and 0.1 mole of Co^{2+} systems at different calcination temperatures using N, N-bis-(3-amino propyl) oxalamide as fuel.

system	Temperature	L*	a*	b*	ΔE
٠,٠١	٥٠٠	٩٠,٣٦	-٠,٦٣	١,٢٨	٩٠,٣٧
	٧٠٠	٩٧,٦٧	-٠,٧٧	-٣,٢٩	٩٧,٧٣
	٨٠٠	٩٦,٠٧	-١,٦٩	-٥,٣٨	٩٦,٢٤
	٩٠٠	٩٥,٢	-١,٥	-٦,٤٨	٩٥,٤٣
	١٠٠٠	٩٣,٩٨	-١,٨٢	-٧,٨٩	٩٤,٣٣
	١١٠٠	٩١,٣٣	-٢,٧	-١١,٠١	٩٢,٠٣
	١٢٠٠	٩٠,٧٥	-٢,٨١	-١١,٢٧	٩١,٥٠
٠,٠٥	٥٠٠	٨٩,٤٦	-٠,١٠	١,٠٣	٨٩,٤٧
	٧٠٠	٩٣,٦٥	-٠,٩٥	-٢,٨٥	٩٣,٧٠
	٨٠٠	٩٢,٤٥	-١,٧٣	-٦,١١	٩٢,٦٧
	٩٠٠	٩١,١٧	-٢,٢٤	-١١,٤٧	٩١,٩٢
	١٠٠٠	٨٦,٨٧	-٢,٩٦	-١٤,٨٥	٨٨,١٨
	١١٠٠	٨٤,٤٨	-٣,٤٨	-١٥,٥١	٨٥,٩٦
	١٢٠٠	٨٣,٥٧	-٣,٦٣	-١٨,٠١	٨٥,٥٧
٠,١٠	٥٠٠	٨٧,٠٤	-٠,٠٧	١,٢٠	٨٧,٠٥
	٧٠٠	٩٢,٩٩	-٣,٢٦	-٥,٢٥	٩٣,٢٠
	٨٠٠	٨٩,٦٨	-٥,٩٥	-٩,٩٨	٩٠,٤٣
	٩٠٠	٨٩,٠٩	-٧,٦٧	-١٢,٥٧	٩٠,٣٠
	١٠٠٠	٨٦,٦٥	-١٠,٠٦	-١٥,٤٤	٨٨,٦٠
	١١٠٠	٨٥,٥٥	-١٠,٠٠	-١٧,٠٠	٨٧,٨٠
	١٢٠٠	٧٨,٩٦	-١١,٨٣	-٢٠,٥١	٨٢,٤٣

Temperature, °C	٠,٠١ mole of Co^{2+}	٠,٠٥ mole of Co^{2+}	٠,١٠ mole of Co^{2+}
٥٠٠			
٧٠٠		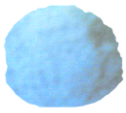	
٨٠٠	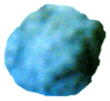	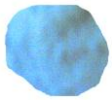	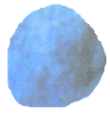
٩٠٠			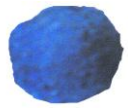
١٠٠٠	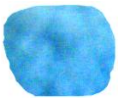	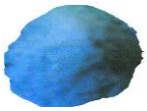	
١١٠٠٠			
١٢٠٠	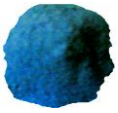		
Blank	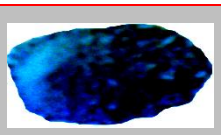 $CoAl_2O_4$		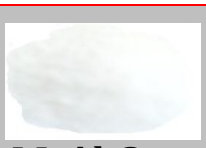 $MgAl_2O_4$

Figure(20): The color of ceramic powder for 0.01, 0.05 and 0.010 mole of Co^{2+} systems using N, N-bis-(3-amino-propyl) oxalamide as fuel at different calcination temperatures.

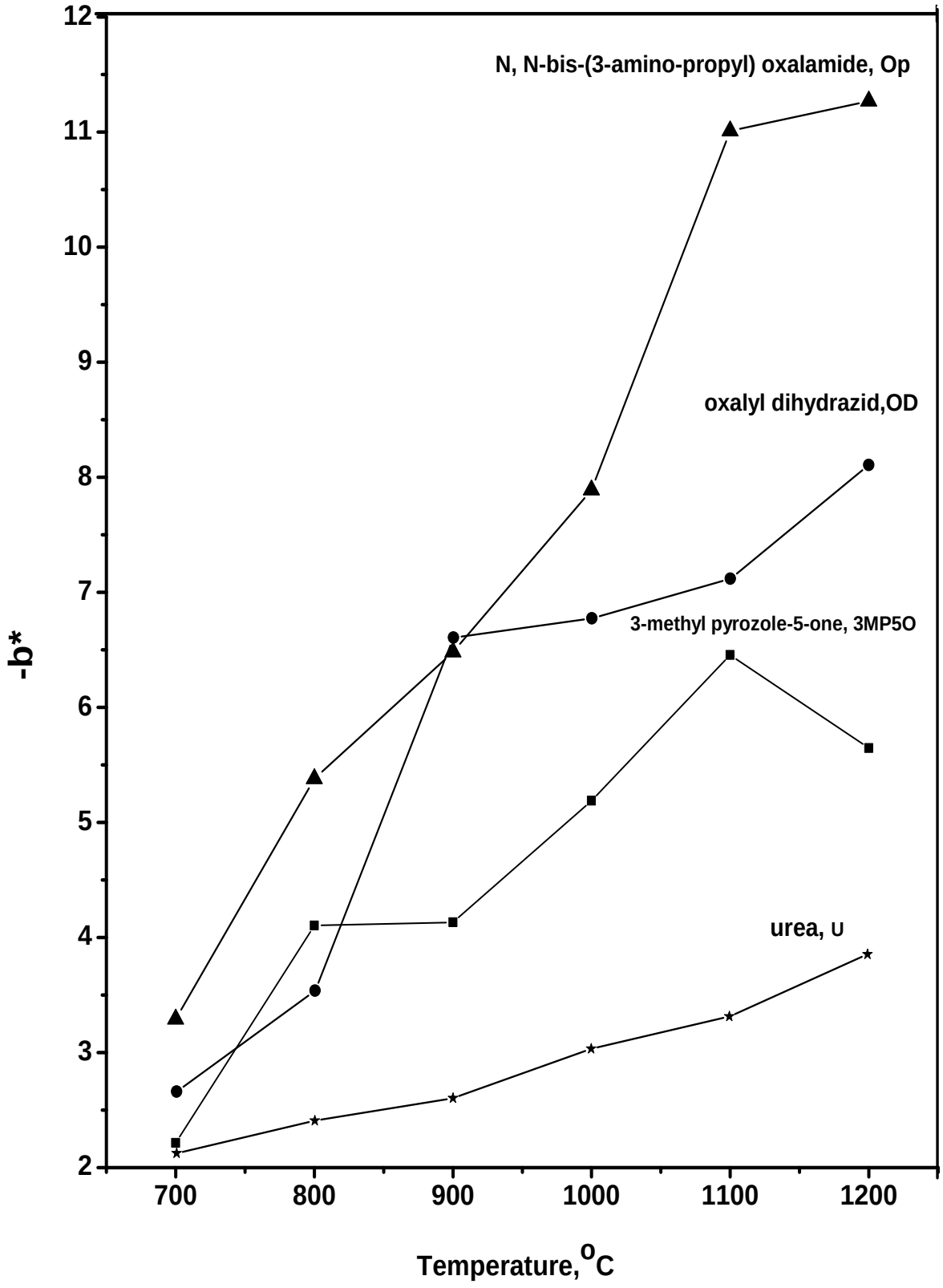

Figure(21): Colorimetric data for 0.01 mole of Co^{2+} system at different calcination temperatures by using different fuels.

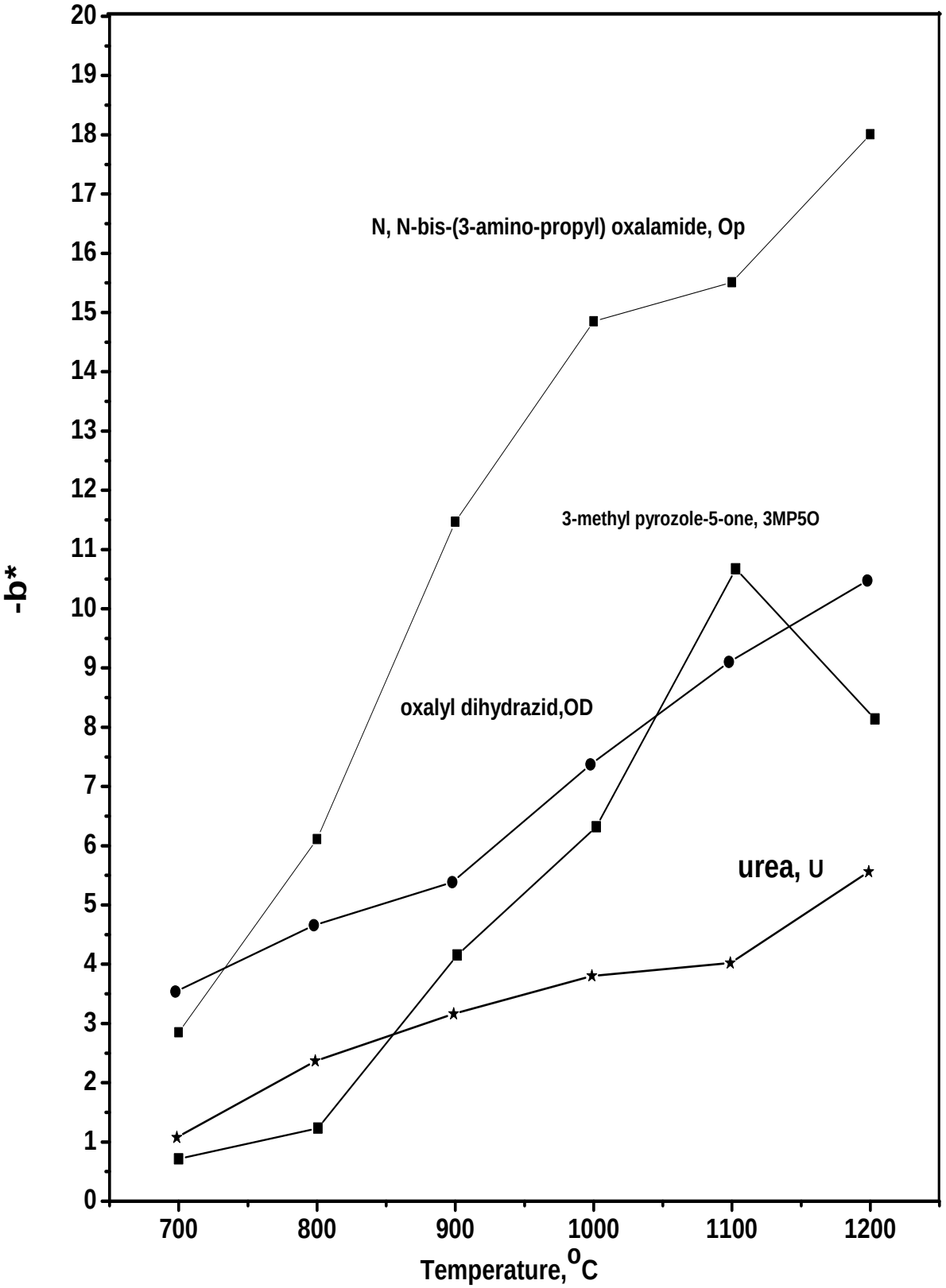

Figure(22): Colorimetric data for 0.05 mole of Co^{2+} system at different calcination temperatures by using different fuels.

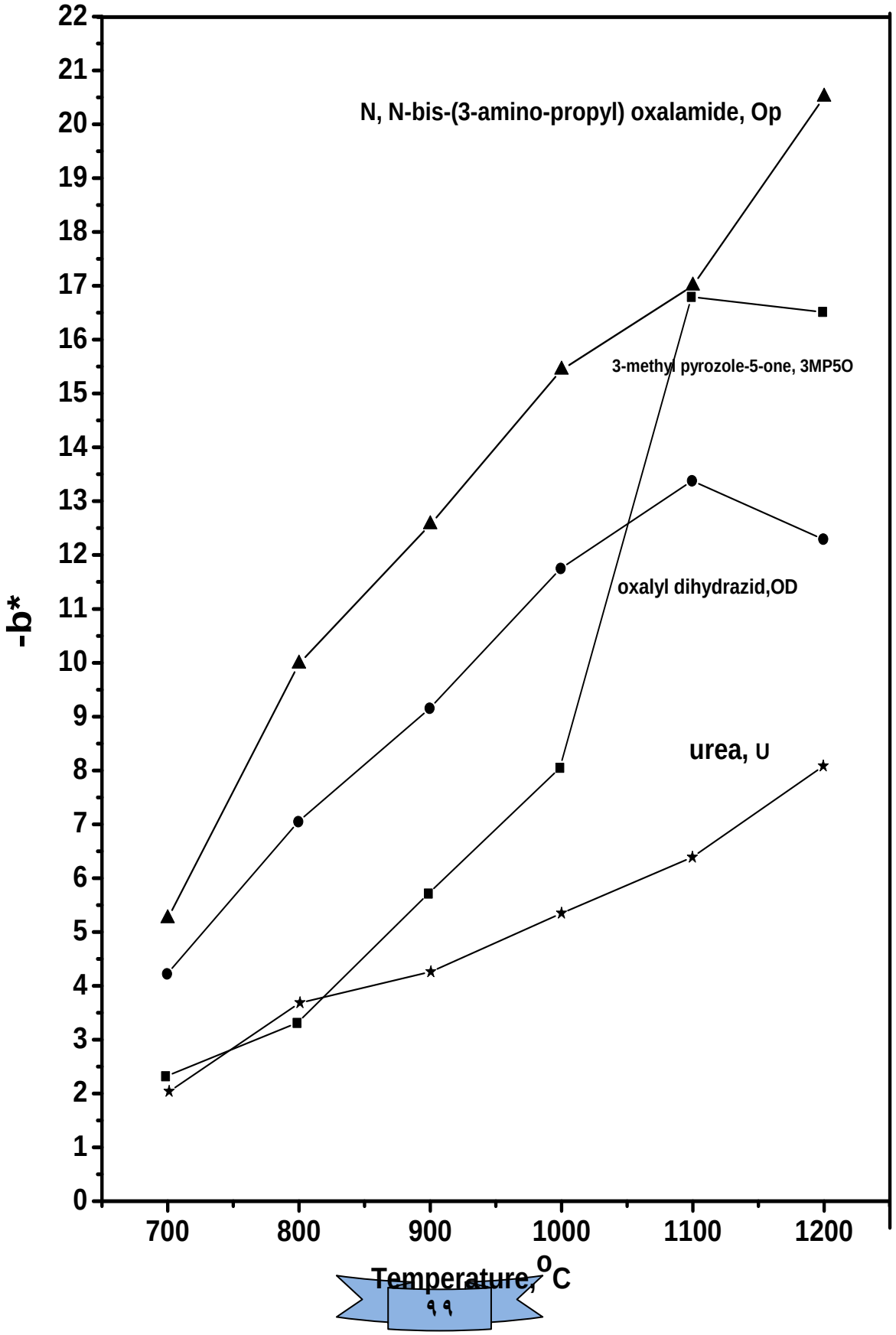

Figure(23): Colorimetric data for 0.10 mole of Co^{2+} system at different calcination temperatures by using different fuels.

3.1.3. The electronic spectra for cobalt systems in nujol mull using different fuels.

3.1.3.1. The electronic spectra for cobalt system using urea as fuels.

The electronic spectra of A, F and M systems of cobalt using urea as fuel show the present of broad band at 575 nm for A system, 600 nm for M system and no bands for F system at 500 ^{o}C. Absorption of these bands increase with calcination temperatures from 700-1200 ^{o}C. These bands become three broad absorption bands at 543 nm (green region), 582 nm (yellow-orange region) and 625nm (red region) for A system, 543nm, 587 nm and 628 nm for F system and 543 nm, 582 nm and 625 nm for M system at 1200^{o}C. All these bands indicate for tetrahedral co-ordination [104-106] of cobalt which gives rise to the blue coloration as present in Figure (24).

3.1.3.2. The electronic spectra for cobalt system using oxalyl dihydrazide as fuels.

The electronic spectra of A, F and M systems of cobalt using oxalyl dihydrazide as fuel show the present of broad band at 600 nm for M system and no bands for F and A systems at 500 ^{o}C. The absorption of these bands increases with calcination temperatures from 700-1200 ^{o}C. These bands appear three broad absorption bands at 543 nm (green region), 588 nm (yellow-orange region) and 630 nm (red region) for A system, 543 nm, 588 nm and 625 nm for F system and 543 nm, 588 nm and 625 nm for M system

at 1200°C. These indicate the tetrahedral co-ordination [104-106] of cobalt which gives rise to the blue coloration as present in Figures (25).

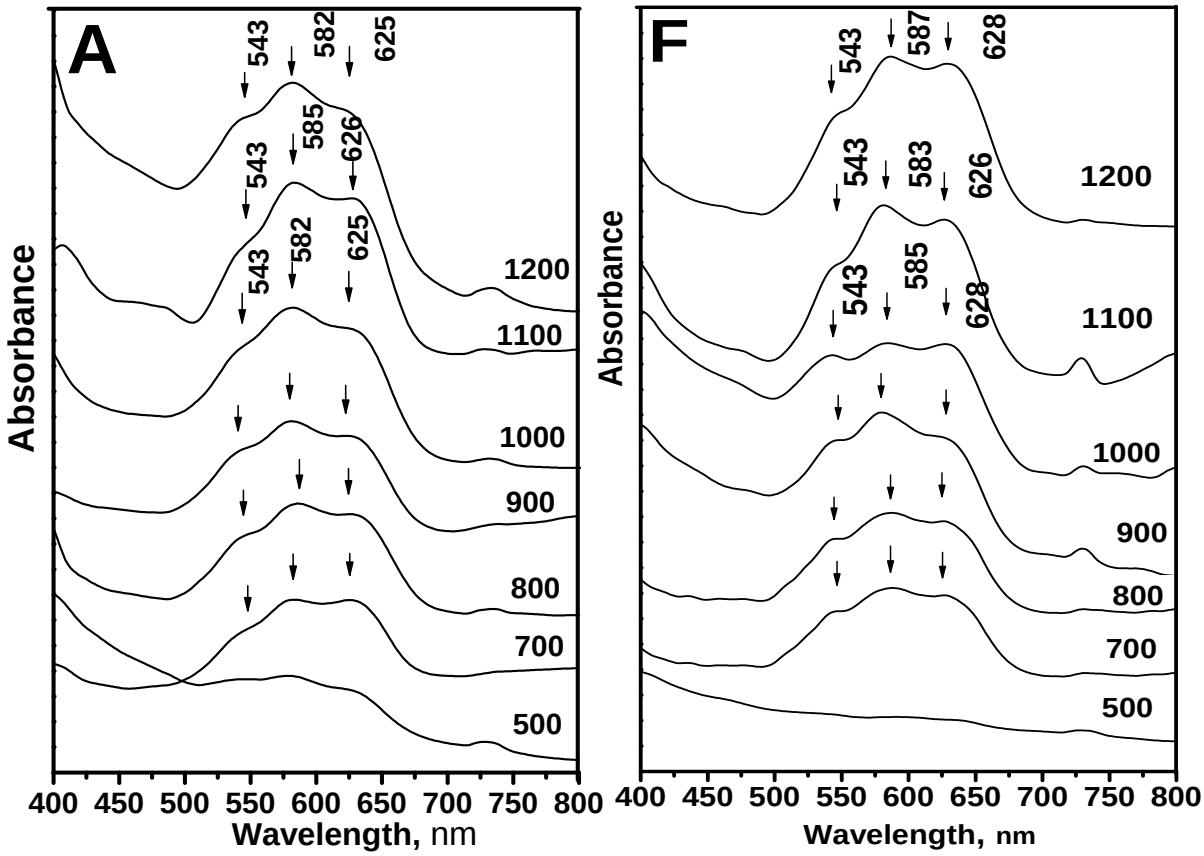

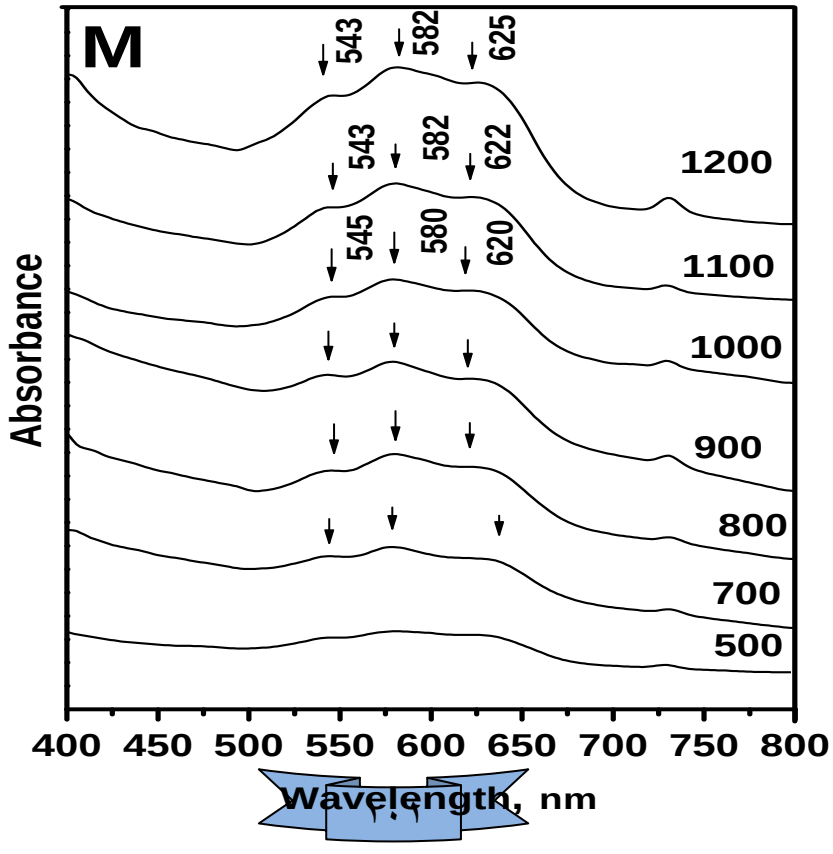

Figure(24): Electronic spectra for 0.01(A), 0.05 (F) and 0.10 (M) mole of Co^{2+} systems in nujol mull at different calcination temperatures using urea as fuel.

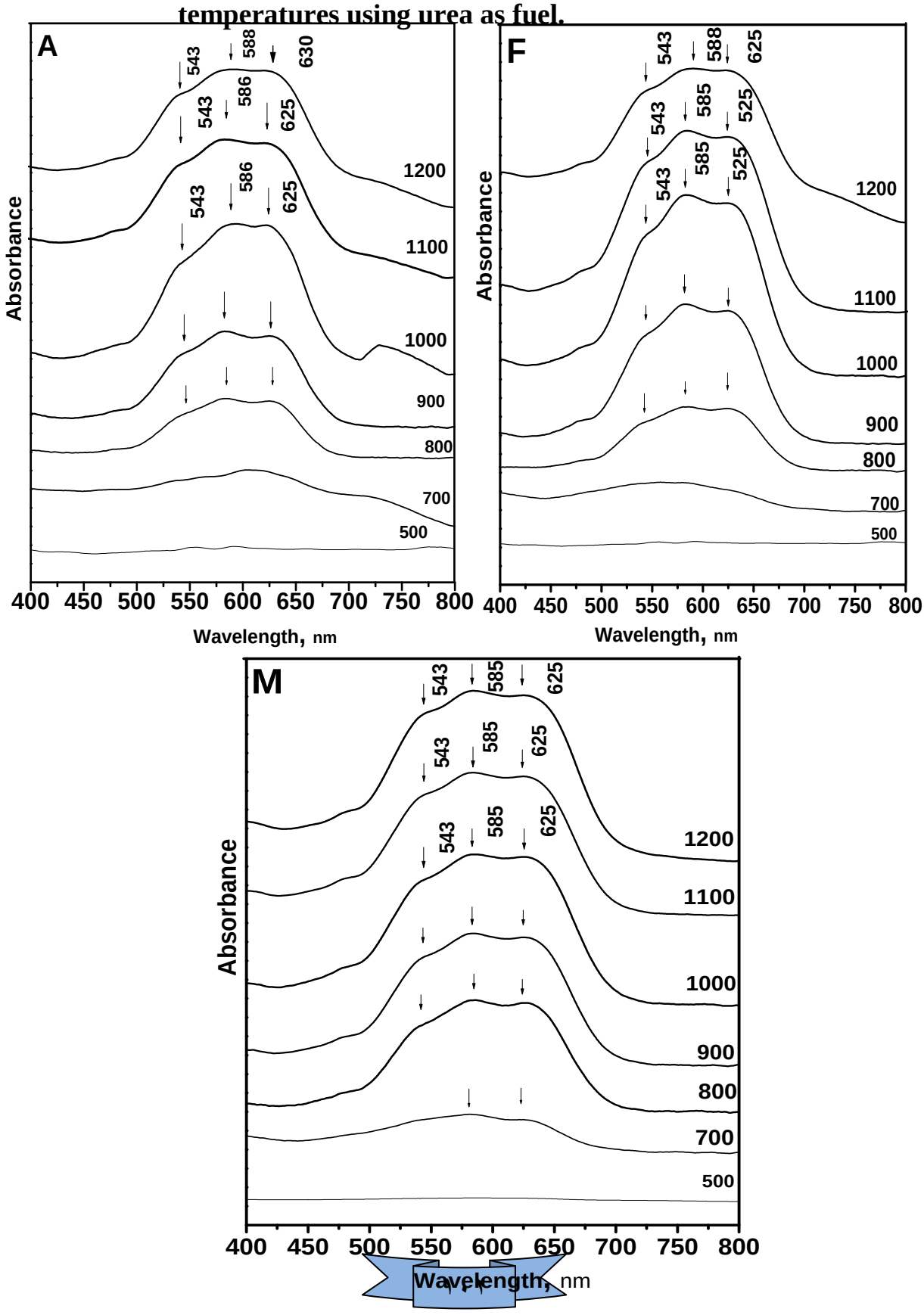

Figure(25): Electronic spectra for 0.01(A), 0.05 (F) and 0.10 (M) mole of Co^{2+} systems in nujol mull at different calcination temperatures using oxalyl dihydrazide as fuel.

3.1.3.3. The electronic spectra for cobalt system using 3-methyl pyrozole-5-one as fuels.

The electronic spectra of A, F and M systems of cobalt using 3-methyl pyrozole-5-one (3MP5O) as fuel show the present of broad band at 600 nm for F system and no bands for A and M systems at 500 °C. The appearance bands at 700 °C for A, F and M systems and the absorption of these bands increase with calcination temperatures from 700-1200 °C. These bands appear that three broad absorption bands at 543 nm (green region), 585 nm (yellow-orange region) and 622nm (red region) for A system, 543 nm, 585 nm and 624 nm for F system and 543 nm, 585 nm and 625 nm for M system at 1200°C. These mean the formation of tetrahedral [104-106] co-ordination of cobalt which gives rise to the blue coloration as present in Figures (26).

3.1.3.4. The electronic spectra for cobalt system using N, N-bis-(3-amino-propyl) oxalamide as fuels.

The electronic spectra of A, F and M systems of cobalt using N, N-bis-(3-amino-propyl) oxalamide as fuel show the present of broad band at 600 nm for A system and no bands for F and M systems at 500 °C. The present of bands at 700 °C for A, F and M systems and absorption of these bands increase with calcination temperatures from 700-1200 °C. The broad band with three absorption head appear at 543 nm (green region), 586 nm (yellow-orange region) and 625nm (red region) for A system, 543 nm, 586

nm and 530 nm for F system and 543 nm, 585 nm and 625 nm for M system at 1200°C. This means the formation of tetrahedral [104-106] co-ordination of cobalt leading to the blue coloration as present in Figure (27).

All four system, The energy level diagram gives d-d transitions of cobalt Co(II) ($3d^7$) from Orgel diagram shows the present of three transition states of $^4A_2(F) \rightarrow {}^4T_2(F)$, $^4A_2(F) \rightarrow {}^4T_1(F)$ and $^4A_2(F) \rightarrow {}^4T_1(P)$. The broad and intense absorption band between 500-700 nm could attributed to third transition from $^4A_2(F)(e^4t^3_2)$ as ground state to the excited $^4T_1(P)(e^3t^4_2)$ state. This triple band in visible region can be attributed to Jahn-Teller distortion of tetrahedral structure [107-108].

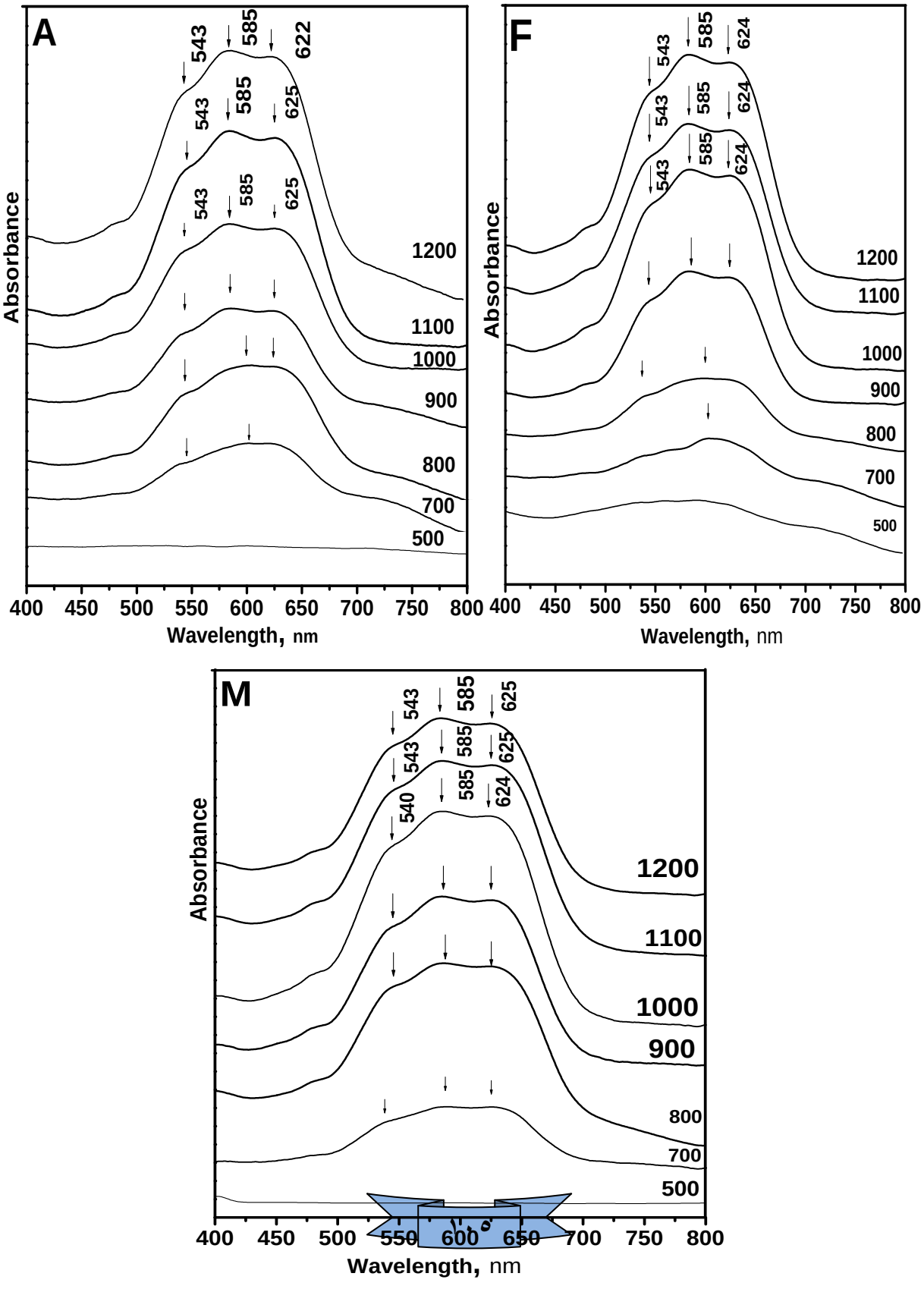
A
543
585
622
543
585
625
543
585
625
1200
1100
1000
900
800
700
500
Absorbance
400 450 500 550 600 650 700 750 800
Wavelength, nm
F
543
585
624
543
585
624
543
585
624
1200
1100
1000
900
800
700
500
Absorbance
400 450 500 550 600 650 700 750 800
Wavelength, nm
M
543
585
625
543
585
625
540
585
624
1200
1100
1000
900
800
700
500
Absorbance
400 450 500 550 600 650 700 750 800
Wavelength, nm

Figure(26): Electronic spectra for 0.01(A), 0.05 (F) and 0.10 (M) mole of Co^{2+} systems in nujol mull at different calcination temperatures using 3-methyl pyrozole-5-one as fuel.

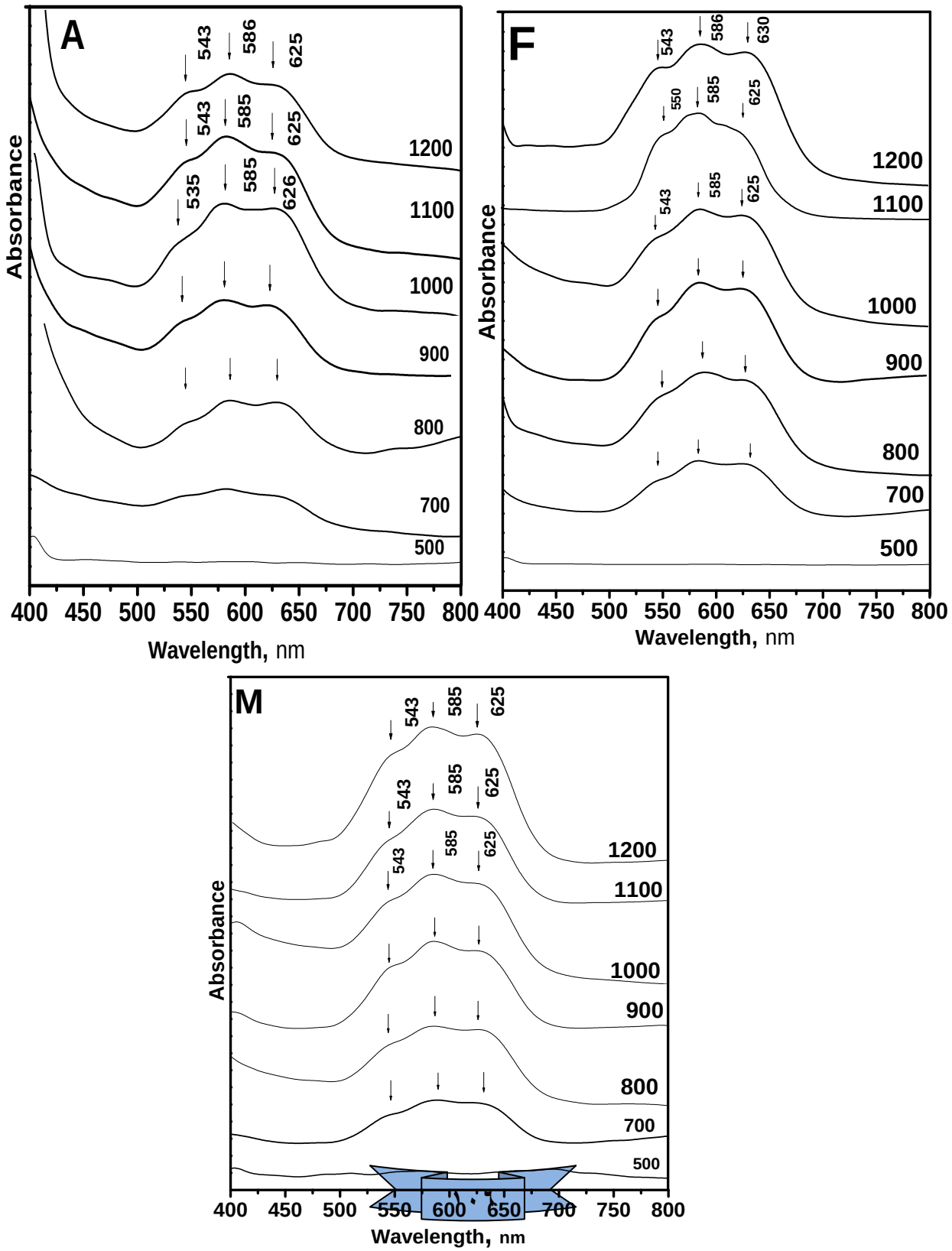

Figure(٢٧): Electronic spectra for 0.01(A), 0.05 (F) and 0.10 (M) mole of Co^{2+} systems in nujol mull at different calcination temperatures using N, N-bis-(3-amino-propyl) oxalamide as fuel.

3.2. The spectral characterization for $Ni_yMg_{1-y}Al_2O_4$ systems using different fuels.

3.2.1. Fourier Transform Infrared Spectra for $Ni_yMg_{1-y}Al_2O_4$ system using urea as fuel.

Infrared spectra (IR) for 0.10 (A), 0.50 (F), 0.80 (M) mole of nickel systems using urea as fuel are present in Figure (28). IR curves demonstrated that the samples at ignition temperature 500 °C contain a broad absorption band around 3500 cm^{-1} for A system, 3490 cm^{-1} for F system and 3450 cm^{-1} for M system are related to the stretching vibration of free (–OH) group of water molecules. The absorption bands in range 1650 -1050 cm^{-1} for A and F systems and1630 cm^{-1} for M system are related to the stretching vibration of carbonyl (C=O and C–O) groups of residual organic fuel [84]. The absorption bands at 1650, 1450 and 858 cm^{-1} for A and F systems and 1630, 1450 and 820 cm^{-1} for M system correspond to undecomposed nitrate ions. The absorption bands at 2950 for A and F systems and 2920 for M system related to C-H aliphatic in sample [85].

A weak absorption bands in range 400–700 cm^{-1} appearance due to the formation of trace amounts of metal oxides. After calcination at different temperatures from 500-1200 ◦C, the observed absorption bands in the range 800–4000 cm^{-1} are decreased gradually until disappeared at 1100 ◦C except, the strong absorption band at 3450 cm^{-1} for A and M systems and 3500 cm^{-1} for F system are related to the stretching vibration of adsorption water [109]

molecules. The three absorption bands 780,740 and 530 cm^{-1} for A system and 770,710 and 550 cm^{-1} for F and 760, 730 and 540 cm^{-1} for M systems are corresponding to AlO_4/AlO_6 groups building up the magnesium spinel as a result of vibration of ions of valence Al^{3+} in tetrahedral and octahedral positions compared with 700, 530 and 425 cm^{-1} for $MgAl_2O_4$ spinel. Other broad [87-89] bands at 700, 535 and 425 cm^{-1} for A system, 710, 550 and 425cm^{-1} for F system and 760, 730 and 425 for M system are corresponding to NiO_6/NiO_4 and MgO_6/MgO_4 groups for the Nickel and magnesium spinel as a result of vibration in the octahedral sites or to mixed vibration of them in octahedral and tetrahedral sites [110-111] compared with 760-720-520 cm^{-1} for $NiAl_2O_4$ spinel as present in Figure (29).The weak absorption band at 610 cm^{-1} that characterize for $NiAl_2O_4$ structure [112]. Assignment of an important bands in the IR spectra for 0.10, 0.50 and 0.80 mole of Ni^{2+} systems at different calcination temperatures using urea as fuel are given in Table (9).

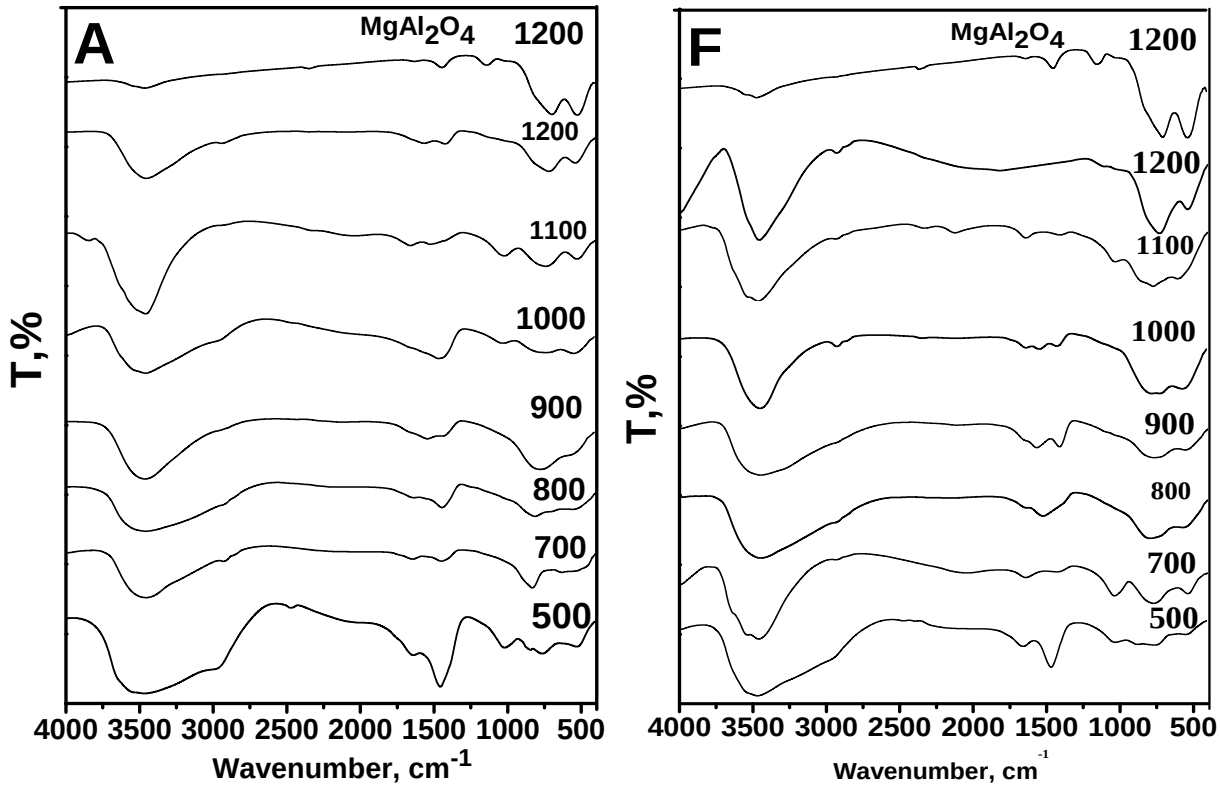
A
MgAl2O4
1200
1200
1100
1000
900
800
700
500
T,%
4000 3500 3000 2500 2000 1500 1000 500
Wavenumber, cm-1
F
MgAl2O4
1200
1200
1100
1000
900
800
700
500
T,%
4000 3500 3000 2500 2000 1500 1000 500
Wavenumber, cm-1

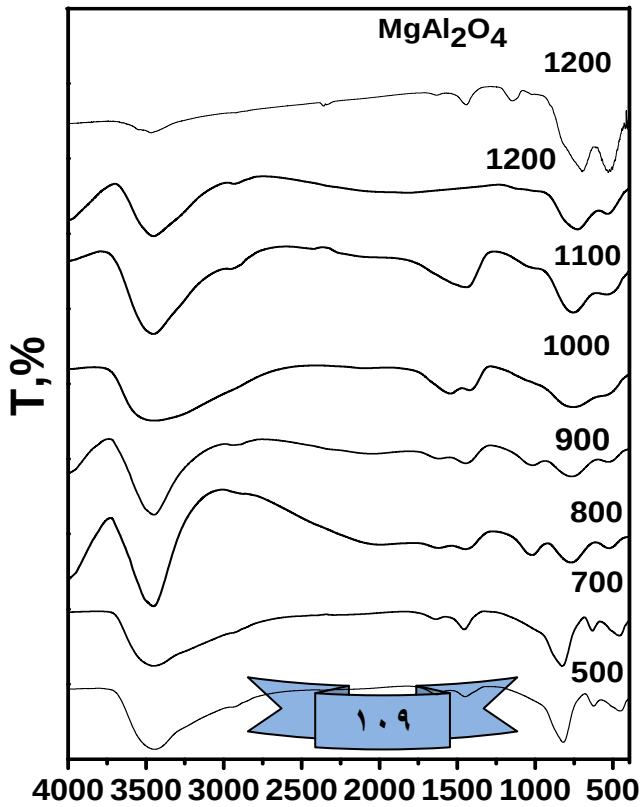
MgAl2O4
1200
1200
1100
1000
900
800
700
500
T,%
4000 3500 3000 2500 2000 1500 1000 500

Figure (28): Infrared spectra for $Ni_{0.1}Mg_{0.9}Al_2O_4$ (A), $Ni_{0.5}Mg_{0.5}Al_2O_4$ (F) and $Ni_{0.8}Mg_{0.2}Al_2O_4$ (M) systems using urea as fuel at different calcination temperatures.

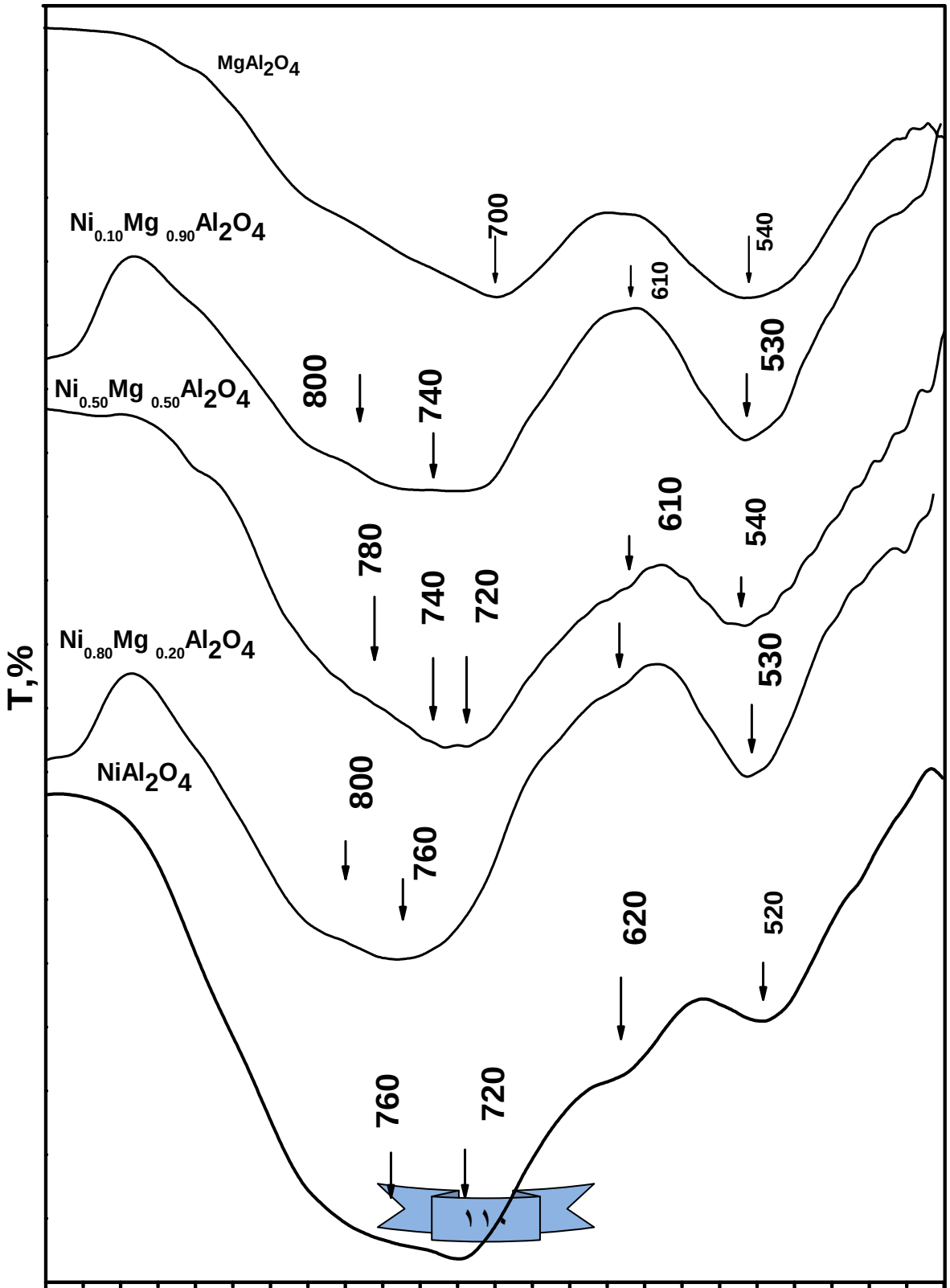

Temperature, °C	system 0.01 mole of Ni^{2+}

Figure (29): Infrared spectra for 0.10, 0.50, 0.80 mole of Ni^{2+} systems, $NiAl_2O_4$ and $MgAl_2O_4$ by using urea as fuel in rang 400-1000 cm^{-1}

	υ -OH	υ-CH	υ C=O	υC-O	υC-N	υ N=O	υ M-O
٥٠٠	٣5٠٠	٢٩5٠	١٦٥٠	١05٠	1450	٨٥٨	700,٥٣٠
٧٠٠	٣٤5٠	2920	1650	-	١٤٥٠	٨٥٠	800,50٠
٨٠٠	٣٤٥٠	-	١٦٥٠	-	١٤٥٠	-	٨٠٠,٥٢٠
٩٠٠	٣٤٥٠	-	1650	-	-	-	7٤٠,610, ٥٣٠
١٠٠٠	٣٤5٠	-	-	-	-	-	740,600,٥٣٠
١١٠٠	٣٤50	-	-	-	-	-	770,740,620,530,425
١٢٠٠	٣٤٥0	-	-	-	-	-	770,740,620,530,425
	0.05 mole of Ni^{2+}						
٥٠٠	٣49٠	٢٩٥٠	١٦٥٠	١05٠	١٤٥٠	٨٥8	٧٥٠,٦٠٠
٧٠٠	٣٤٥٠	-	١٦٥٠	١٠٥٠	١٤9٠	-	750,٥2٠
٨٠٠	٣٤٥٠	-	١٦٥٠	-	١٤٥٠	-	760,٥٣٠
٩٠٠	٣٤٥٠	-	-	-	-	-	750,٥٣٠
١٠٠٠	٣٤٥٠	-	-	-	-	-	770,740,620,530
١١٠٠	٣٤٥٠	-	-	-	-	-	770,740,620,530,425
١٢٠٠	٣٥٠٠	-	-	-	-	-	770,740,620,530,425
	0.80 mole of Ni^{2+}						
٥٠٠	٣45٠	٢٩٢٠	١٦٣٠	-	١٤٥٠	٨2٠	٦٢٠,450
٧٠٠	٣٤٥٠	٢٩٢٠	١٦٥٠	-	١٤٥٠	٨٢٠	٦٢٠,450
٨٠٠	٣٤٥٠	-	١٦٥٠	١٠٥٠	١٤٥٠	-	760,٥٣٠
٩٠٠	٣٤٥٠	-	١٦٥٠	١٠٥٠	١٤٥٠	-	760,550
١٠٠٠	٣٤٥٠	-	-	-	-	-	760,٥٣٠,425
١١٠٠	٣٤٥٠	-	-	-	-	-	760,730, 530,425
١٢٠٠	٣٤٥٠	-	-	-	-	-	760,730, 530,425

Table (9): Assignment of the important bands in the IR spectra for 0.10, 0.50 and 0.80 mole of Ni^{2+} systems at different calcination temperatures using urea as fuel.

3.2.2. Fourier Transform Infrared Spectra for nickel system using 3-methyl pyrozole-5-one as fuel.

Infrared of spectra (IR) for 0.10 (A), 0.50 (F), 0.80 (M) mole of Ni^{2+} systems using 3-methyl pyrozole-5-one (3MP5O) as fuel are present in Figure (30). From this curves, we can be explain that the samples at ignition temperature 500 ◦C contain a broad absorption band around 3400 cm^{-1} for A and M systems and 3450 cm^{-1} for F system related to the stretching vibration of free (–OH) group of water molecules. The absorption bands at 1650, 1090 cm^{-1} for A system and 1637, 1050 cm^{-1} for F and M systems are related to the symmetrical and asymmetrical stretching vibration of carbonyl C=O and C–O groups of residual organic fuel [84]. The absorption bands at 1650, 1382 and 800 cm^{-1} for A system and 1637, 1050 and 800 cm^{-1} for F and M systems correspond to undecomposed nitrate ions [85].

The weak absorption bands in the range 400–700 cm^{-1} corresponding to the formation of trace amounts of metal oxides. After calcinations at different temperatures in range 500 to 1200 ◦C, the revealed absorption bands in the region 800–4000 cm^{-1} which are decreased gradually until disappeared at 1100 ◦C except, the strong absorption band at 3500 cm^{-1} for A system, 3490 cm^{-1} for F system and 3450 cm^{-1} for M system related to the stretching vibration of adsorption water [109] molecules. The absorption bands at high frequency 760,710 and 540cm^{-1} for A system, 760, 720 and 520 cm^{-1} for F system and 780, 730 and 535 cm^{-1} for M system are corresponding to AlO_4/AlO_6 groups building up the magnesium spinel as a result of vibration of ions of valence Al^{3+} in tetrahedral and octahedral positions [87-89]. These bands compared with 700, 530 and 425 cm^{-1} for $MgAl_2O_4$ spinel as blank system. Three other bands at 710, 535 and 425 cm^{-1} for A system, 740, 520 and 420

cm^{-1} for F system and 730, 530 and 425 cm^{-1} for M system are corresponding to NiO_6/NiO_4 and MgO_6/MgO_4 groups for the nickel and magnesium spinel as a result of vibration in the octahedral sites or to mixed vibration of them in octahedral and tetrahedral sites [110-111]. These bands compared with 760,720 and 525 cm^{-1} for $NiAl_2O_4$ spinel as present in Figure (31). Assignment of the important bands in the IR spectra for 0.10, 0.50 and 0.80 mole of Ni^{2+} at different calcinations temperatures using urea as fuel are given in Table (10).

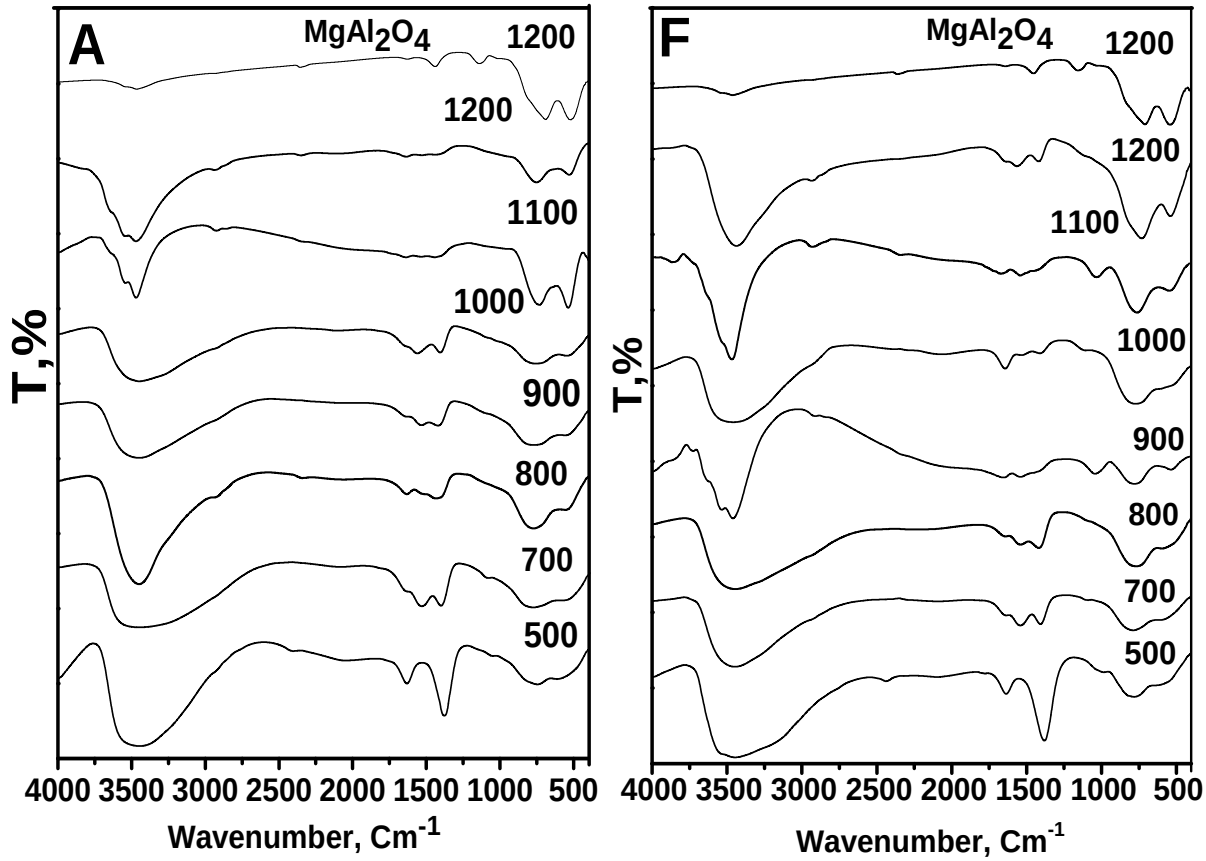
A
MgAl2O4
1200
1200
1100
1000
900
800
700
500
T,%
4000 3500 3000 2500 2000 1500 1000 500
Wavenumber, Cm-1
F
MgAl2O4
1200
1200
1100
1000
900
800
700
500
T,%
4000 3500 3000 2500 2000 1500 1000 500
Wavenumber, Cm-1

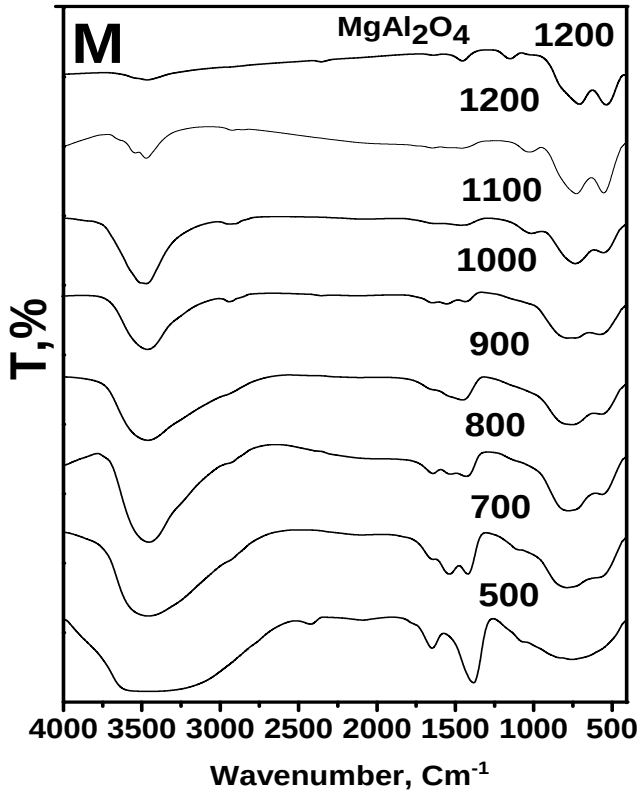
M
MgAl2O4
1200
1200
1100
1000
900
800
700
500
T,%
4000 3500 3000 2500 2000 1500 1000 500
Wavenumber, Cm-1

Figure (30): Infrared spectra for $Ni_{0.1}Mg_{0.9}Al_2O_4$ (A), $Ni_{0.5}Mg_{0.5}Al_2O_4$ (F) and $Ni_{0.8}Mg_{0.2}Al_2O_4$ systems using 3-methyl pyrozole-5-one as fuel at different calcination temperatures.

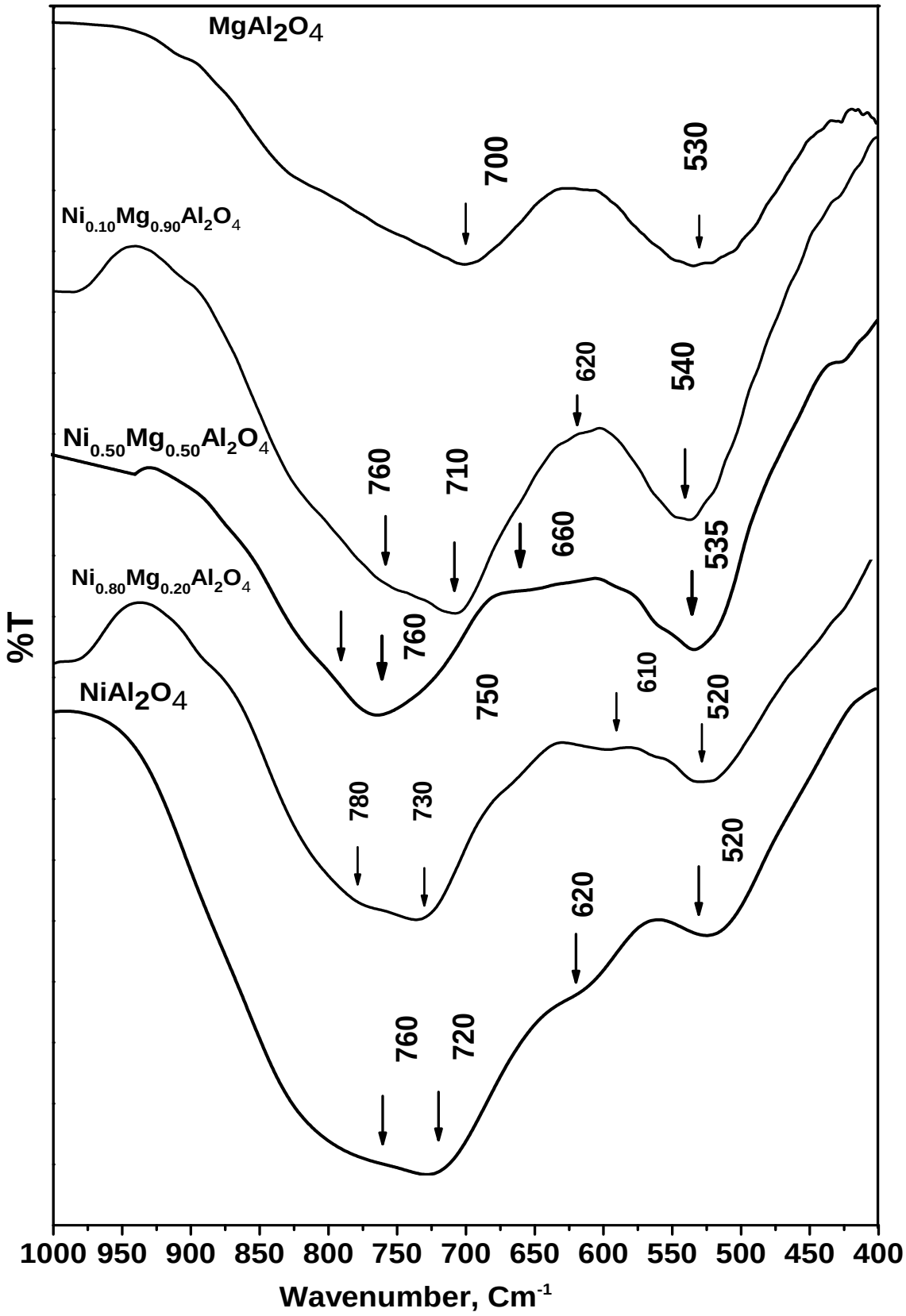

Figure (31): Infrared spectra for 0.1, 0.5, 0.80 mole of Ni^{2+} systems, $NiAl_2O_4$ and $MgAl_2O_4$ by using 3-methyl pyrozole-5-one as fuel in rang 400-1000 cm^{-1} .

Temperature, °C	system 0.10 mole of Ni^{2+}						
	υ -OH	υ-CH	υ C=O	υC-O	υC-N	υ N=O	υ M-O
٥٠٠	٣4٠٠	-	١٦٥٠	١09٠	1382	٨00	700,٥٣٠
٧٠٠	٣٤5٠	-	1650	-	١٤٥٠	-	800,50٠
٨٠٠	٣٤٥٠	-	١٦٥٠	-	١٤٥٠	-	٨٠٠,٥٢٠
٩٠٠	٣٤٥٠	-	1650	-	-	-	7٤٠,610, ٥٣٠
١٠٠٠	٣٤5٠	-	-	-	-	-	740,600,٥٣٠
١١٠٠	٣٤50	-	-	-	-	-	760,710,620,540,425
١٢٠٠	٣٥٠٠	-	-	-	-	-	760,710,620,540,425
	0.50 mole of Ni^{2+}						
٥٠٠	٣45٠	-	١٦37	١0٥٠	١٤٥٠	٨00	٧60,٦٠٠
٧٠٠	٣٤٥٠	-	١٦٥٠	-	١٤٩٠	-	760,٥2٠
٨٠٠	٣٤٥٠	-	١٦٥٠	-	١٤٥٠	-	760,٥٣٠
٩٠٠	٣٤٥٠	-	1650	-	-	-	760,٥٣٠
١٠٠٠	٣٤٥٠	-	-	-	-	-	770,740,660,530
١١٠٠	٣٤٥٠	-	-	-	-	-	770,740,660,535,425
١٢٠٠	٣٤٩٠	-	-	-	-	-	760,720,660,535,425
	0.80 mole of Ni^{2+}						
٥٠٠	٣45٠	-	١٦٣٠	١٠٥٠	١٤٥٠	٨2٠	750
٧٠٠	٣٤0٠	-	١٦٥٠	١٠٥٠	١٤٥٠	٨٢٠	٧٦٠,500
٨٠٠	٣٤٥٠	-	١٦٥٠	-	١٤٥٠	-	760,٥٢٠
٩٠٠	٣٤٥٠	-	١٦٥٠	-	١٤٥٠	-	760,530
١٠٠٠	٣٤٥٠	-	-	-	-	-	760,٥٣٠,425
١١٠٠	٣٤٥٠	-	-	-	-	-	780,730, 520,425
١٢٠٠	٣٤٥٠	-	-	-	-	-	780,730, 530,425

Table (١٠): Assignment of the important bands in the IR spectra for 0.10, 0.50 and 0.80 mole of Ni^{2+} systems at different calcination temperatures using3-methyl pyrozole-5-one as fuel.

3.2.2. The diffuse reflectance spectra for $Ni_yMg_{1-y}Al_2O_4$ systems using urea as fuel.

3.2.2.1. Diffuse reflectance spectra of nickel system using urea as fuel

Diffuse reflectance spectra for (A) 0.10, (F) 0.50 and (M) 0.80 mole of Ni^{2+} systems by using urea as fuel are given in Figure (32). These systems show the appearance of band around 612,500 and 460 nm for A system, 618, 500 and 445 nm for F system and 618, 500 and 450 nm for M system at 700º C. These bands are corresponds to pale green-blue (cyan) color of sample under investigation. The bands shift to cyan band as calcination temperatures increase until reaching around 612, 570, 500, 505 and 460 nm for A system, 618, 560, 505 and 445 nm for F system and 618, 568, 505 and 450 nm for M system at 1000ºC for green-blue (cyan) color. These bands increase its shift to 460, 505 and 612 for A system, 445, 510 and 610 nm for F system and 450, 505, 560 and 606 nm for M system at 1200ºC [110-111] which show the good green-blue (cyan) color pigment.

From colorimetric data present in Table (11), the values of b* and a* increase in the negative direction while L* values decrease as result of increasing calcination temperatures. The increasing in negative values of a*, means the higher intensity of green color and the increasing values of b* in negative direction indicate for the appearance of blue color as shown in Figures (33-34). The increasing of a* in negative direction is more than the increasing values of b* in negative direction. This means the present of two

mixed color green and blue that the green is more than blue color intensity. The decreasing in L* parameter corresponds to reduce the lightness of sample. The values of a* and b* increase in negative direction with the depth of green-blue color as result of calcination temperatures and the increasing of the amount of nickel ions. The lower value of hue variation ΔE tends to a good color matching [102]. Colorimetric data show the high value of a* and b* and lower value of hue variation ΔE at 1200ºC for all doping nickel percents as show in Table (11). This means that the appearance of good pigment powder color and a good color matching occur at 1200ºC.The color of different doping with change temperature shown in Figure (35).

3.2.2.2. Diffuse reflectance spectra of nickel system using 3-methyl pyrozole-5-one as fuel

Diffuse reflectance spectra of A, F and M doping Ni^{2+} systems using 3-methyl pyrozole-5-one (3MP5O) as fuel shown in Figure (36). The appearance of bands in range 618, 500 and 450 nm for A system, 612, 506 and 440 nm for F system and 500 nm for M system at 700º C which are produced the pale green-blue (cyan) color of sample. These bands shift to cyan band as calcination temperatures increase until reaching around 612, 560, 505 and 455 nm for A system, 612, 562, 506 and 468 nm for F system and 618, 560, 505 and 468 nm at 1000ºC for green-blue (cyan) color. These bands show more shift to 612, 560, 505 and 455 nm for A system, 612, 562, 506 and 468 nm for F system and 618, 560, 505 and 468 nm for M system at 1200ºC [110-111], where the sample show the good green-blue (cyan) color pigment.

From colorimetric data present in Table (11) the values of b* and a* values increase in negative direction while L* values decrease as result of the increasing of calcinations temperatures. The increasing of a* in negative direction is more than the increasing values of b* in negative direction. This

means that the present of two mixed color of green and blue. The decreasing in L* parameter tends to reduce the lightness of sample. In the same time, the increasing of amount of nickel percent, the value of a* and b* increases as shown in Figures (37-38), leading to the depth of green-blue (cyan) color as result of calcinations temperatures. The l ower value of hue variation ΔE tends to a good color matching [102]. Colorimetric data show high value of a* and b* and lower value of hue variation ΔE at 1200ºC for 0.10 and 0.80 mole of nickel as shown in Table (12). This means the appearance of good pigment powder color and a good color matching occur at 1200ºC. Colorimetric data show high values of a* and b* at 1200 ºC for 0.50 mole nickel and a good color matching occur at 1100ºC. The color of different doping with change temperatures are shown in Figure (39). The doping of nickel is leading to the present of higher amount of defects in structure. These defects are due to distorted tetrahedral and octahedral sites in spinel structure, changing the ligand-field around the chromophore **[103]** and hence changing the observed color.

As comparison between two fuels, the values of a* for 0.10 mole system using urea as fuel are more than 3-methyl pyrozole-5-one except at 700^{o}C. Under 1000^{o}C, the values of b* for 0.10 mole system using 3-methyl pyrozole-5-one is more than urea as fuel and up to 1000^{o}C. This means the intensity of cyan color for 3-methyl pyrozole-5-one is higher than urea under 1000^{o}C. Up to this temperature, the intensity of cyan color using urea is more than 3-methyl pyrozole-5-one as shown in Figures (40-41).

For 0.50 mole system, the values of a* using urea as fuel is more than 3-methyl pyrozole-5-one up to 800^{o}C and b* values for the system using urea is more than 3-methyl pyrozole-5-one as fuel except at 700^{o}C. This means the

intensity of cyan color is higher for urea than 3-methyl pyrozole-5-one as fuel up to 800^{o}C as shown in Figures (42-43).

For 0.80 mole system, the values of a* using urea as fuel is more than 3-methyl pyrozole-5-one except 1200^{o}C and b* values for the system using urea is more than 3-methyl pyrozole-5-one as fuel. This means the intensity of cyan color is higher for urea than 3-methyl pyrozole-5-one as fuel except at 1200^{o}C as shown in Figures (44-45).

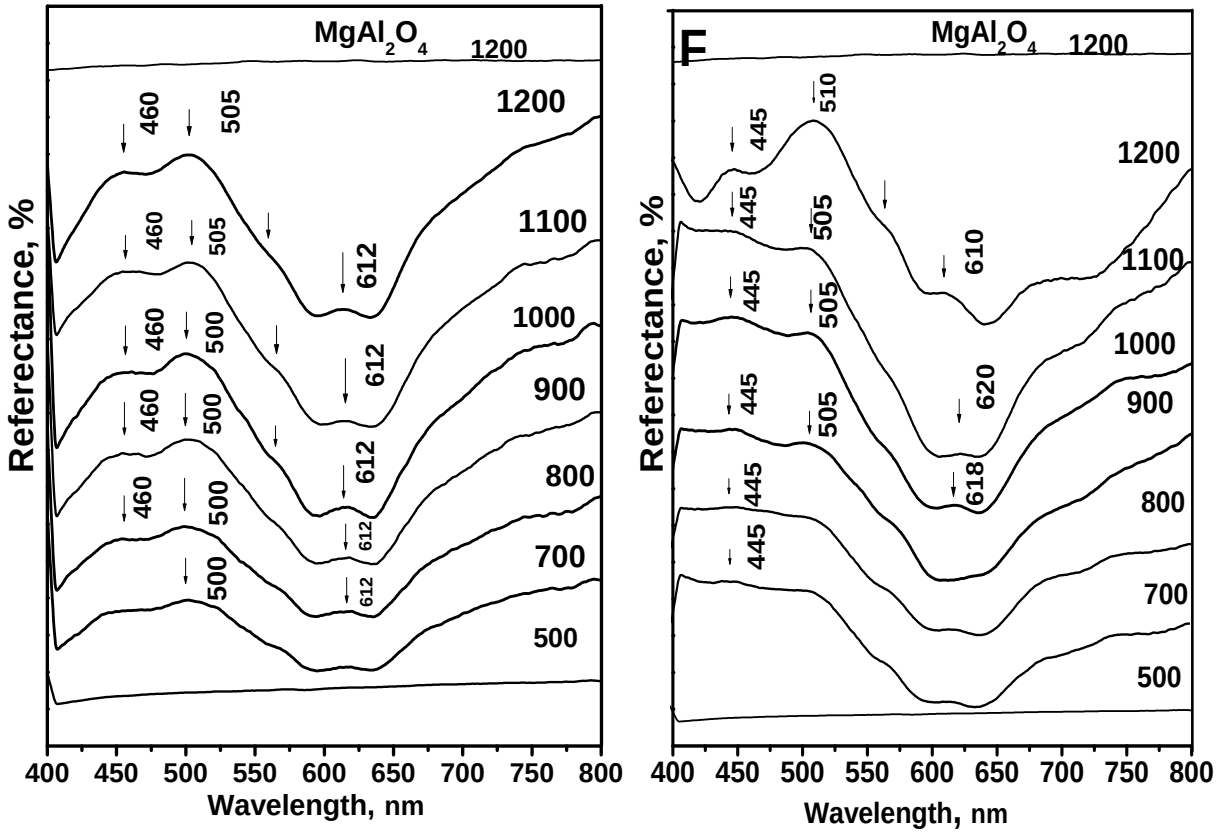

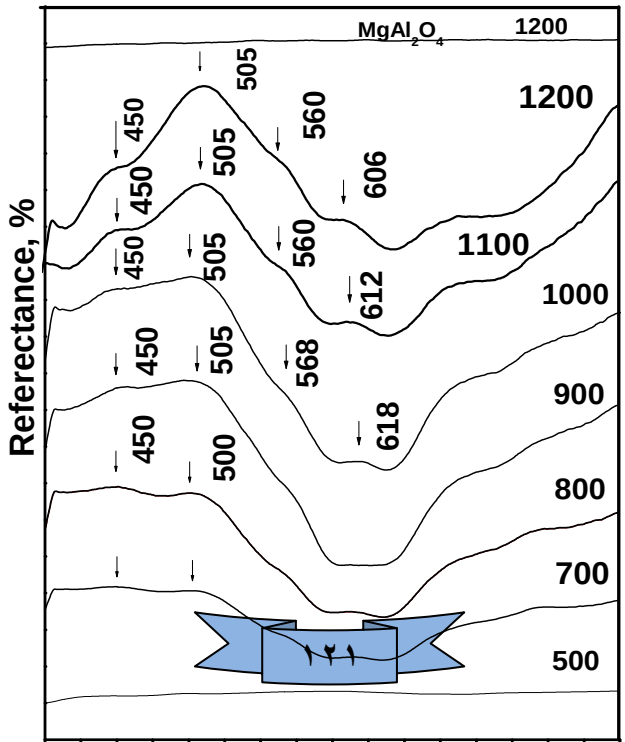

Figure (32): The diffuse reflectance spectra for $Ni_{0.10}Mg_{0.90}Al_2O_4$ (A), $Ni_{0.50}Mg_{0.50}Al_2O_4$ (F) and $Ni_{0.80}Mg_{0.20}Al_2O_4$ systems at different calcination temperatures by using urea as fuel.

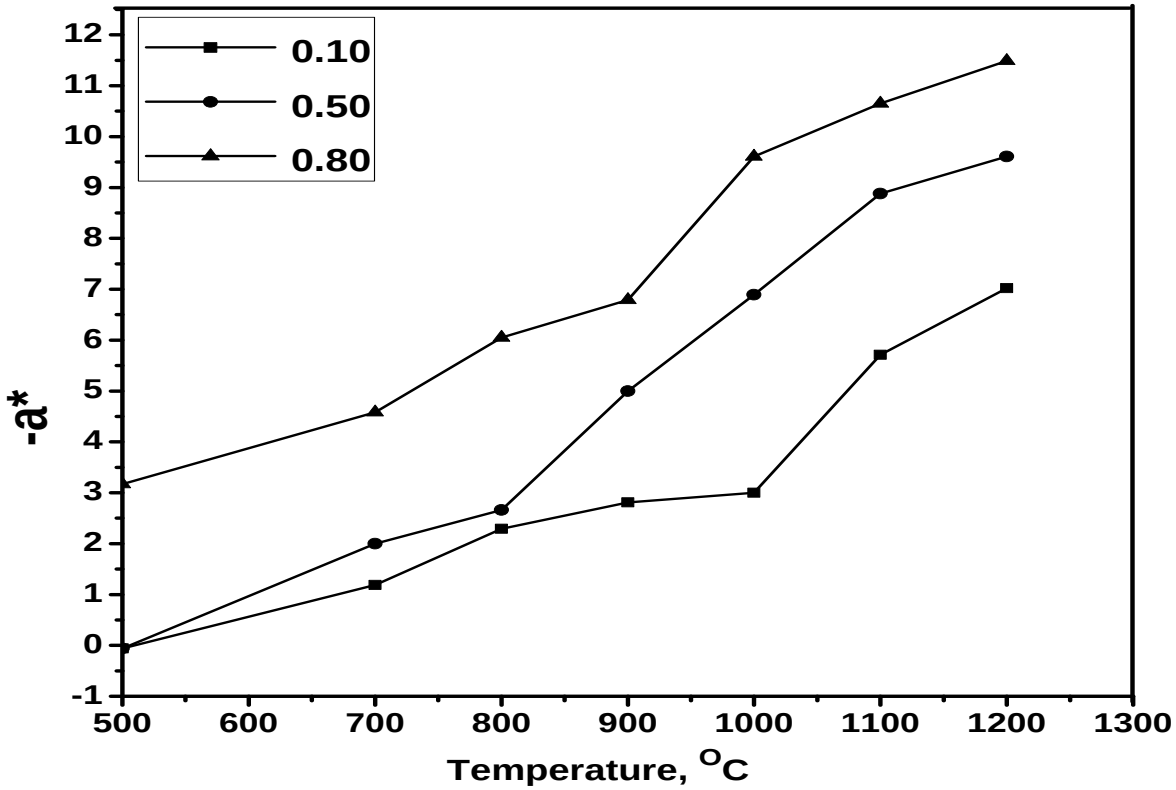

Figure (٣٣): Colorimetric data for different doping of 0.10, 0.50 and 0.80 mole of Ni^{2+} systems at different calcination temperature by using urea as fuel.

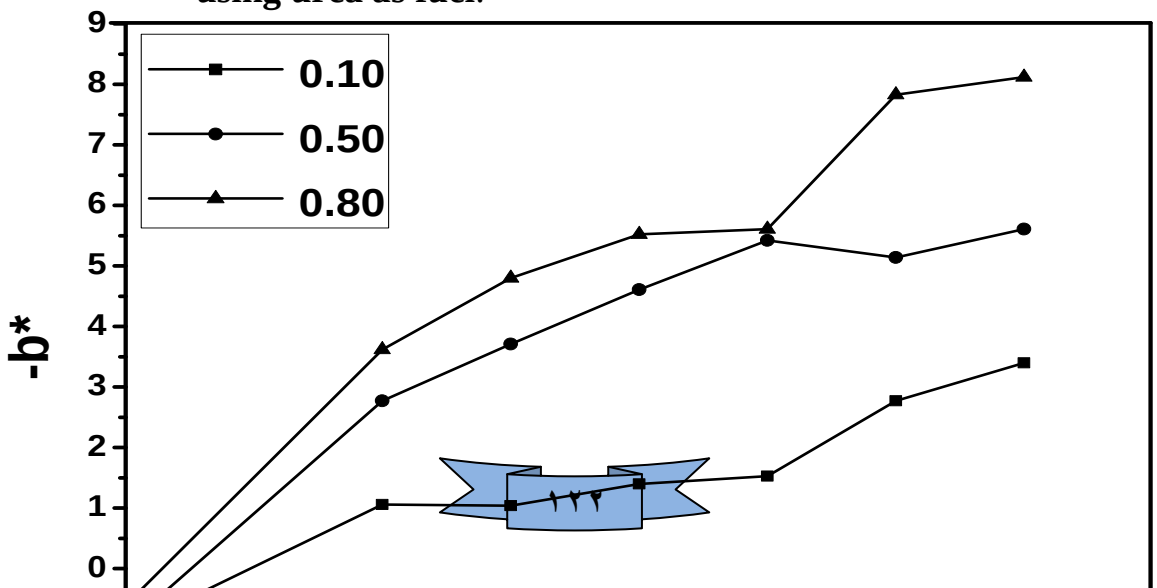

Figure (٣٤): Colorimetric data for different doping of 0.10, 0.50 and 0.80 mole of Ni^{2+} system at different calcination temperatures by using urea as fuel.

system	Temperature, °C	L*	a*	b*	ΔE
0.10	٥٠٠	96.94	٠,٠٦	١,٠٠	٩٦,٩٥
	٧٠٠	98.94	-١,١٩	-١,٠٦	٩٨,٩٥
	٨٠٠	٩٧,٩٥	-٢,٢٩	-١,٠٤	٩٧,٩٨
	٩٠٠	٩٧,٦٠	-٢,٨١	-١,٤٠	٩٧,٦٥
	١٠٠٠	٩٧,٥٨	-٣,٠٠	-١,٥٣	٩٧,٦٤
	١١٠٠	٩٥,١١	-٥,٧١	-٢,٧٧	٩٥,٣٢
	١٢٠٠	٩٣,٤٨	-٧,٠٢	-٣,٤٠	٩٣,٨١
٠,٥٠	٥٠٠	٩٦,٩٤	٠,٠٦	٠,٩٥	٩٦,٩٥
	٧٠٠	٩٧,٨٩	-٢,٠٠	-٢,٧٧	٩٧,٩٥
	٨٠٠	٩٧,٢٥	-٢,٦٦	-٣,٧١	٩٧,٣٦
	٩٠٠	٩٦,٣٧	-٥,٠٠	-٤,٦١	٩٦,٦١
	١٠٠٠	٩٣,٧٨	-٦,٨٩	-٥,٤٢	٩٤,١٩
	١١٠٠	٩٢,٤٨	-٨,٨٨	-٥,١٤	٩٣,١٠
	١٢٠٠	٩٢,٣٥	-٩,٦١	-٥,٦١	٩٣,٠٢

٠,٨٠	٥٠٠	٩٤,٦٥	-٣,١٧	٠,٦٠	٩٤,٧١
	٧٠٠	٩٧,٩٢	-٤,٥٨	-٣,٦٢	٩٨,١٠
	٨٠٠	٩٦,١١	-٦,٠٥	-٤,٨٠	٩٦,٤٢
	٩٠٠	٩٦,٠٤	-٦,٧٩	-٥,٥٢	٩٦,٤٤
	١٠٠٠	٩٤,٤٨	-٩,٦١	-٥,٦١	٩٥,١٣
	١١٠٠	٩٣,٥٤	-١٠,٦٥	-٧,٨٣	٩٤,٤٧
	١٢٠٠	٩٢,٤٢	-١١,٤٩	-٨,١٢	٩٣,٤٩

Table (11): Colorimetric data for different doping of 0.10, 0.50 and 0.80 mole of Ni^{2+} systems at different temperatures using urea as fuel..

Temperature, °C	٠,١٠ mole of Ni^{2+}	٠,٥٠ mole of Ni^{2+}	٠,٨٠ mole of Ni^{2+}
٥٠٠			
٧٠٠	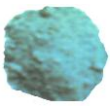	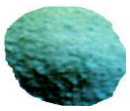	
٨٠٠			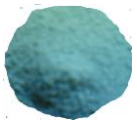
٩٠٠			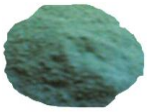
١٠٠٠			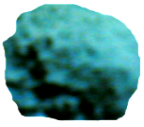

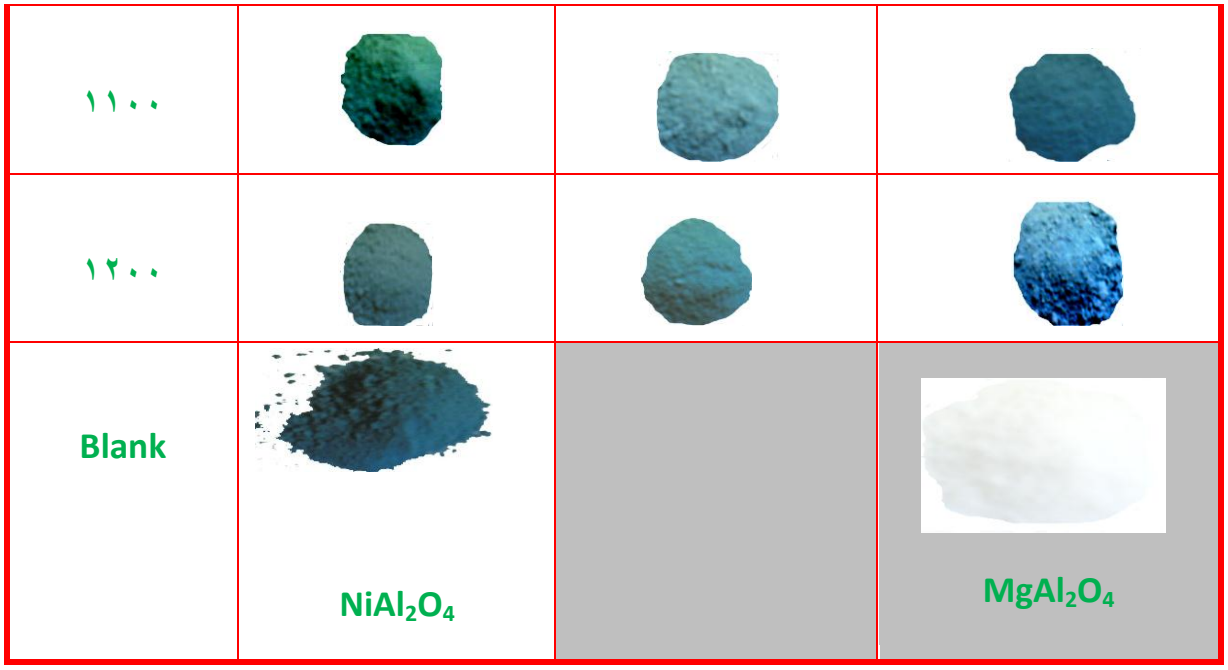

Figure (٣٥): The color of ceramic powder for 0.10, 0.50 and 0.80 mole of Ni^{2+} systems using urea as fuel at different calcination temperatures.

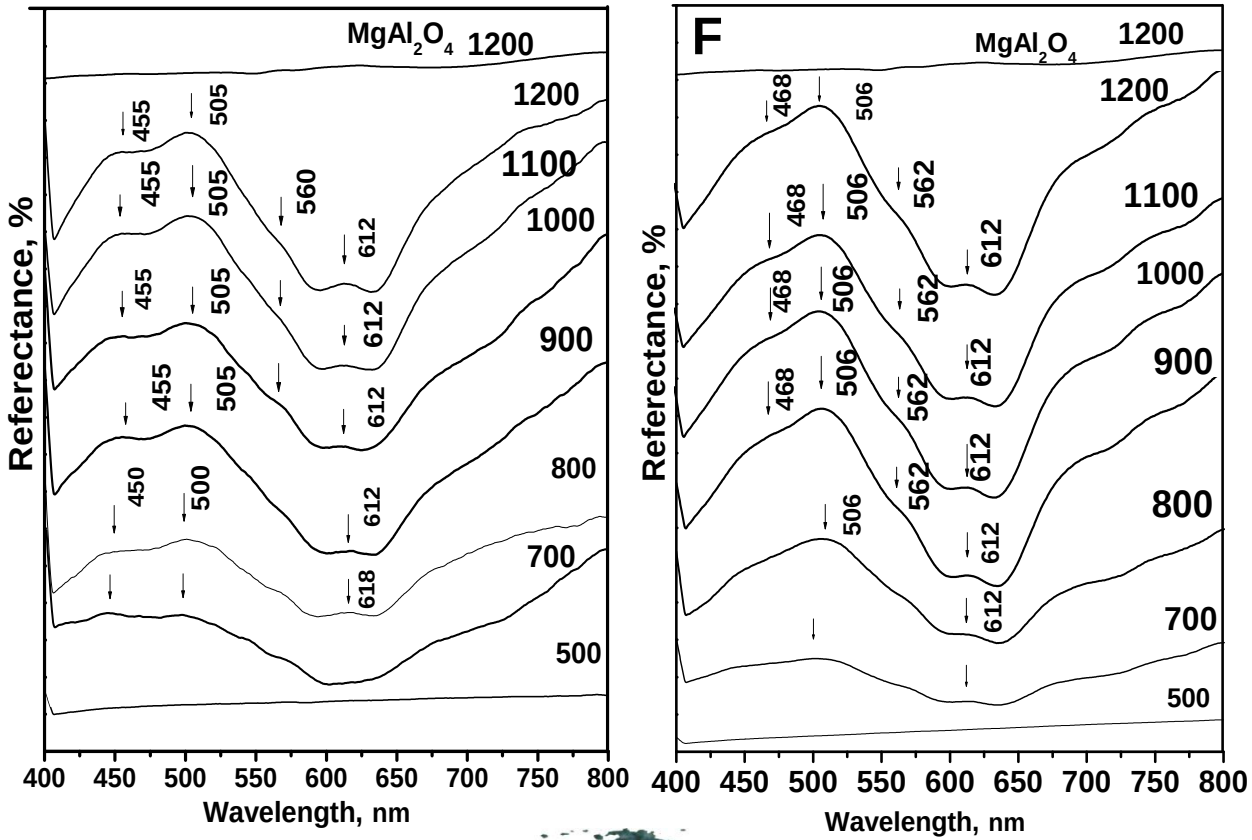

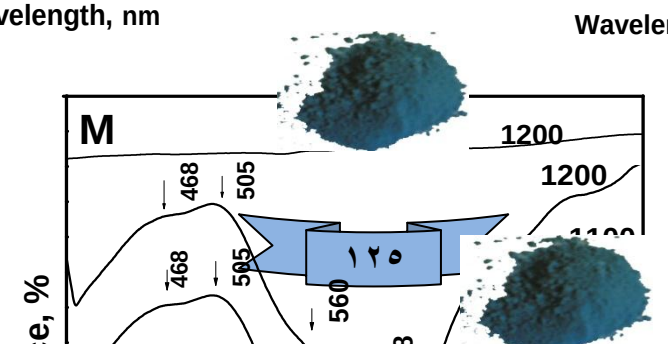

Figure (36): The diffuse reflectance spectra for $Ni_{0.10}Mg_{0.90}Al_2O_4$ (A), $Ni_{0.50}Mg_{0.50}Al_2O_4$ (F) and $Ni_{0.80}Mg_{0.20}Al_2O_4$ (M) systems at different calcination temperatures by using 3-methyl pyrozole-5-one as fuel.

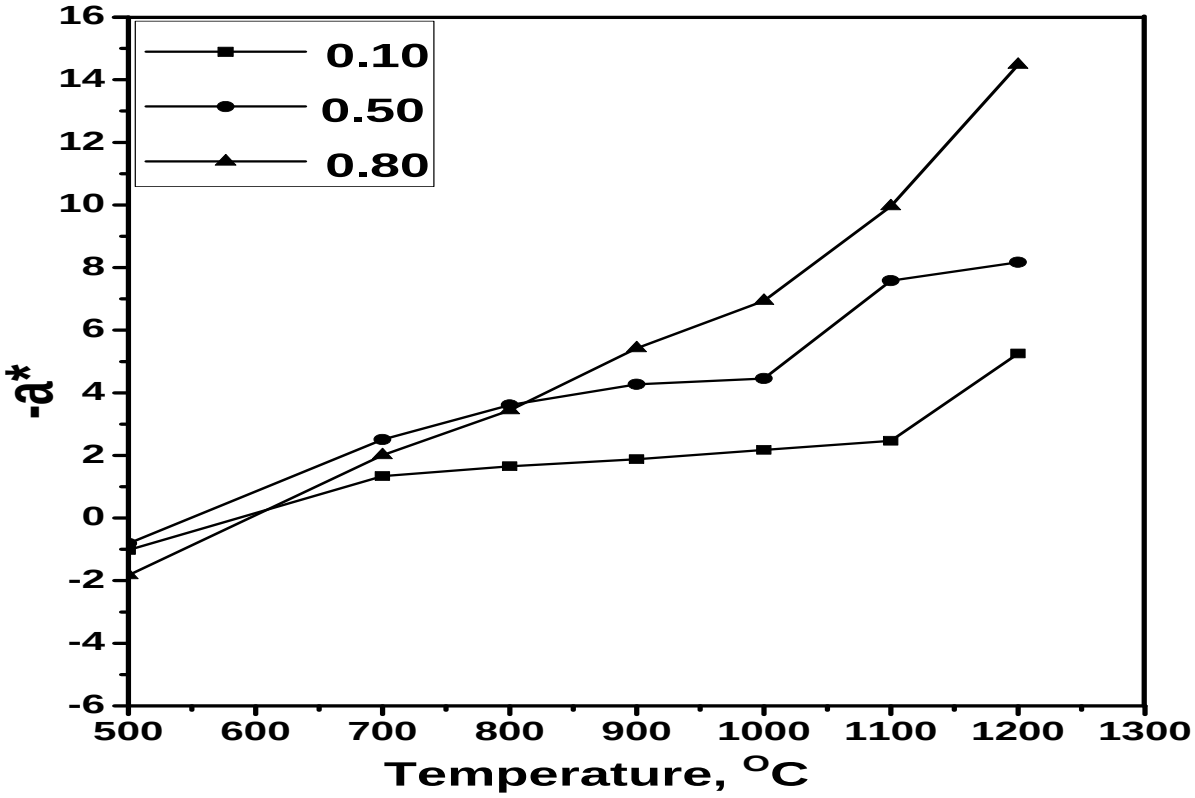

Figure (37): Colorimetric data for 0.10, 0.50 and 0.80 mole of Ni^{2+} systems at different calcination temperature by using 3MP5O as fuel.

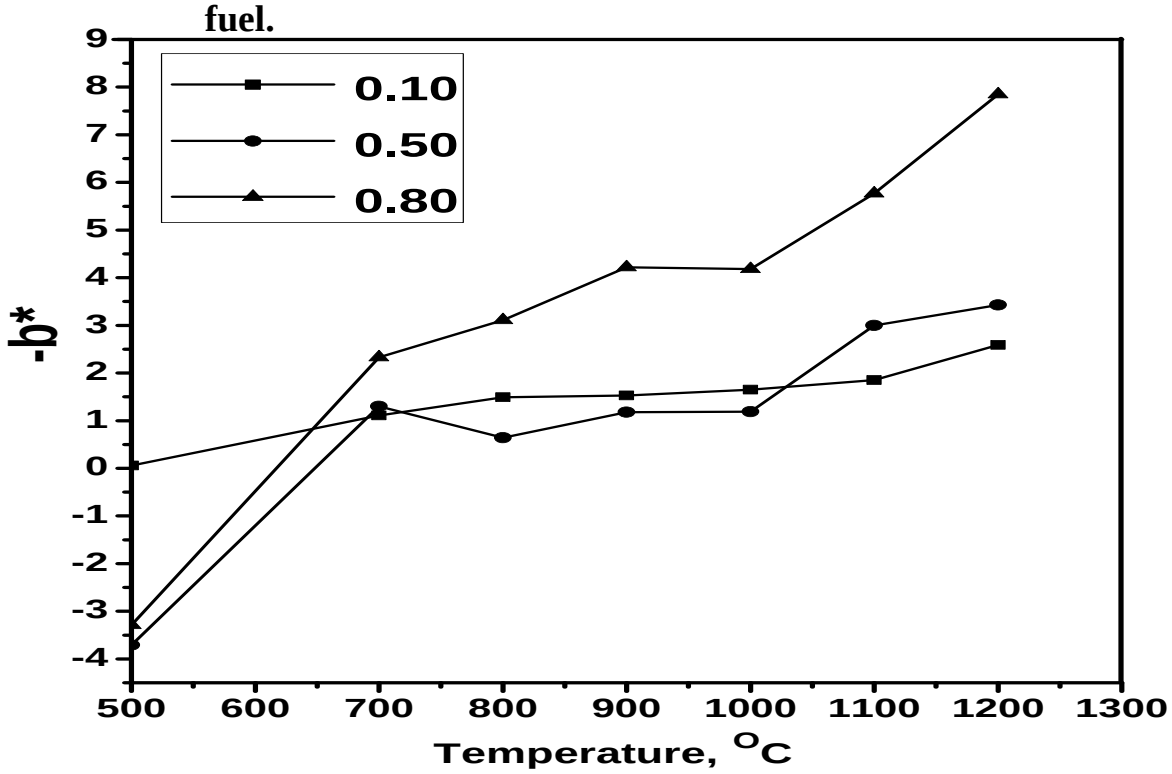

Figure (38): Colorimetric data for 0.10, 0.50 and 0.80 mole of Ni^{2+} systems at different calcination temperature by using 3-methyl pyrozole-5-one as fuel.

system	Temperature	L*	a*	b*	ΔE
٠,١٠	٥٠٠	٩٦,٩٤	١,٠٢	٠,٠٦	٩٦,٩٥
	٧٠٠	٩٥,١٧	-١,٣٤	-١,١١	٩٥,١٩
	٨٠٠	٩٤,٤	-١,٦٥	-١,٤٩	٩٤,٤٣
	٩٠٠	٩٣,٨٩	-١,٨٨	-١,٥٣	٩٣,٩٢
	١٠٠٠	٩١,٩٨	-٢,١٨	-١,٦٥	٩٢,٠٢
	١١٠٠	٩١,٥٦	-٢,٤٧	-١,٨٥	٩١,٦١
	١٢٠٠	٩٠,٠٠	-٥,٢٥	-٢,٥٩	٩٠,١٩

٠,٥٠	٥٠٠	٨٩,٢١	٠,٨١	٣,٧١	٨٩,٢٩
	٧٠٠	٩٢,٩٧	-٢,٥١	-١,٣٠	٩٣,٠٠
	٨٠٠	٩١,٧٩	-٣,٦١	-٠,٦٤	٩١,٩٠
	٩٠٠	٨٩,٢٨	-٤,٢٧	-١,١٨	٨٩,٣٩
	١٠٠٠	٨٦,٣٤	-٤,٤٦	-١,١٩	٨٦,٤٦
	١١٠٠	٨٥,٩٢	- ٧,٥٨	-٣,٠٠	٨٦,٣١
	١٢٠٠	٨٥,٩٣	-٨,١٧	-٣,٤٣	٨٦,٣٩
٠,٨٠	٥٠٠	٨١,١٣	١,٨٣	٣,٢٩	٨١,٢٢
	٧٠٠	٩٤,٨٤	-٢,٠١	-٢,٣٣	٩٤,٨٩
	٨٠٠	٩٣,٤١	-٣,٤٤	-٣,١١	٩٣,٥٣
	٩٠٠	٩١,٦٦	-٥,٤٢	-٤,٢٢	٩١,٩٢
	١٠٠٠	٨٨,٩١	-٦,٩٤	-٤,١٨	٨٩,٢٨
	١١٠٠	٨٨,٦٠	-٩,٩٦	-٥,٧٧	٨٩,٣٥
	١٢٠٠	٨٤,١٨	-١٤,٤٨	-٧,٨٥	٨٥,٧٨

Table (12): Colorimetric data for 0.10, 0.50 and 0.80 mole of Ni^{2+} systems at different temperatures using 3-methyl pyrozole-5-one as fuel.

Temperature, °C	٠,١٠ mole of Ni^{2+}	٠,٥٠ mole of Ni^{2+}	٠,٨٠ mole of Ni^{2+}
٥٠٠	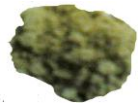		
٧٠٠	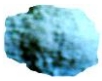		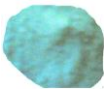
٨٠٠			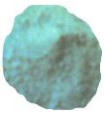
٩٠٠	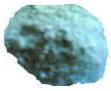		
١٠٠٠			
١١٠٠٠			
١٢٠٠			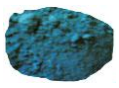
Blank	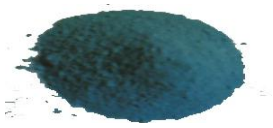 $NiAl_2O_4$		 $MgAl_2O_4$

Figure (39): The color of ceramic powder for 0.10, 0.50 and 0.80 mole of Ni^{2+} systems using 3-methyl pyrozole-5-one as a fuel with change temperatures.

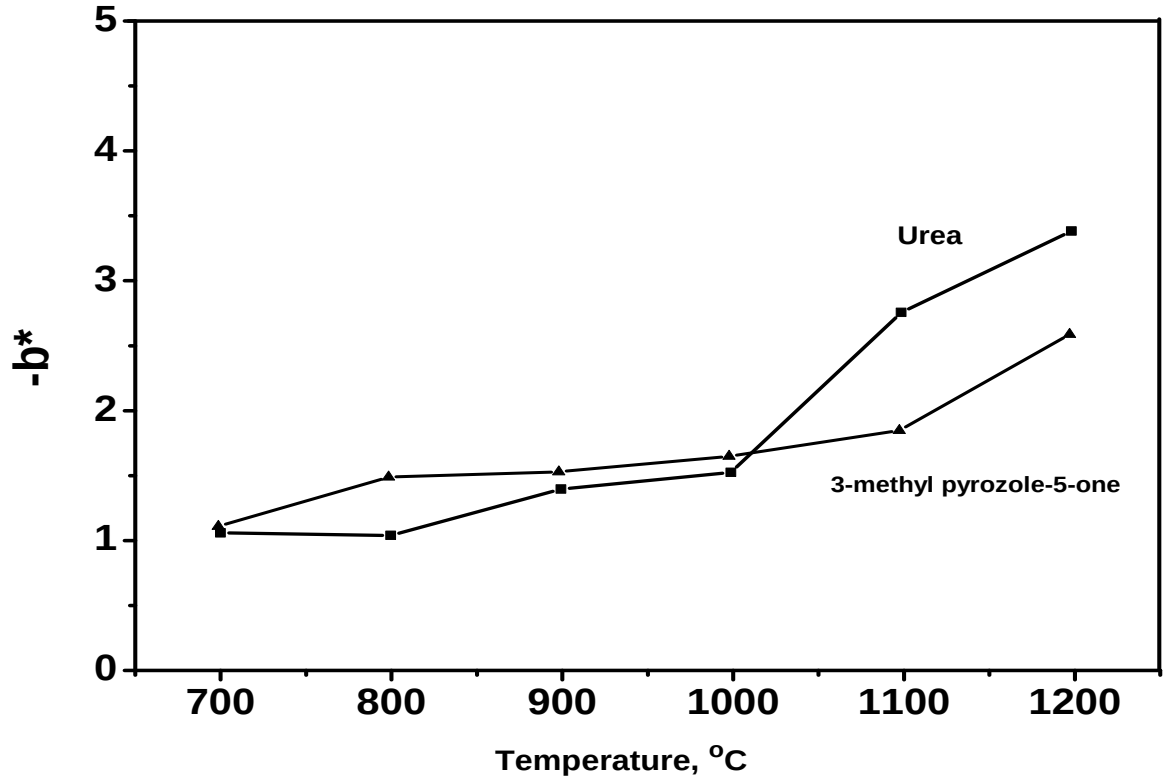

Figure (40): Colorimetric data (b* in blue direction) for 0.10 mole of Ni^{2+} system at different calcination temperature by using urea and 3-methyl pyrozole-5-one as fuel.

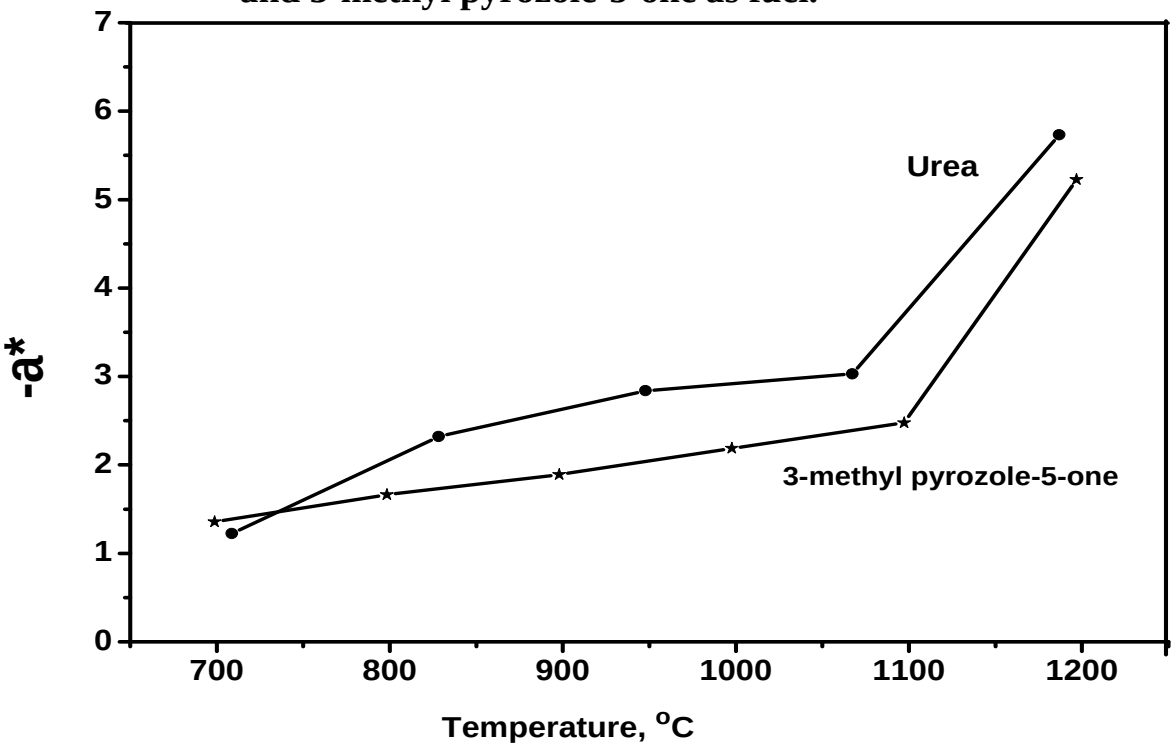

Figure (41): Colorimetric data (a* in green direction) for 0.10 mole of Ni^{2+} system at different calcination temperature by using urea and 3-methyl pyrozole-5-one as fuel.

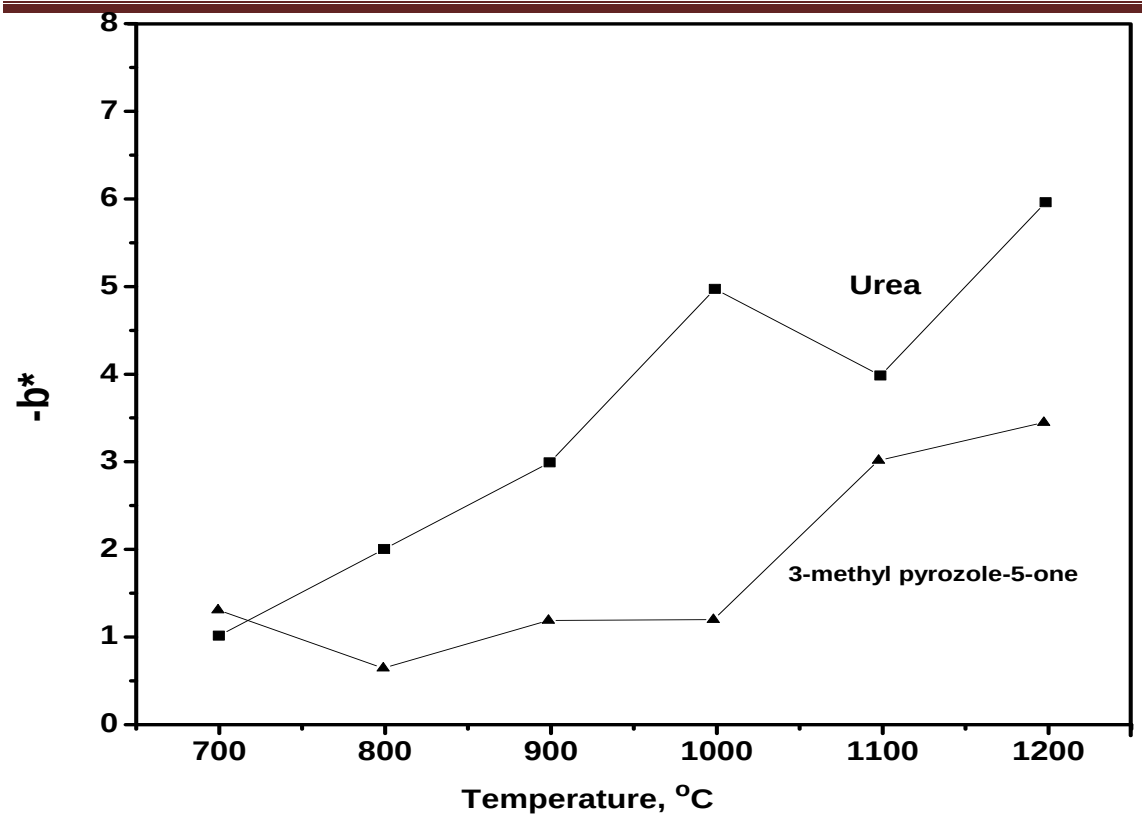

Figure (42): Colorimetric data (b* in blue direction) for 0.50 mole of Ni^{2+} system at different calcination temperature by using urea and 3-methyl pyrozole-5-one as fuel.

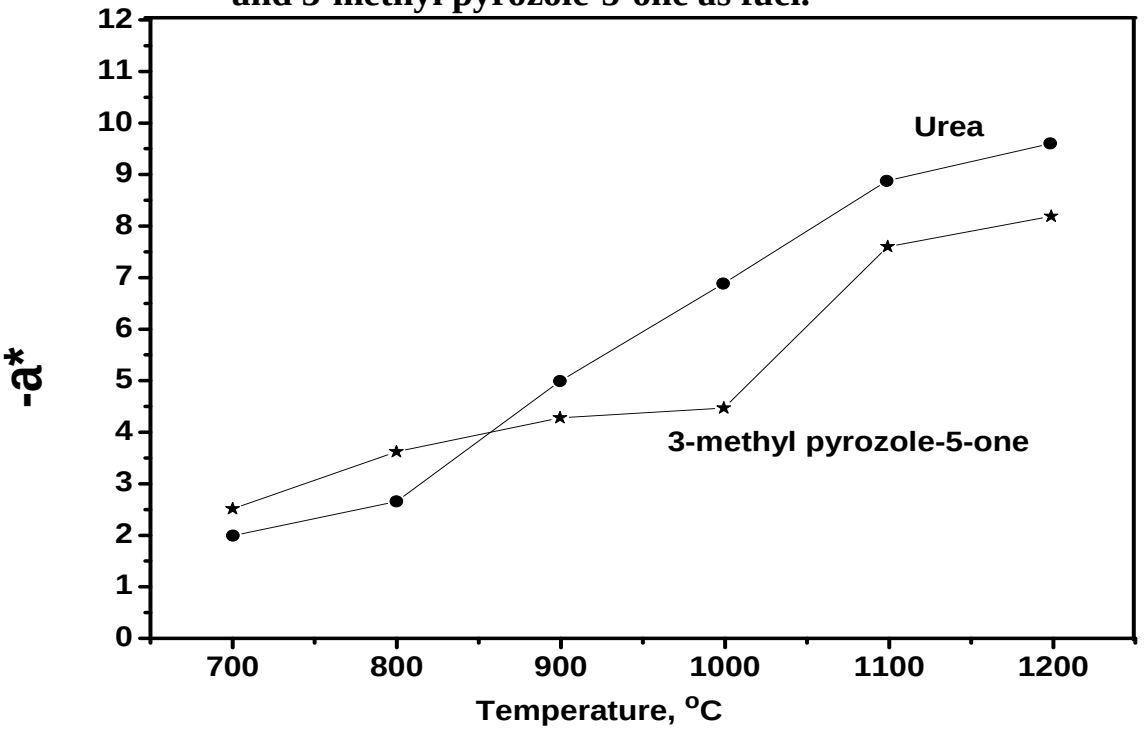

Figure (43): Colorimetric data (a* in green direction) for 0.50 mole of Ni^{2+} system at different calcination temperature by using urea and 3-methyl pyrozole-5-one as fuel.

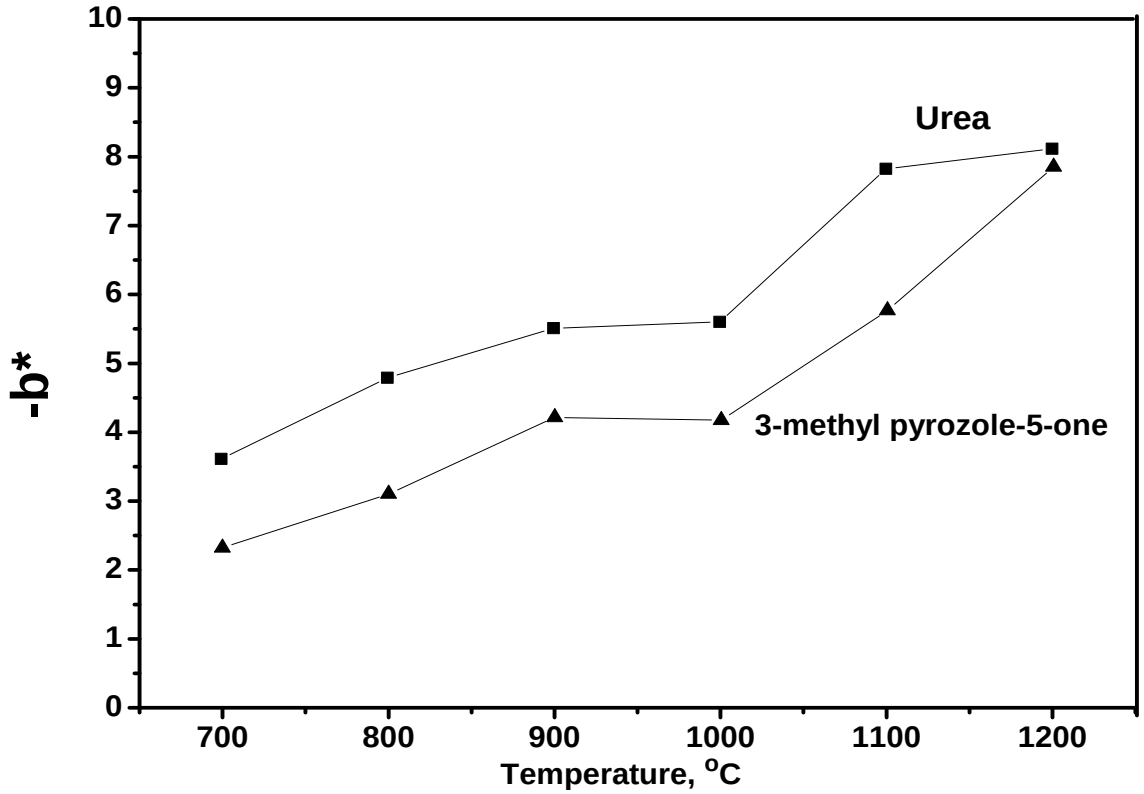

Figure (44): Colorimetric data (b* in blue direction) for 0.80 mole of Ni^{2+} system at different calcination temperature by using urea and 3-methyl pyrozole-5-one as fuel.

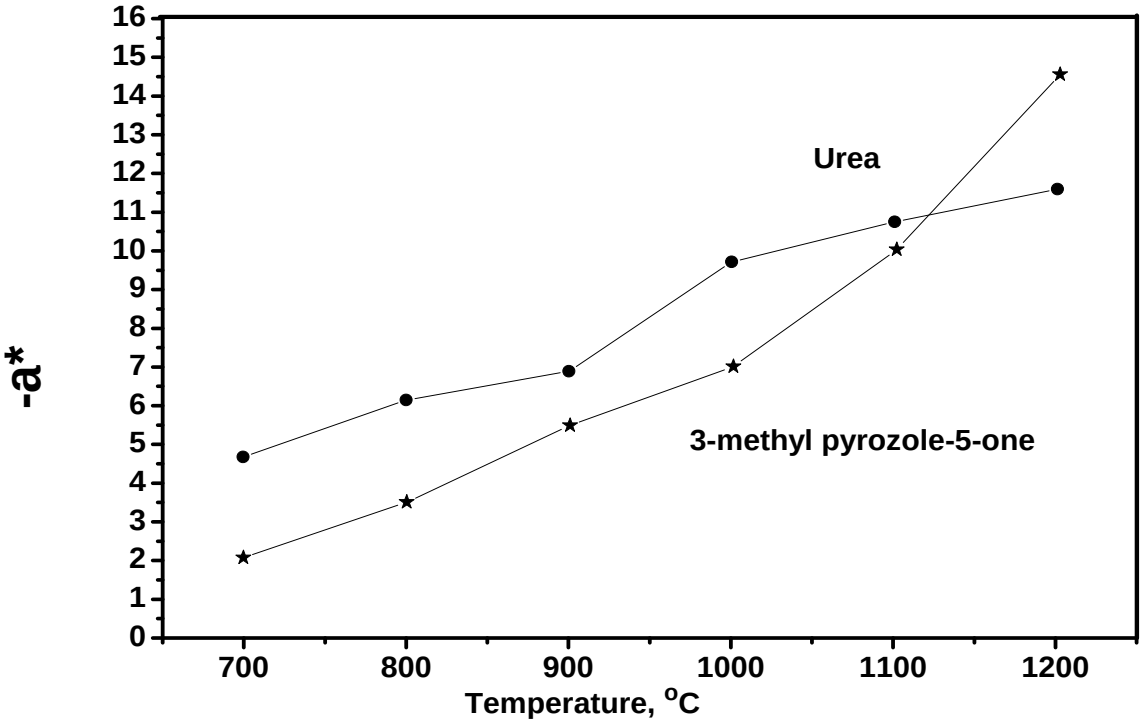

Figure (45): Colorimetric data (a* in green direction) for 0.10 mole of Ni^{2+} system at different calcination temperature by using urea and 3-methyl pyrozole-5-one as fuel.

3.2.3. The electronic spectra $Ni_yMg_{1-y}Al_2O_4$ systems using different fuel

3.2.3.1. The electronic spectra of nickel system using urea as fuel

The electronic spectra of 0.10 (A), 0.50 (F) and 0.80 (M) mole of Nickel systems using urea as fuel at different calcination temperatures present as shown in Figures (46). Three broad absorption bands at 540 nm for A system, 560 nm for F system and 545 nm for M system (green region), 595 nm for A and F systems and 600 nm for M system (yellow-orange region) and 637 nm for A system, 535 nm for F and M systems (red region). These bands indicate for tetrahedral co-ordination for Ni^{2+} in the Al_2O_3 lattice which gives rise to the green-blue coloration.

From Orgel diagram, the d-d transitions of Ni^{2+} ($3d^{8}_{Td}$) shows the present of three transition states of $^3T_{1g}(F) \longrightarrow {}^1T_{2g}$, $^3T_{1g}(F) \longrightarrow {}^3T_{1g}(P)$ and $^3T_{1g}(F) \longrightarrow {}^3A_{2g}$. The two weak absorption bands at 475, 480 nm and 725, 715 nm for indicate for octahedral co-ordination of Ni^{2+} in the Al_2O_3 lattice [112-113] and The energy level diagram gives d-d transitions of Ni(II) ($3d^{8}_{Oh}$) from Orgel diagram shows $^3A_{2g} \longrightarrow {}^3T_2(D)$, $^3A_{2g} \longrightarrow {}^3T_1(F)$. This triple band in visible region can be attributed to Jahn-Teller [110-111] distortion of tetrahedral structure.

3.2.3.2. The electronic spectra of nickel system using 3-methyl pyrozole-5-one as fuel.

The electronic spectra of 0.01, 0.05 and 0.1 mole of Ni^{2+} systems using 3-methyl pyrozole-5-one as fuel is shown in Figures (47). Three broad absorption bands show at 575 nm for A system, 555 nm for F system and 560 nm for M system (green region), 600 for A system, 595 nm for F system and 605 nm for M system (yellow-orange region) and 537 nm for A system, 627 nm for F system and 630 nm for M system (red region) as result of different calcination temperatures. These bands indicate for tetrahedral [114] co-

ordination of Ni^{2+} in the Al_2O_3 lattice which gives rise to the green-blue coloration.

Using Orgel diagram, The d-d transitions of Ni^{2+} ($3d^{8}_{Td}$) shows the present of three transition states of $^3T_1(F) \longrightarrow {}^1T_2$, $^3T_1(F) \longrightarrow {}^3T_1(P)$ and $^3T_1(F) \longrightarrow {}^3A_{2g}$. The two weak absorption bands at 475, 480 nm and 725,715 nm are appeared for octahedral co-ordination of Ni^{2+} in the Al_2O_3 lattice. The energy level diagram gives d-d transitions of Ni^{2+} ($3d^{8}_{Oh}$) from Orgel diagram shows $^3A_2g \longrightarrow {}^3T_2(D)$ and $^3A_{2g} \longrightarrow {}^3T_1(F)$. This triple band in visible region can be attributed to Jahn-Teller distortion of tetrahedral structure.

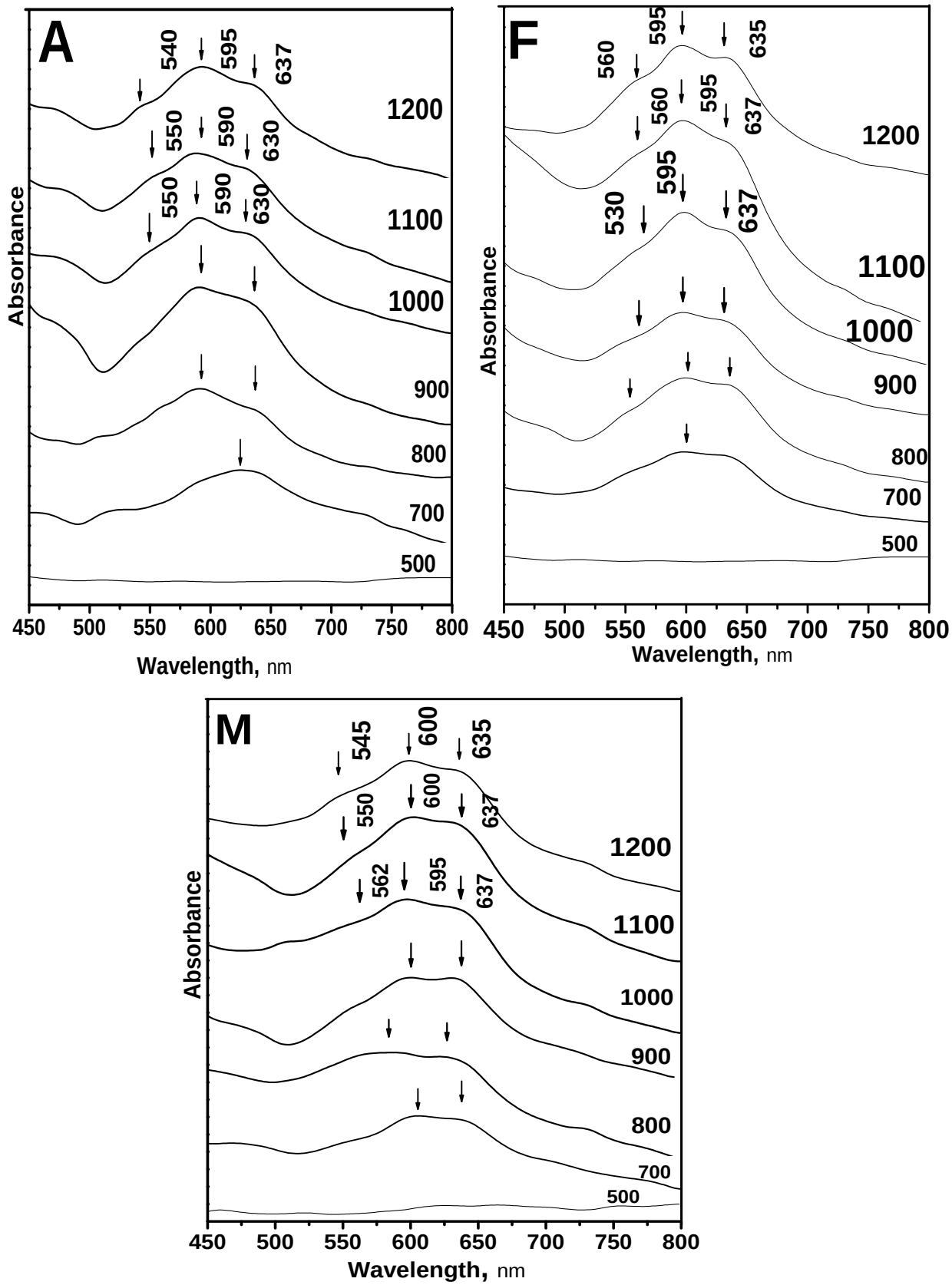

Figure (46): The electronic spectra for $Ni_{0.10}Mg_{0.90}Al_2O_4$ (A), $Ni_{0.50}Mg_{0.50}Al_2O_4$ (F) and $Ni_{0.80}Mg_{0.20}Al_2O_4$ (M) system at different calcination temperatures by using urea as fuel.

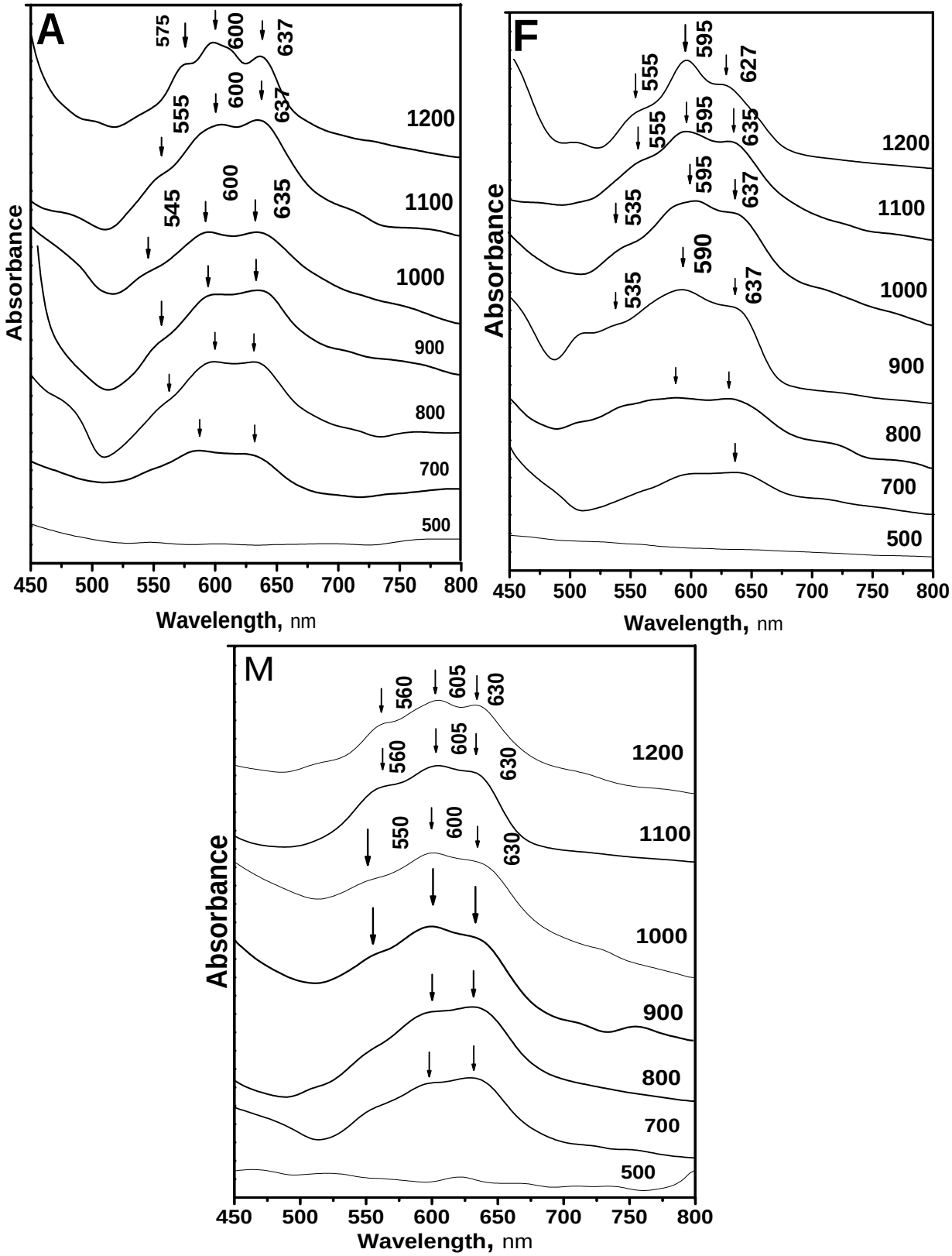

Figure (٤٧):The electronic spectra for $Ni_{0.10}Mg_{0.90}Al_2O_4$ (A), $Ni_{0.50}Mg_{0.50}Al_2O_4$ (F) and $Ni_{0.80}Mg_{0.20}Al_2O_4$ (M) systems at different calcination temperatures by using 3-methyl pyrozole-5-one as fuel.

3.3. The crystal structure characterization of $Co_xMg_{1-x}Al_2O_4$ systems ceramic pigment

3.3.1. Thermal analysis for $Co_xMg_{1-x}Al_2O_4$ system using different fuels

A good fuel used in a combustion process should react non-violently, produce non-toxic gases, and act as a complexing agent for metal cations. Different pmetal cations and organic fuels with different functional groups (caboxylic group and/or amine group) are exhibited different complex power. The fuel is one of the important factors that affect the phase formation and morphology of the final product. In addition, the released chemical energy from the exothermic reaction between various metal nitrates and fuels is different [115-116]. Also, energy is important factor that affects the phase formation of the product because the high temperature is a favorable of the stable phase formation and particle aggregation of the final product. The thermal analysis (TG, DTG and DTA) of $Co_xMg_{1-x}Al_2O_4$ system using different fuels carried out on ash powders.

From TG-curves, the weight losses were calculated for the different steps and compared with those theoretically calculated for the suggested decomposition based on the results of the elemental analysis by the tangent method, calculated from the curve of the mass loss versus temperature. The calculations on the range of temperature with respective mass losses were performed with the aid of shimadzu software and excell programs. The kinetic parameter as activation energies are calculated from TG-curves in temperature range 200-1000 ºC by using Coats-Redfern[117] method.

3.3.1.1. Thermal analysis for 0.05 mole of Co^{2+} using urea as fuel.

The thermogravimetric curves in Figure (48) show four thermal decomposition steps by using urea as fuel. The first and second steps show the losing of 12.5 % (calc. 13.6%) by weight at temperature range 50-200 ºC due to the elimination of the humidity and co-ordination water in sample. The third in range 200-450ºC and the fourth in range 450-690ºC steps show the losing of 30.8 % (calc. 28.9%) by weight occurs for evolution of CO gas from sample. We can say that phase formation starts at 700º C with stable of TG-curve. The differential thermal analysis (DTA) shows three endothermic steps at 100, 150 and 690 ºC and one exothermic step at 400 ºC. The first and second endothermic reactions occur for elimination of the water in sample. The third one exothermic step occurs for elimination of the residual organic material in sample. The fourth endothermic reaction step appears at 690 ºC due to the phase formation. The activation energy is calculated from TG-curves by using Coats-Redfern [117] method. The activation energy of this system equals to 8.314kJ/mol. The decomposition of sample under investigation for 0.05 mole of Co^{2+} system can occur as the following

$$Co_{0.05}\,Mg_{0.95}Al_2(OH)_4(CO_3)_2.0.5H_2O \xrightarrow{\text{50-200 º C}} Co_{0.05}\,Mg_{0.95}Al_2(O)_2(CO_3)_2+2.5H_2O$$

$$Co_{0.05}\,Mg_{0.95}Al_2(O)_2(CO_3)_2 \xrightarrow{\text{200-650 º C}} Co_{0.05}Mg_{0.95}Al_2O_4+2CO_2$$

3.3.1.2. Thermal analysis for 0.05 mole of Co^{2+} using oxalyl dihydrazide as fuel.

The weight losing of 0.05 mole Co^{2+} system using oxalyl dihydrazide as fuel changes in three steps as shown in TGA curve for ash as shown in Figures (49). The losing of 13% (calc. 13.5%) by weight in the first range 50-200ºC and the second range 200-450ºC occur due to elimination of the humidity and co-ordination water in sample. The losing of 10 % (calc. 11%) by weight in the third step in the range 450-650ºC occur due to evolution of CO, CO_2 and NOx gases from sample. We can say that phase formation starts around 700º C from TGA curve. DTG shows three endothermic steps at 100, 300 and 500 ºC. The differential thermal analysis (DTA) shows two endothermic steps and only exothermic step. The first endothermic step occurred for elimination of the water in sample. The second exothermic step occurred for elimination of the residual organic material in sample. The third endothermic reaction step shows phase formation and appearance of phase under study. The activation energy of this system equals to 9.70kJ/mol. We can explain the calcinations steps as the following equations.

$$\mathbf{0.05CoCO_3.\ 0.95MgO.Al_2O_3.1.5\ H_2O \xrightarrow{50\text{-}200\ ^\circ C} 0.05CoCO_3.0.95MgO.Al_2O_3+1.5H_2O}$$

$$\mathbf{0.05CoCO_3.0.95MgO.Al_2O_3 \xrightarrow{200\text{-}450\ ^\circ C} Co_{0.05}Mg_{0.95}Al_2O_4+0.05CO_2}$$

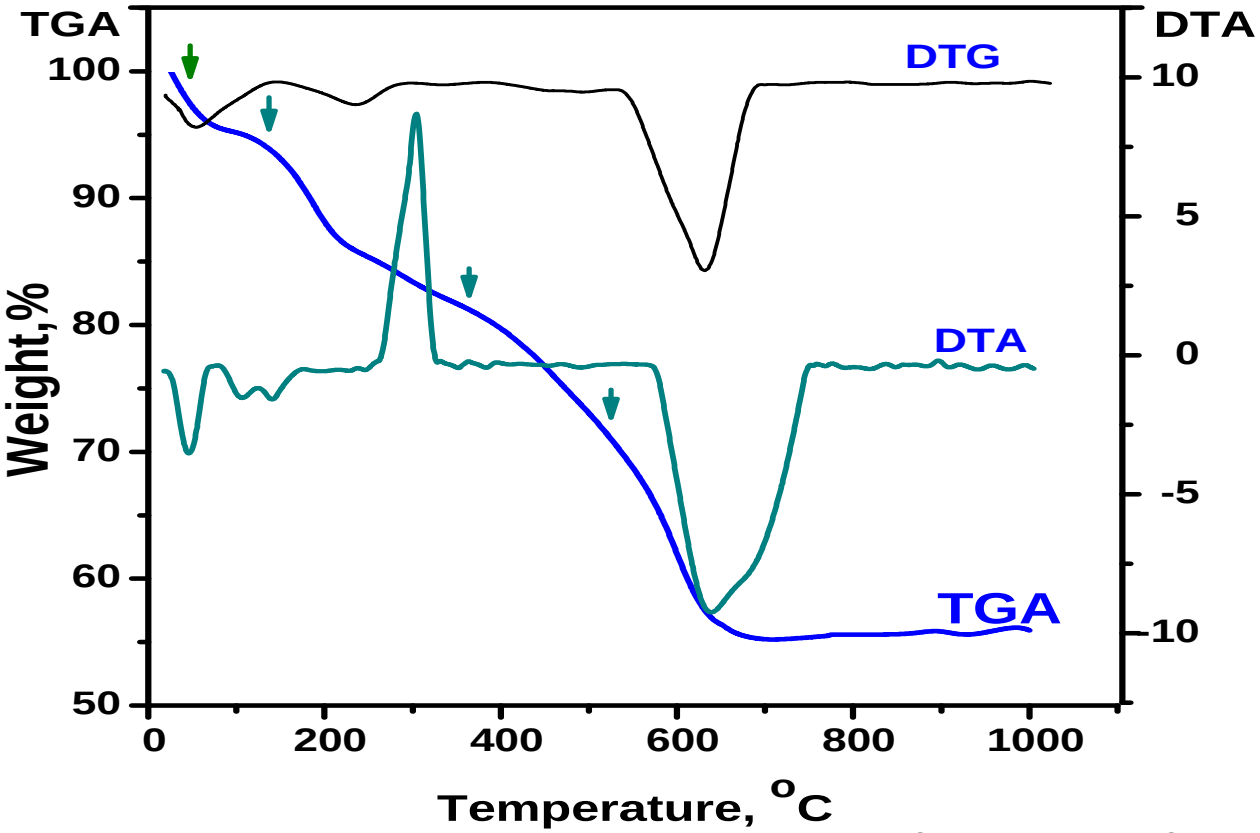

Figure (48): Thermal analysis (TGA, DTG and DTA) for 0.05 mole of Co^{2+} system using urea as fuel.

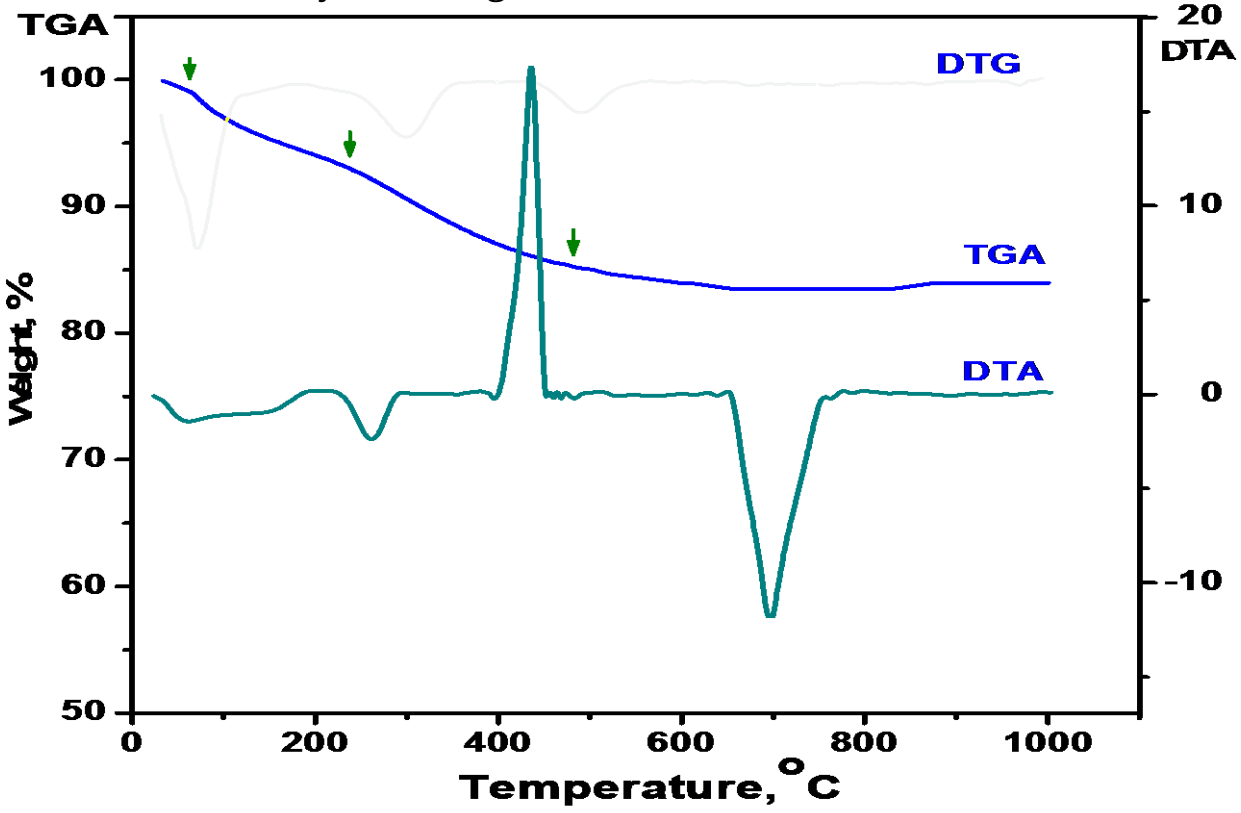

Figure (49): Thermal analysis (TGA, DTG and DTA) for 0.05 mole of Co^{2+} system using oxalyl dihydrazide as fuel.

3.3.1.3. Thermal analysis for 0.05 mole Co^{2+} using 3-methyl pyrozole-one (3MP5O) as fuel.

The weight losing of 0.05 mole Co^{2+} system using 3-methyl pyrozole-5-one (3MP5O) as fuel are present in four steps as shown in TGA curve for ash as present in Figure (50). The weight loss 8.5% (calc. 7.9%) in range 50–100 ◦C, this can be attributed to elimination of the co-ordination water in sample. The weight loss of 23%, at the temperature 100–500 ◦C, represents the removal of the ligand molecule. The mass losing at 500-700 °C were 22.5%(calc. 23.8%) corresponding to the removal of CO,CO_2 gases from the sample then the solid solution of cobalt aluminate and magnesium aluminate began to be formed at 650°C. DTG shows three endothermic steps at 100, 250 and 690 ºC. DTA shows second endothermic steps at 100 and 690 ºC and one exothermic step at 250 ºC. The first endothermic step occurred due to elimination of the water and the second exothermic step for elimination of the residual organic material in sample. The third endothermic reaction step shows phase formation and appearance of phase under study. The activation energy of this system equals to 13.86kJ/mol.The calculated calcinations steps occurred according the following equations.

$$Co_{0.05}\,Mg_{0.95}O.\,Al_2(OH)_2(CO_3)_2.0.50H_2O.\,0.7(C_4H_6N_2O) \xrightarrow{\text{50-100 ° C}} Co_{0.05}\,Mg_{0.95}Al_2(O)_2(CO_3)_2\,.\,0.7(C_4H_6N_2O)+1.5H_2O$$

$$Co_{0.05}\,Mg_{0.95}Al_2(O)_2(CO_3)_2\,.\,0.7(C_4H_6N_2O) \xrightarrow{\text{100-500 ° C}} Co_{0.05}\,Mg_{0.95}Al_2(O)_2(CO_3)_2 +0.7(C_4H_6N_2O)$$

$$Co_{0.05}\,Mg_{0.95}Al_2(O)_2(CO_3)_2 \xrightarrow{\text{500-700 ° C}} Co_{0.05}\,Mg_{0.95}Al_2O_4 + CO_2 + CO$$

3.3.1.4. Thermal analysis for 0.05 mole Co^{2+} using N, N-bis-(3-amino-propyl) oxalamide using as fuel.

The weight losing of 0.05 mole Co^{2+} using N, N-bis-(3-amino-propyl) oxalamide as fuel changes in three steps as shown in TGA curve for ash as present in Figure (51). The losing of 13% (calc. 14.2%) by weight in the first (50-100 ºC) and the second (100-200ºC) steps occurs for elimination of the humidity and co-ordination water in sample. The losing of 13.8 % (calc. 14.7%) by weight in the third (200-650ºC) occurs for evolution of CO, CO_2 and NO*x* gases from sample. We can say that phase formation starts around 700º C from TGA curve. DTG shows three endothermic steps at 100, 250 and 650 ºC. DTA shows two endothermic steps at 100 and 700ºC and one exothermic reaction at 300 ºC. The first endothermic step occurred for elimination of the water and the second exothermic step for elimination of the residual organic material in sample. The third endothermic reaction step shows phase formation and appearance of phase under study. The activation energy of this system equals to 7.30kJ/mol

$$\mathbf{0.05CoO.0.95Mg\ CO_3.Al_2O_3\ H_2O \xrightarrow{50\text{-}200\ ^\circ C} 0.05CoCO_3.0.95MgO.Al_2O_3+H_2O}$$

$$\mathbf{0.05CoO.0.95Mg\ CO_3.Al_2O_3 \xrightarrow{200\text{-}650\ ^\circ C} Co_{0.05}\ Mg_{0.95}Al_2O_4 +0.95\ CO_2}$$

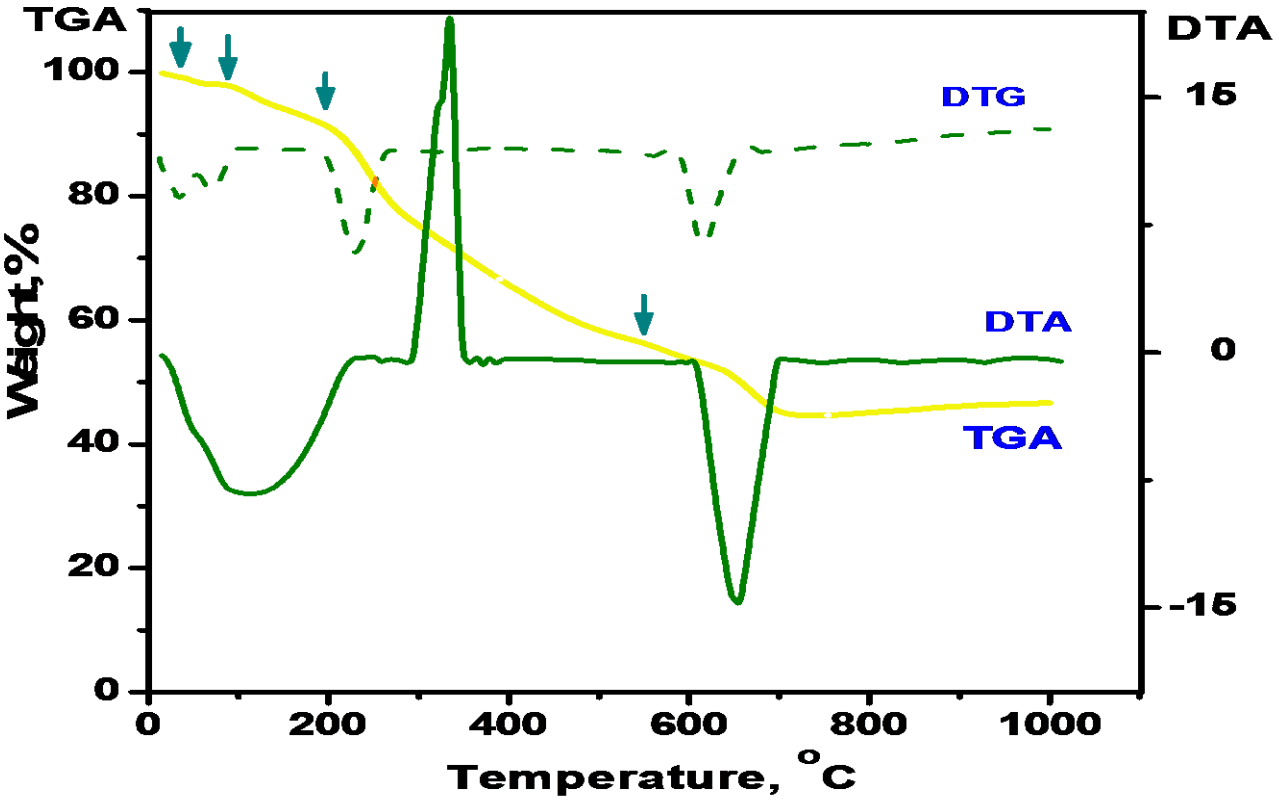

Figure (٥٠): Thermal analysis (TGA, DTG and DTA) for 0.05 mole of Co^{2+} system using 3-methyl pyrozole-5-one as fuel.

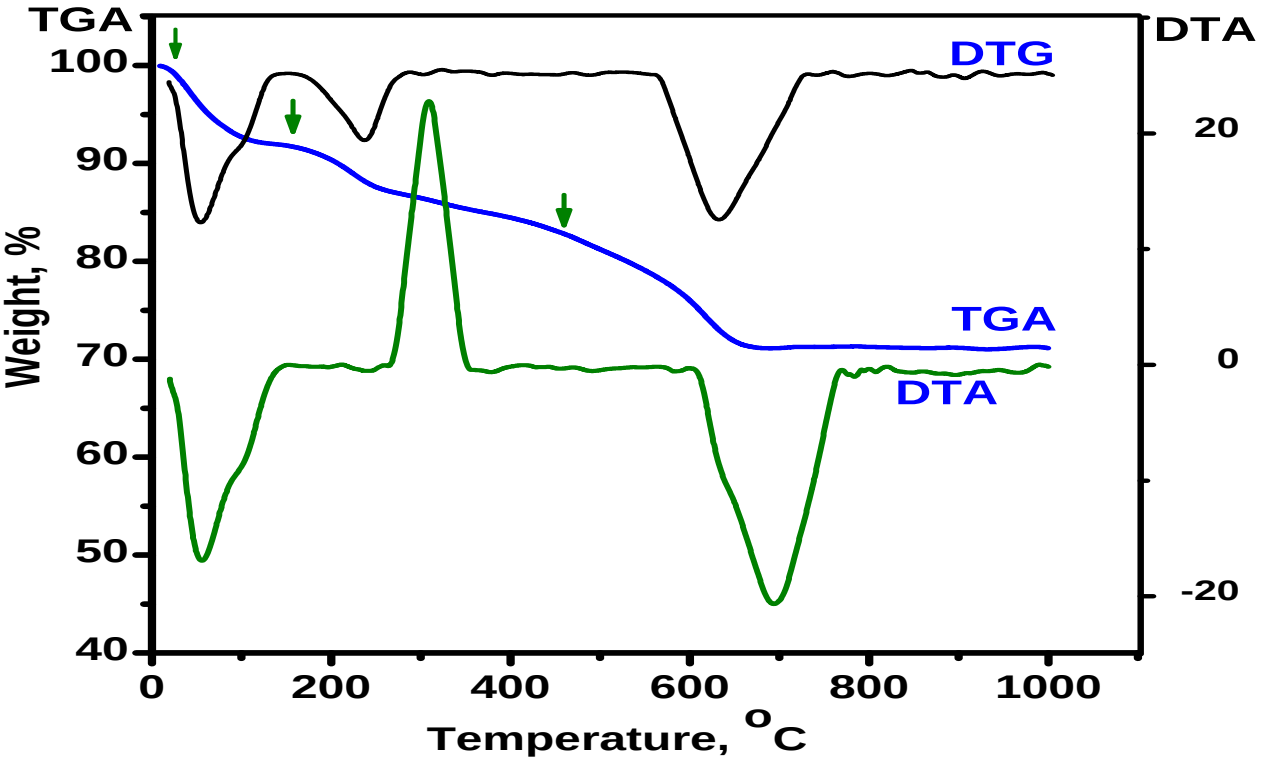

Figure (٥١): Thermal analysis (TGA, DTG and DTA) for 0.05 mole of Co^{2+} system using N, N-bis-(3-amino-propyl) oxalamide as fuel.

3.3.2. X-ray diffraction:

3.3.2.1. X-ray diffraction for $Co_xMg_{1-x}Al_2O_4$ system using urea as fuel.

The X-ray diffraction of $Co_xMg_{1-x}Al_2O_4$ systems using urea as fuel at different firing calcinations temperatures are shown in Figure (52). At 700º C, the XRD of powders remained amorphous or contained only small crystallites that indicated by the broadening lines. At 900º C, the calcinated powders begin to show the spinel crystalline from amorphous phase. With increasing the temperature of calcination above 900º C, the intensities of peaks increase gradually until sharpen peaks are observed in temperature range 1100-1200ºC [118-119].

The average crystallite sizes are calculated from the X-ray diffraction peaks by using scherrer equation [120-121] ($D=0.9\lambda/\beta\cos\theta$), where

λ is wavelength,

θ is the diffraction angle

and β is the corrected halfwidth.

The crystalline spinel phase content and the particles size increase with increasing calcinations temperatures that shown in Figure (53). The particles sizes for different doping Co^{2+} using urea systems from XRD are shown in Table (13).The density of 0.01, 0.05 and 0.10 mole Co^{2+} systems calculated from x-ray and compared with the experimental present using Archimedes rule in Table (15).

3.3.2.2.X-ray diffraction for $Co_xMg_{1-x}Al_2O_4$ system using oxalyl dihydrazide as fuel.

The X-ray diffraction for cobalt ion as doping for $Co_xMg_{1-x}Al_2O_4$ system using oxalyl dihydrazide as fuel are investigated as powders at different calcination temperatures. Figures (54) show the X-ray bands

intensities against (2ɵ) for three systems. From these curves, it is clear that the intensity of the bands is increasing with calcined temperature. The calcinated powders begin to exhibit the spinel crystalline and the disappearance of Al_2O_3 at 1000ºC. With increasing the temperature above 1000 ºC, intensities of the peaks increase gradually until sharpen peaks are observed at 1200ºC [122-123].

The average crystallite sizes calculated from the X-ray diffraction peaks by using scherrer equation. The crystalline spinel phase content and the particles size increase with increasing calcination temperatures that shown in Figure (55). The particle sizes of different doping Co^{2+} systems using oxalyl dihydrazide from XRD are shown in Table (13). The densities of Cobalt systems under investigation calculated from x-ray and compared with the experimental obtained from Archimedes' law in table (16).

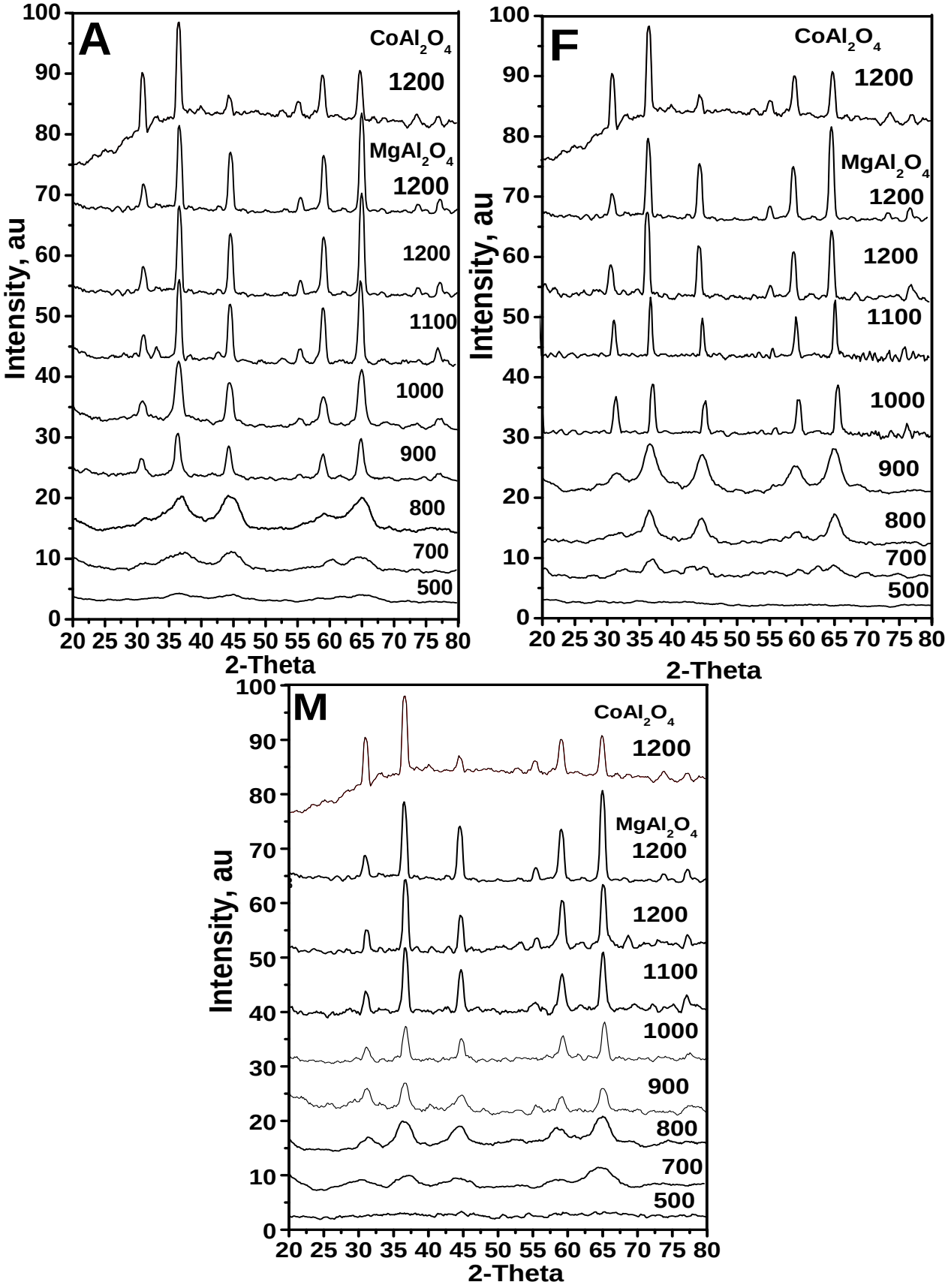

Figure(52): X-ray diffraction for 0.01(A), 0.05 (F) and 0.10 (M) mole of Co^{2+} systems at different calcination temperatures using urea as fuel.

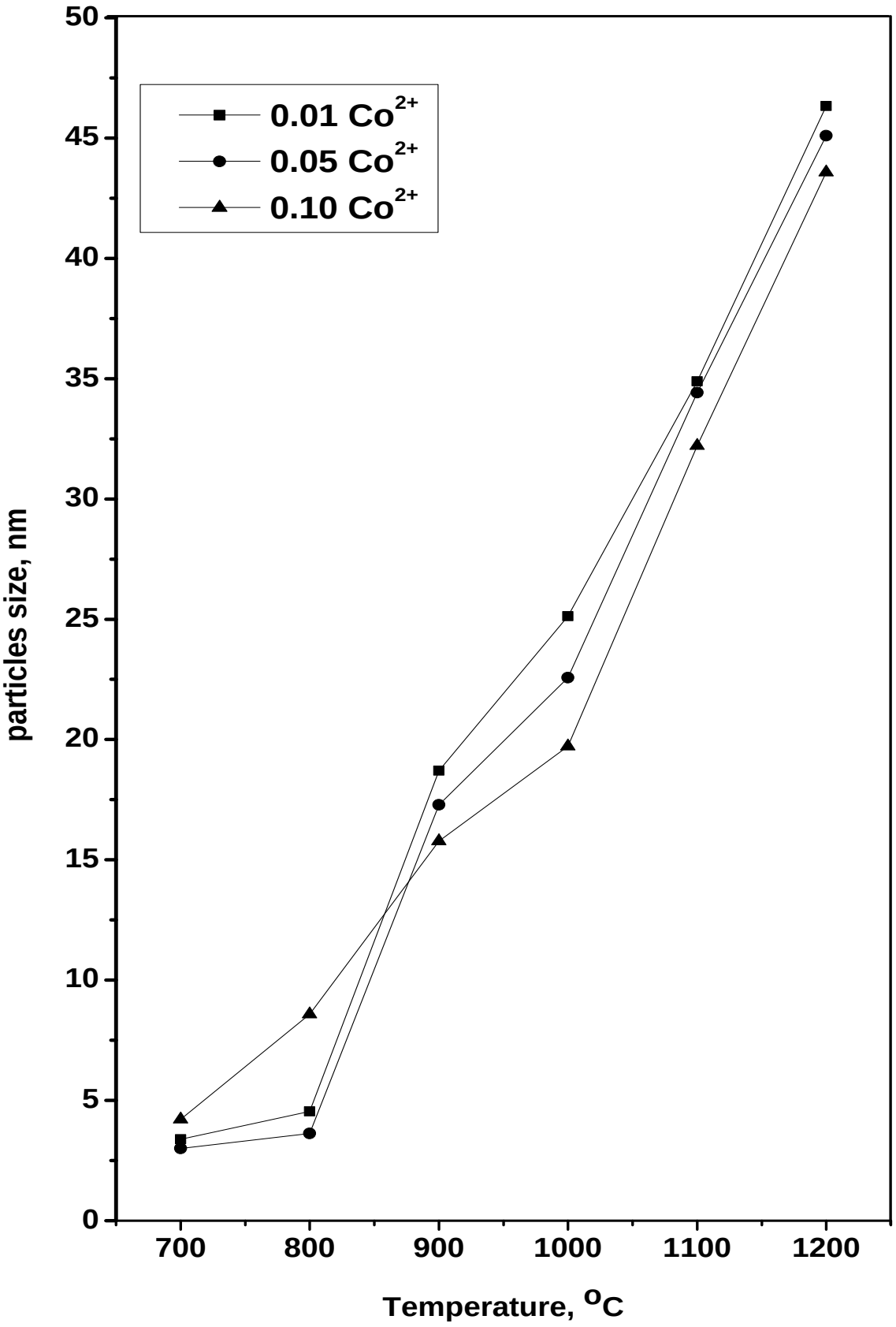

Figure (٥٣): The relation between particle size from X-ray diffraction for 0.01, 0.05 and 0.1 mole of Co^{2+} systems at different calcination temperatures using urea as fuel.

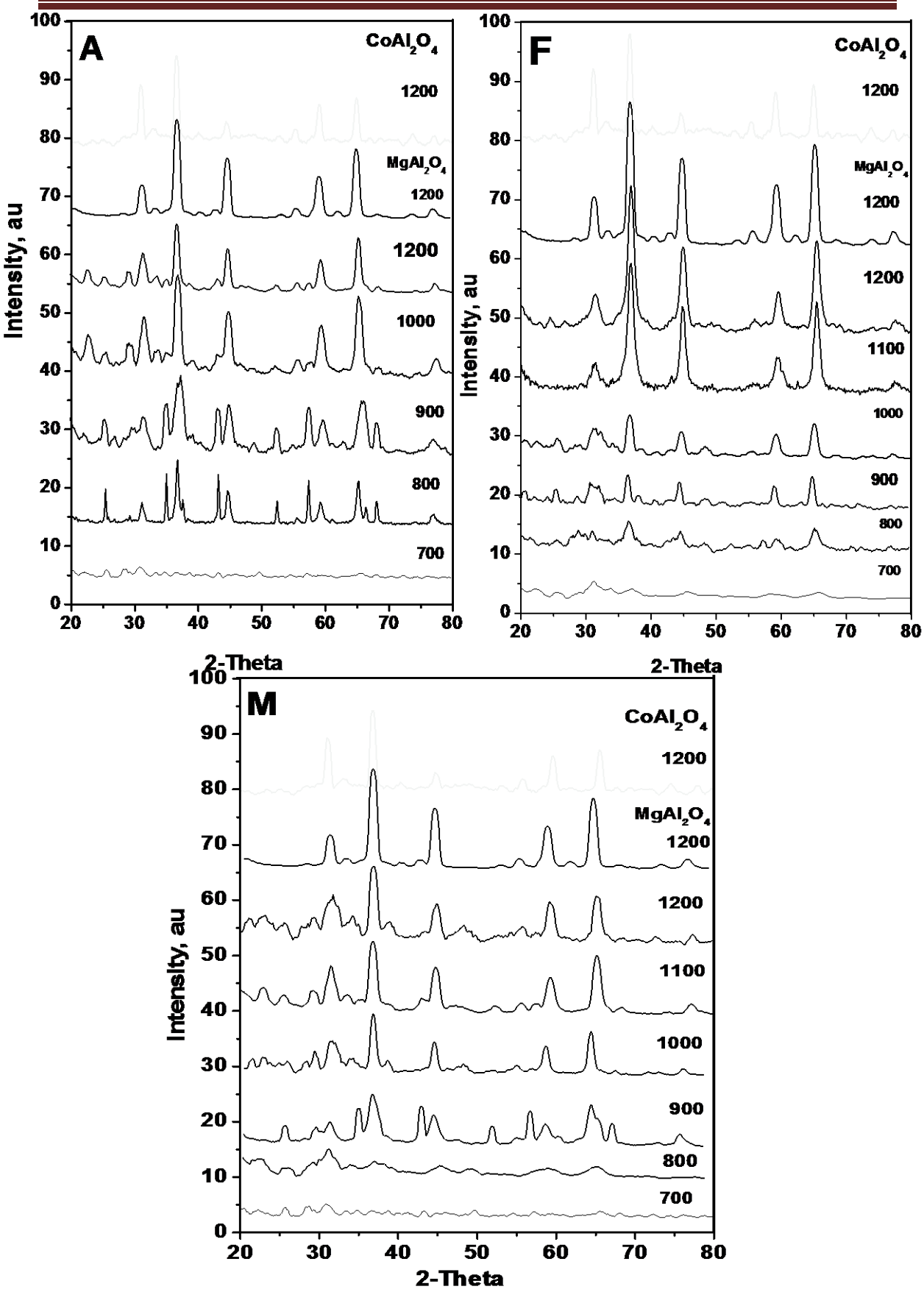

Figure (54): X-ray diffraction for 0.01(A), 0.05(F) and 0.10 (M) mole of Co^{2+} systems at different calcination temperatures using oxalyl dihydrazide as fuel.

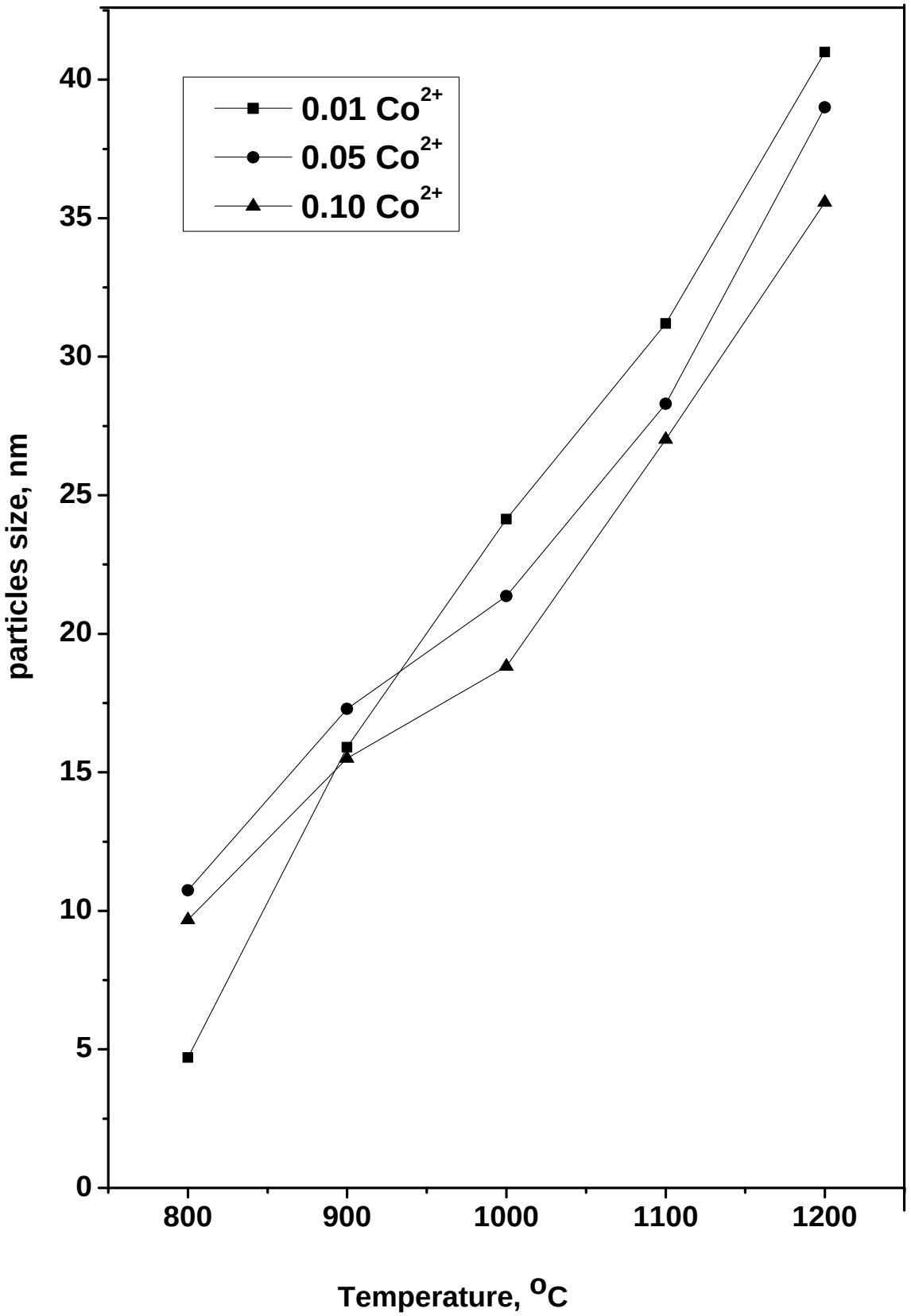

Figure (55): The relation between particle size from X-ray diffraction for 0.01, 0.05 and 0.1 of Co^{2+} systems at different calcinations temperatures using oxalyl dihydrazide as fuel.

3.3.2.3. X-ray diffraction for $Co_xMg_{1-x}Al_2O_4$ system using 3-methyl pyrozole-5-one (3MP5O) as fuel.

The X-ray diffraction for $Co_xMg_{1-x}Al_2O_4$ system, where ($0.10 \geq x \geq 0.01$) using 3-methyl pyrozole-5-one (3MP5O) as fuel is investigated at different calcination temperatures as shown in Figures (56). The peaks intensities of X-ray diffract-gram for amorphous or contained only small crystallites indicated by the broadening lines agree will with data of thermal analysis for the formation of the stable phase. As the calcination temperatures increases the continuously powders begin to exhibit the spinel crystalline. By increasing temperature, the intensities of peaks increase gradually until sharpen peaks are observed at 1200º C.

The average crystallite sizes calculated from the X-ray diffraction peaks by using scherrer equation. The crystalline spinel phase content and the particles size increase with increasing calcination temperatures that shown in Figure (57)**.** The particles sizes of different doping Co^{2+} system using 3-methyl pyrozole-5-one (3MP5O) as fuel from XRD data are given in Table (13). The densities for this system calculated from x-ray diffraction and compared with that experimental obtained from Archimedes' law and given in Table (17).

3.3.2.4. X-ray diffraction for $Co_xMg_{1-x}Al_2O_4$ system using N, N-bis-(3-amino-propyl) oxalamide as fuel.

The X-ray diffraction for cobalt systems using N, N-bis-(3-amino-propyl) oxalamide as fuel at different calcination temperatures are shown in Figures (58). Up to 800º C the peaks intensity of the powders remained X-ray amorphous with only small crystallites that indicated by the broadening lines that agree will with data obtained from thermal analysis for the formation of the stable phase. At 1000ºC, the intensity of peaks increases and

begins to exhibit the spinel crystalline from amorphous phase. By increasing temperature above 1000 ºC, the intensities of the peaks increase gradually until sharpen peaks are observed at 1100º C and 1200º C.

The average crystallite sizes calculated from the X-ray diffraction peaks using scherrer equation. The crystalline spinel phase content and the particles size increase with increasing calcination temperatures shown in Figure (59)**.** The particles sizes of different doping Co^{2+} systems using N, N-bis-(3-amino-propyl) oxalamide as fuel from XRD are calculated as shown in Table (13). Also, the densities of cobalt systems calculated from x-ray and compared with that experimentally obtained from Archimedes' law in Table (18).

The particles sizes for all systems using different fuels decrease as result of the amount of Co^{2+} ion increases. At 900^{o}C, there is no relationship between the sizes of the particles and the type of fuel used for all systems. For 0.01 mole of Co^{2+} system and up to 900^{o}C, the sizes of the particles are much greater for this system using urea as fuel, while particles sizes are smaller ones using N, N-bis-(3-amino-propyl) oxalamide as fuel and overlap and lack of organization of the size of the particles using other two fuels as shown in Figure (60).

Figure (61) shows the particles sizes of 0.05 mole of Co^{2+} system. Up to 900^{o}C, the sizes of the particles is much greater for this system using urea as fuel, while particles sizes are smaller ones using N, N-bis-(3-amino-propyl) oxalamide as fuel and there is a slight increase the particles sizes in the case of the use of oxalyl dihydrazide than 3-methyl pyrozole-5-one (3MP5O) as fuel. For 0.10 mole of Co^{2+} system and up to 900^{o}C, the decreasing of the particle sizes with increase the power and number of the carbon in each fuel as shown in Figure (62).

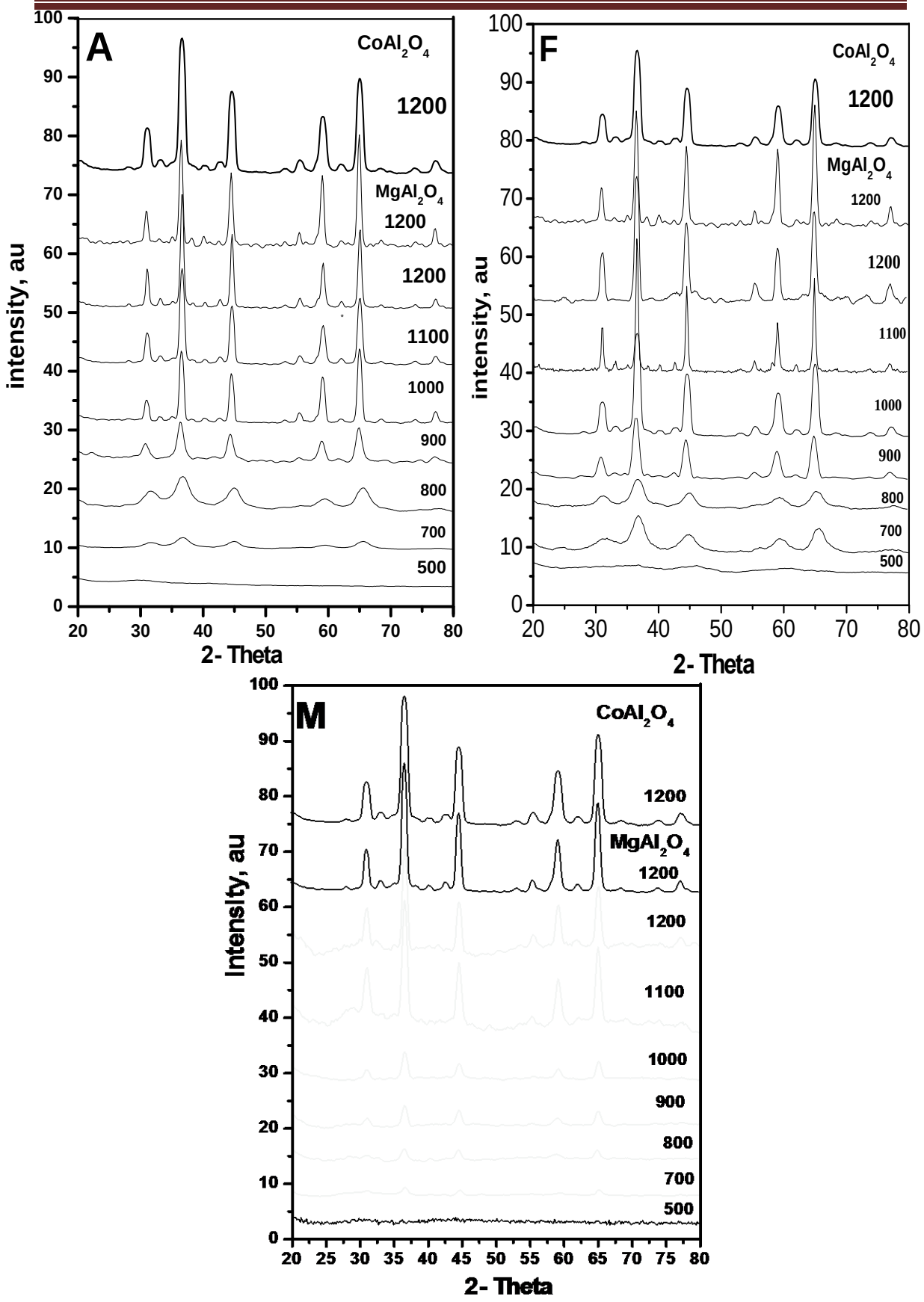

Figure (56): X-ray diffraction for 0.01(A), 0.05 (F) and 0.10(M) mole of Co^{2+} systems at different calcination temperatures using 3-methyl pyrozole-5-one as fuel.

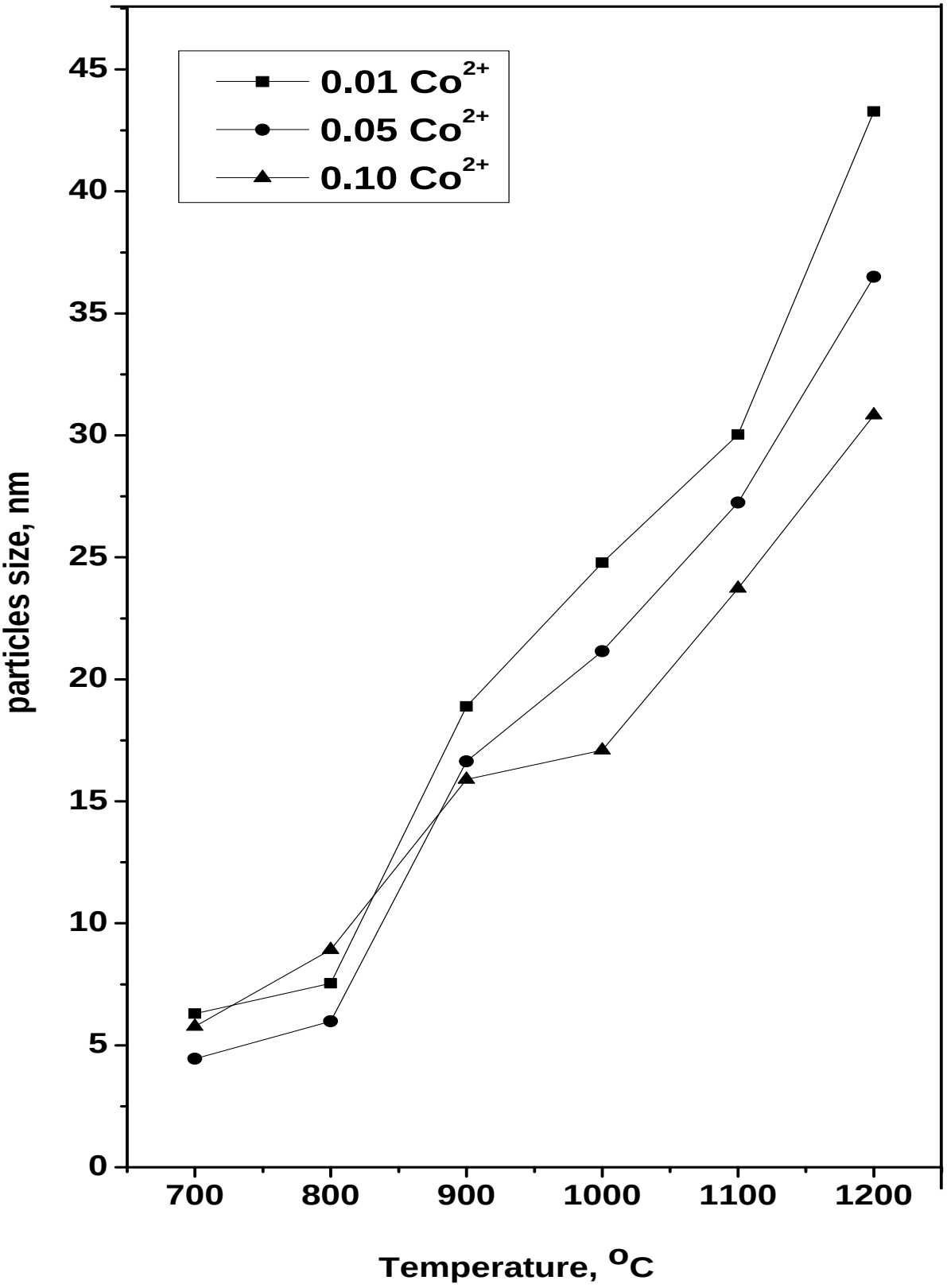

Figure (57): The relation between particle size from X-ray diffraction for 0.01, 0.05 and 0.10 mole Co^{2+} systems at different calcination temperatures using 3-methyl pyrozole-5-one as fuel.

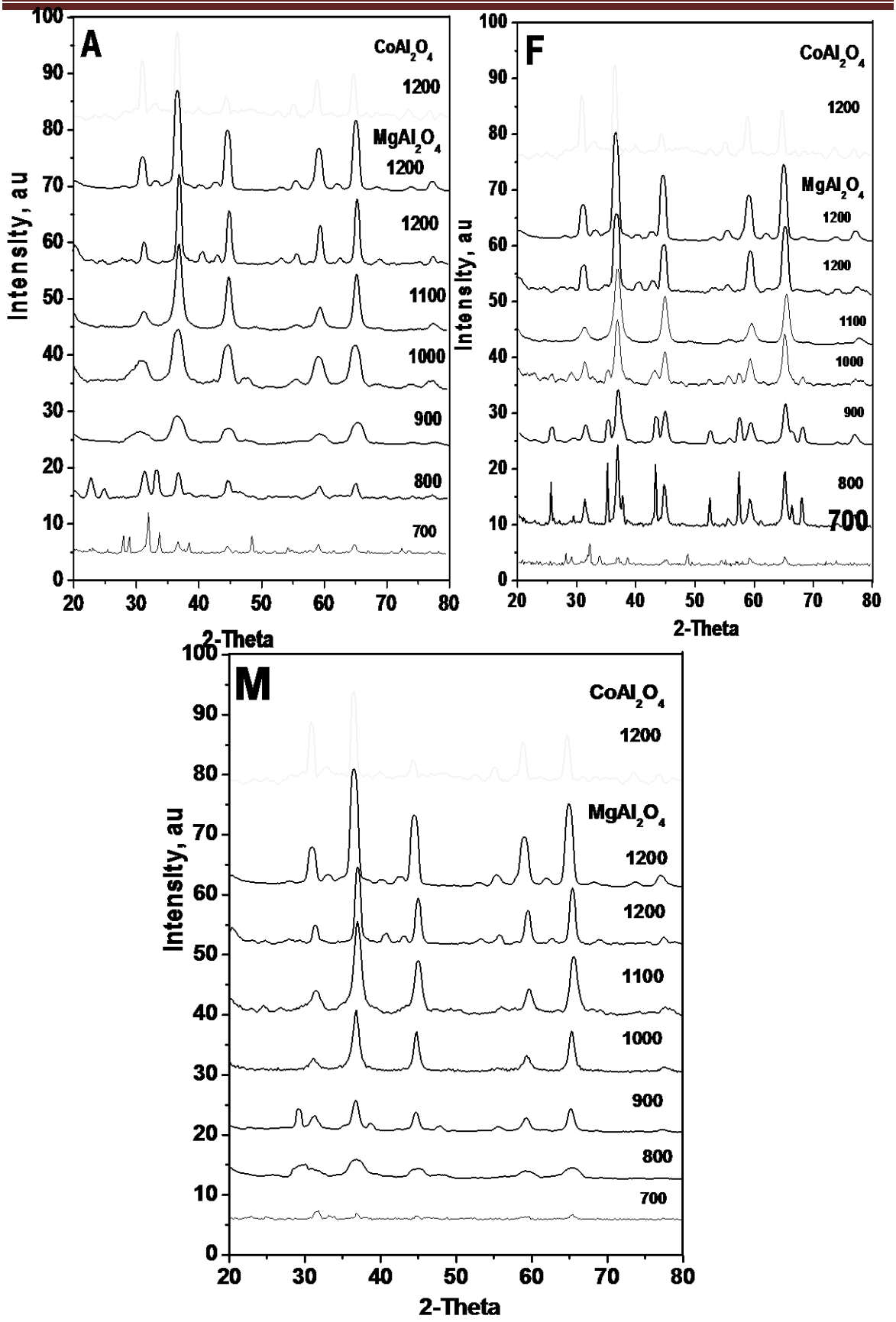

Figure (58): X-ray diffraction for 0.01(A), 0.05 (F), 0.10 (M) mole of Co^{2+} systems at different calcination temperatures using N, N-bis-(3-amino-propyl) oxalamide as fuel.

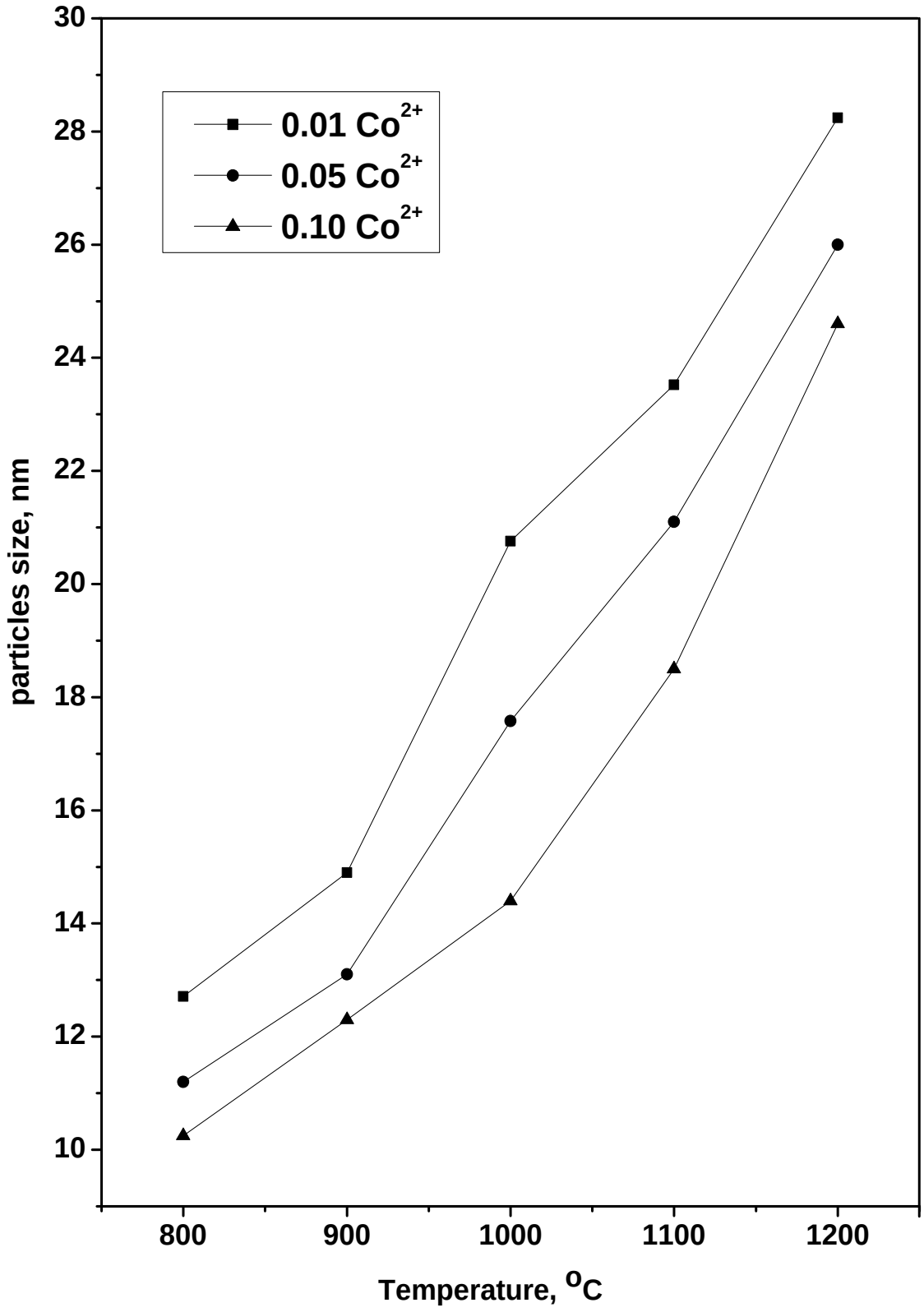

Figure (59): The relation between particle size from X-ray diffraction for 0.01, 0.05 and 0.10 mole of Co^{2+} systems at different calcination temperatures using N, N-bis-(3-amino-propyl) oxalamide as fuel.

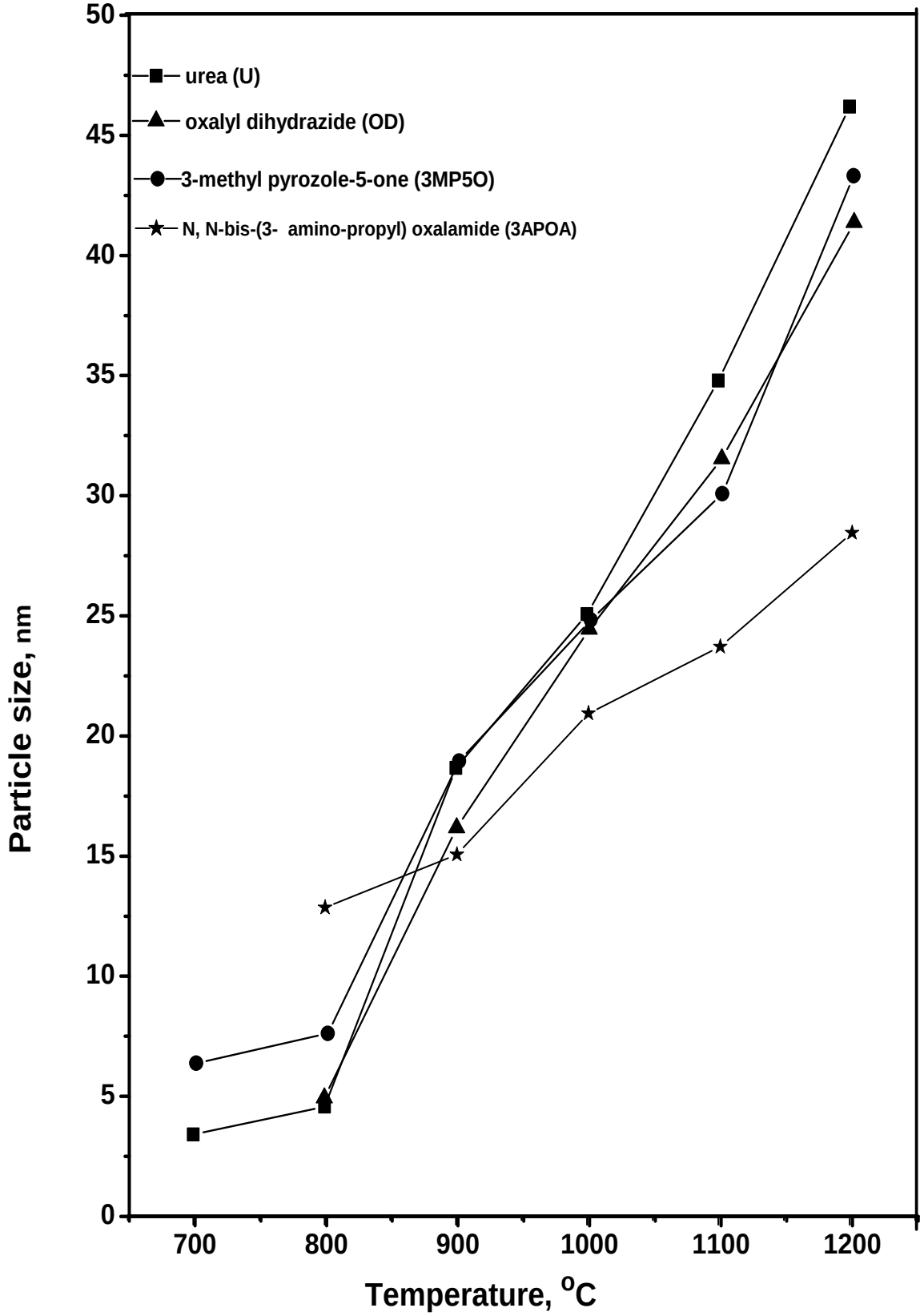

Figure (60): The relation between particle size from X-ray diffraction for 0.01 mole of Co^{2+} systems at different calcination temperatures using different fuels.

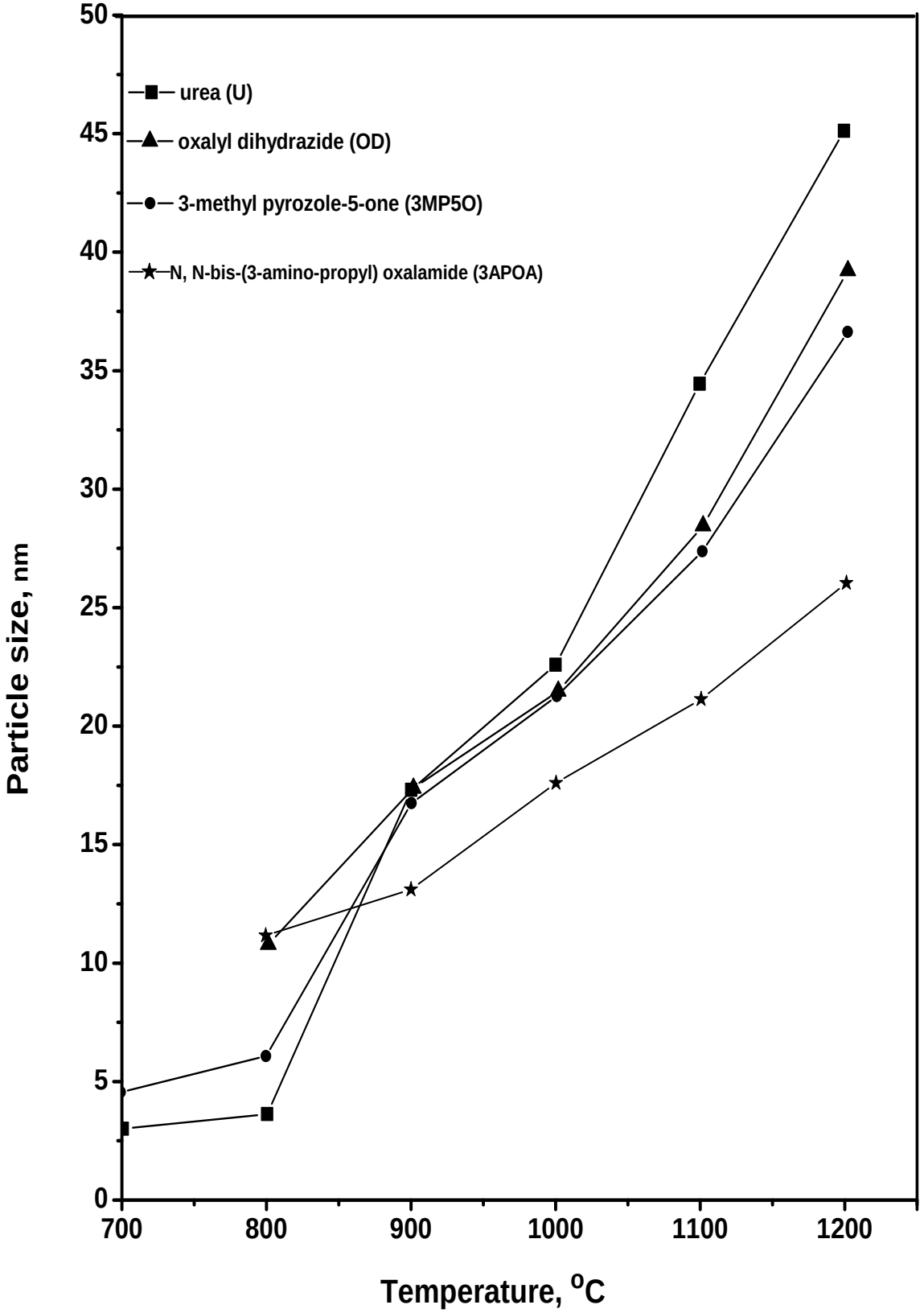

Figure (61): The relation between particle sizes from X-ray diffraction for 0.05 mole of Co^{2+} systems at different calcination temperatures using different fuels.

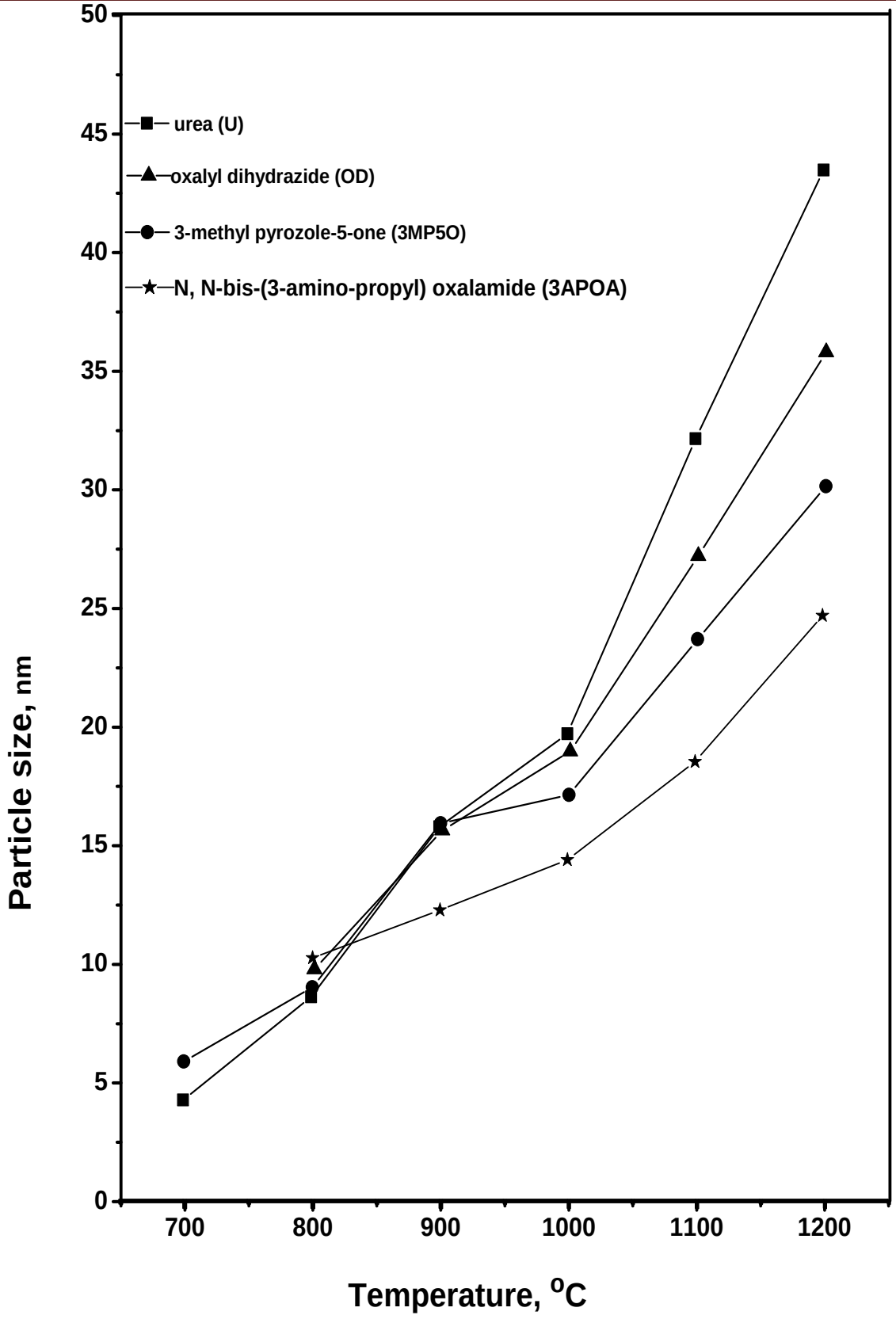

Figure (62): The relation between particle sizes from X-ray diffraction for 0.10 mole of Co^{2+} systems at different calcination temperatures different fuels.

Table(13): Particles sizes (nm) from X-ray diffraction for different Co^{2+} systems at different calcination temperatures using different fuels.

Fuel	System	calcination temperatures, ^{o} C						
		٥٠٠	٧٠٠	٨٠٠	٩٠٠	١٠٠٠	١١٠٠	١٢٠٠
Urea	٠,٠١	Am	٣,٣٨	4.54	18.7	٢٥,١٣	34.89	46.33
	٠,٠٥	Am	٣	٣,٦٢	١٧,٧٦	٢٢,٥٧	34.42	٤٥,١٠
	٠,١	Am	4.22	٨,٥٨	15.78	19.72	32.21	43.58
OD	٠,٠١	-	Am	٤,٧	١٥,٩٠	٢٤,١٤	٣١,٢٠	٣٧,٦٩
	٠,٠٥	-	Am	٣,١	١٧,٢٩	٢١,٣٦	٢٨,٣٠	٣١,١٧٥
	٠,١	-	Am	٩,٦٨	١٥,٥٠	١٨,٨٢	٢٧,٠٢	٣٥,٥٧
3MP5O	٠,٠١	Am	٦,٣	٧,٥٤	18.89	٢٤,٧٨	30.03	٤٣,٢٨
	٠,٠٥	Am	٤,٤٥	5.98	16.64	٢١,١٥	27.25	٤٢,١٢
	٠,١	Am	٥,٧٧	8.92	15.90	17.10	23.73	٣٠,٨٣
3APOA	٠,٠١	-	Am	١٢,٧١	١٤,٩٠	٢٠,٧٦	٢٣,٥٢	٢٨,٢٤
	٠,٠٥	-	Am	١١,١٥٧	١٣,١٠	١٧,٥٨	٢١,١٠	٢٦,٠٠
	٠,١	-	Am	١٠,٢٥	١٢,٣٠	١٤,٣٦	١٨,٥٠	٢٤,٦٠

OD =oxalyl dihydrazide, 3MP5O=3-methyl pyrozole-5-one, 3APOA= N, N-bis-(3-amino-propyl) oxalamide, Am=Amorphous

Table (14): XRD crystallite and TEM particle sizes for different Cobalt systems at 1100ºC using different fuels.

Fuel	System	Particle size (nm)	
		X-ray	TEM
Urea	٠,٠١	34.89	35.00
	٠,٠٥	34.42	٣٤,٠٠
	٠,١٠	32.21	33.30
OD	٠,٠١	٣١,٢٠	٣٢,٠٠
	٠,٠٥	٢٨,٣٠	٣٠,٠٠
	٠,١٠	٢٧,٠٢	٢٨,٠٠
3MP5O	٠,٠١	30.03	٣٤,٨٠
	٠,٠٥	27.25	٣٢,٢٠
	٠,١٠	23.73	٢٨,٦٠
3APOA	٠,٠١	٢٣,٥٢	٢٤,٠٠
	٠,٠٥	٢١,١٠	٢٢,٠٠
	٠,١٠	١٨,٥٠	٢٠,٠٠

Tables(15):Lattice parameters and densities of different cobalt systems using urea as fuel.

system	parameters	Calcinations Temperature, ^{o}C					
		٧٠٠	٨٠٠	٩٠٠	١٠٠٠	١١٠٠	١٢٠٠
٠,٠١	a	٨,٠٧٥	٨,٠٨٠٦	٨,٠٨٨٧	٨,١٠٦٦	٨,١٢٣١	٨,١٣٩٣
	a^3	٥٢٦,٥٤	٥٢٧,٦٣	٥٢٩,٢٢	٥٣٢,٧٥	٥٣٦	٥٣٩,٢١
	$d_{theo.}$ g\ml	٣,٥٩١	٣,٥٨٣	٣,٥٧٣	٣,٥٥٠	٣,٥٣٠	٣,٥١٠
	$d_{exp.}$ g\ml	٣,٥٧٠	٣,٥٦٠	٣,٥٥٠	٣,٥٣٠	٥,٥٠٠	٥,٤٩٠
٠,٠٥	a	٨,٠٧٠	٨,٠٨٠٦	٨,٠٨٥	٨,٠٩٤٨	٨,١٢٣١	٨,١٣٩٣
	a^3	٥٢٥,٤٥	٥٢٧,٦٣	٥٢٨,٤٩	٥٣٠,٤٢	٥٣٦	٥٣٩,٢١
	$d_{theo.}$ g\ml	٣,٦٣٢	٣,٦١٨	٣,٦١٢	٣,٥٩٨٤	٣,٥٦٢	٣,٥٤٠
	$d_{exp.}$ g\ml	٣,٥٨٠	٣,٥٧٠	٣,٥٥٠	٣,٥٣٣	٣,٥١٠	٣,٥٠٠
٠,١٠	a	٨,٠٧٥	٨,٠٨٠٦	٨,٠٨٥	٨,٠٩٤٨	٨,١٠٦٦	٨,١٣٩٣
	a^3	٥٢٦,٥٤	٥٢٧,٦٥	٥٢٨,٤٩	٥٣٠,٤٢	٥٣٢,٢٧	٥٣٩,٢١
	$d_{theo.}$ g\ml	٣,٦٦٨	٣,٦٦٠	٣,٦٥٤	٣,٦٤٢	٣,٦٣٠	٣,٥٨١
	$d_{exp.}$ g\ml	٣,٦٥٠	٣,٦٣٠	٣,٦١٠	٣,٦٠٠	٣,٥٨٠	٣,٥٦٠

a= Lattice parameters, d_{theo}= theoretical density and d_{exp}= experimental density

Tables(16): Lattice parameters and densities of different cobalt systems using oxalyl dihydrazide as fuel.

system	parameters	Calcinations Temperature, ^{o}C				
		٨٠٠	٩٠٠	١٠٠٠	١١٠٠	١٢٠٠
٠,٠١	a	٨,٠٧٥	٨,٠٨٥	٨,٠٨٨٧	٨,١٠٦٦	٨,١٢٣١
	a^3	٥٢٦,٥٤	٥٢٨,٤٩	٥٢٩,٢٢	٥٣٢,٢٧	٥٣٦
	d_{theo} g\ml	٣,٥٩٠	٣,٥٧٩٨	٣,٥٧٢	٣,٥٥٢	٣,٥٤٨
	d_{exp} g\ml	٣,٥٧٠	٣,٥٦٠	٣,٥٥٠	٣,٥٣٠	٣,٥١٠
٠,٠٥	a	٨,٠٧٠	٨,٠٧٥	٨,٠٨٠٦	٨,٠٨٥	٨,٠٩٤٨
	a^3	٥٢٥,٤٥	٥٢٦,٥٤	٥٢٧,٦٥	٥٢٨,٤٩	٥٣٠,٤٢
	d_{theo} g\ml	٣,٧٠٣	٣,٦٢٤	٣,٦١٨	٣,٦١١	٣,٥٩٨
	d_{exp} g\ml	٣,٧٠٠	٣,٦٠٠	٣,٥٧٠	٣,٥٥٠	٣,٥٣٥
٠,١٠	a	٨,٠٧٠	٨,٠٧٥	٨,٠٨٠٦	٨,٠٨٥	٨,٠٨٨٧
	a^3	٥٢٥,٤٥	٥٢٦,٥٤	٥٢٧,٦٥	٥٢٨,٤٩	٥٢٩,٢٢
	d_{theo} g\ml	٣,٦٧٤	٣,٦٦٧٨	٣,٦٦٠	٣,٦٥٤	٣,٦٥٠
	d_{exp} g\ml	٣,٦٥٠	٣,٦٣٣	٣,٦١٠	٣,٦٠٠	٣,٩٥٠

a= Lattice parameters, d_{theo}= theoretical density and d_{exp}= experimental density

Tables(17): Lattice parameters and densities of different cobalt systems using 3-methyl pyrozole-5-one as fuel.

System	parameters	Calcinations Temperature, ^{o}C					
		٧٠٠	٨٠٠	٩٠٠	١٠٠٠	١١٠٠	١٢٠٠
٠,٠١	a	٨,٠٧٠	٨,٠٧٥	٨,٠٨٠٦	٨,٠٨٥	٨,١٠٦٦	٨,١٢٣١
	a^3	٥٢٥,٥٦	٥٢٦,٥٤	٥٢٧,٦٣	٥٢٨,٤٩	٥٣٢,٧٥	٥٣٦
	d_{theo}g\ml	٣,٥٩٨	٣,٥٩١	٣,٥٨٤	٣,٥٧٨	٣,٥٤٩	٣,٥٢٨
	d_{exp}g\ml	٣,٥٦٣	٣,٥٥٤	٣,٥٣٨	٣,٥٢٥	٣,٥١٠	٣,٤٩٠
٠,٠٥	a	٨,٠٧٠	٨,٠٧٥	٨,٠٨٥	٨,٠٨٨٧	٨,١٠٦٦	٨,١٢٣١
	a^3	٥٢٥,٥٦	٥٢٦,٥٤	٥٢٨,٤٩	٥٢٩,٢٢	٥٣٢,٧٥	٥٣٦
	d_{theo} g\ml	٣,٦٣٢	٣,٦٢٥	٣,٦١٢	٣,٦٠٧	٣,٥٨٣	٣,٥٦٢
	d_{exp}g\ml	٣,٦١٥	٣,٦٠٠	٣,٩٥٥	٣,٩١٠	٣,٥٨٠	٣,٥٥٠
٠,١٠	a	٨,٠٧٥	٨,٠٨٠٦	٨,٠٨٥	٨,٠٨٨٧	٨,٠٩٤٨	٨,١٠٦٦
	a^3	٥٢٦,٥٤	٥٢٧,٦٥	٥٢٨,٤٩	٥٢٩,٢٢	٥٣٠,٤٢	٥٣٢,٧٥
	d_{theo}g\ml	٣,٦٧٤	٣,٦٦٠	٣,٦٥٤	٣,٦٥٠	٣,٦٤٢	٣,٦٢٦
	d_{exp}g\ml	٣,٦٥٥	٣,٦٤٥	٣,٦٣٥	٣,٦٢٢	٣,٦١٥	٣,٦٠٠

a= Lattice parameters, d_{theo}= theoretical density and d_{exp}= experimental density

Tables(18): Lattice parameters and densities of different cobalt systems using N, N-bis-(3-amino-propyl) oxalamide as fuel.

System	parameters	Calcinations Temperature, ^{o}C				
		٨٠٠	٩٠٠	١٠٠٠	١١٠٠	١٢٠٠
٠,٠١	a	٨,٠٧٠	٨,٠٧٥	٨,٠٨٠٦	٨,٠٨٨٧	٨,٠٩٤٨
	a^3	٥٢٥,٥٦	٥٢٦,٥٤	٥٢٧,٦٥	٥٢٩,٢٢	٥٣٠,٤٢
	d_{theo}g\ml	٣,٥٩٨	٣,٥٩٠	٣,٥٨٠	٣,٥٧٢	٣,٥٦٠
	d_{exp}g\ml	٣,٥٩٠	٣,٥٦٥	٣,٥٥٠	٣,٥٣٥	٣,٥٢٠
٠,٠٥	a	٨,٠٧٠	٨,٠٧٥	٨,٠٨٠٦	٨,٠٨٥	٨,٠٨٨٧
	a^3	٥٢٥,٥٦	٥٢٦,٥٤	٥٢٧,٦٥	٥٢٨,٤٩	٥٢٩,٢٢
	d_{theo} g\ml	٣,٦٣٢	٣,٦٢٥	٣,٦١٨	٣,٦١٢	٣,٦٠٧
	d_{exp} g\ml	٣,٦٢٥	٣,٦١٠	٣,٦٠٠	٣,٩٥٠	٣,٩٠٠
٠,١٠	a	٨,٠٧٠	٨,٠٧٥	٨,٠٨٠٦	٨,٠٨٥	٨,٠٨٨٧
	a^3	٥٢٥,٥٦	٥٢٦,٥٤	٥٢٧,٦٥	٥٢٨,٤٩	٥٢٩,٢٢
	d_{theo} g\ml	٣,٦٧٥	٣,٦٦٨	٣,٦٦٠	٣,٦٥٤	٣,٦٥٠
	d_{exp} g\ml	٣,٦٥٠	٣,٦٣٥	٣,٦٢٥	٣,٦١٠	٣,٦٠٠

a= Lattice parameters, d_{theo}= theoretical density and d_{exp}= experimental density

3.3.3. Microstructure characterization for $Co_xMg_{1-x}Al_2O_4$ system of ceramic pigments

Microstructure characterizations of ceramic pigments at different calcination temperatures are performed using transmission electron microscopy (TEM). The particle sizes are calculated also from TEM photographs using ultrastructure size calculator or quantitative electron microscopy using an areal analysis. Measurements of at least 20 particles were required to characterize each size distribution from TEM photographs.

3.3.3.1. Microstructure characterization for $Co_xMg_{1-x}Al_2O_4$ system using urea as fuel.

The microstructures for powder compounds under investigation formed using urea as fuel and studied using transmission electron microscopy. Figure (63) give the TEM photographs of samples which show the sheet and spherical shapes for 0.01 mole of Co^{2+} system and spherical particles for 0.05 and 0.1 mole of Co^{2+} systems. The particle sizes are determined using TEM and are compared with that obtained from XRD and collective data in Table (14). The morphology and particle sizes are decreased with increasing the amount of doping Co^{2+} ion.

3.3.3.2. Microstructure characterization for $Co_xMg_{1-x}Al_2O_4$ system using oxalyl dihydrazide as fuel.

Transmission electron microscopy (TEM) photographs shown in Figure (64) for the compounds under investigation using oxalyl dihydrazide as fuel exhibit the spherical particles for 0.01, 0.05 and 0.1 mole of Co^{2+} systems. The particle sizes calculated by XRD are compared with the data obtained from TEM and present in Table (14). Also, the morphology and particle sizes are decreased as the amount of doping Co^{2+} ion increases.

3.3.3.3. Microstructure characterization for $Co_xMg_{1-x}Al_2O_4$ system using 3-methyl pyrozole-5-one (3MP5O) as fuel.

Transmission electron microscopy (TEM) photographs of powder samples using 3-methyl pyrozole-5-one (3MP5O) as fuel show spherical particles that shown in Figure (65). The particle sizes observed by TEM are agreement with that observed by XRD as present in Table (14). The morphology and particle size decrease with increasing the amount of doping.

3.3.3.4. Microstructure characterization for $Co_xMg_{1-x}Al_2O_4$ system using N, N-bis-(3- amino-propyl) oxalamide as fuel.

Transmission electron microscopy (TEM) photographs of powder samples for A, F and M systems using N, N-bis-(3-amino-propyl) oxalamide as fuel show the spherical particles as present in Figure (66). The particle sizes observed by TEM are agreement with that observed by XRD as present in Table (14). The morphology and particle size decrease with increasing the amount Co^{2+} ion.

From all these data, the morphology of $CoAl_2O_4$ and $MgAl_2O_4$ spinel for different systems has the spherical shapes and particles size decrease as the type of fuel is changed. The morphology and particles size depend on the number of carbon atoms in different fuel and amount of energy evaluated as result of ignition.

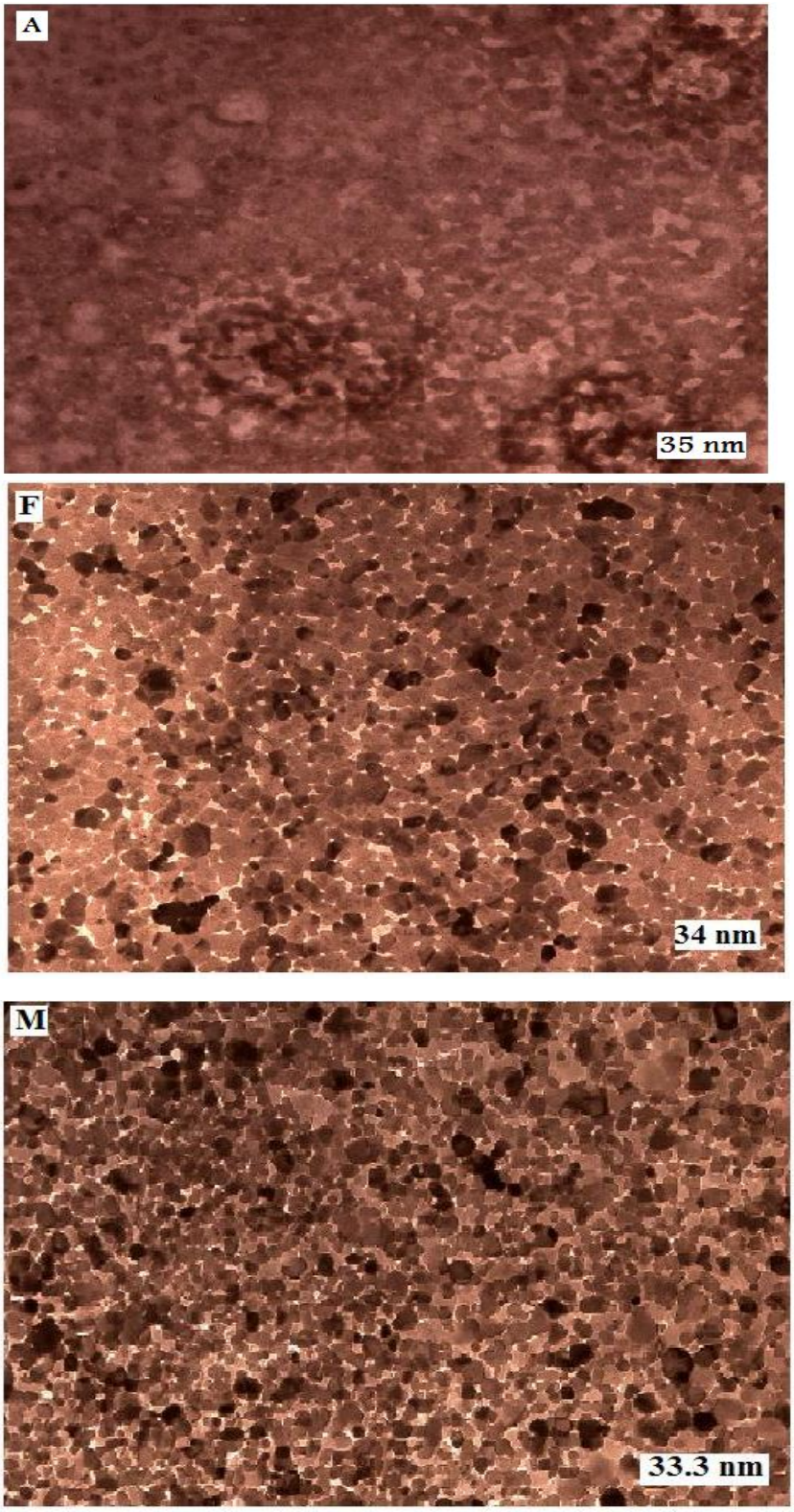

Figure (63):Transmission electron microscopy (TEM) for A=0.01, F=0.05 and M=0.10 mole of Co^{2+} systems at 1100ºC by using urea as fuel.

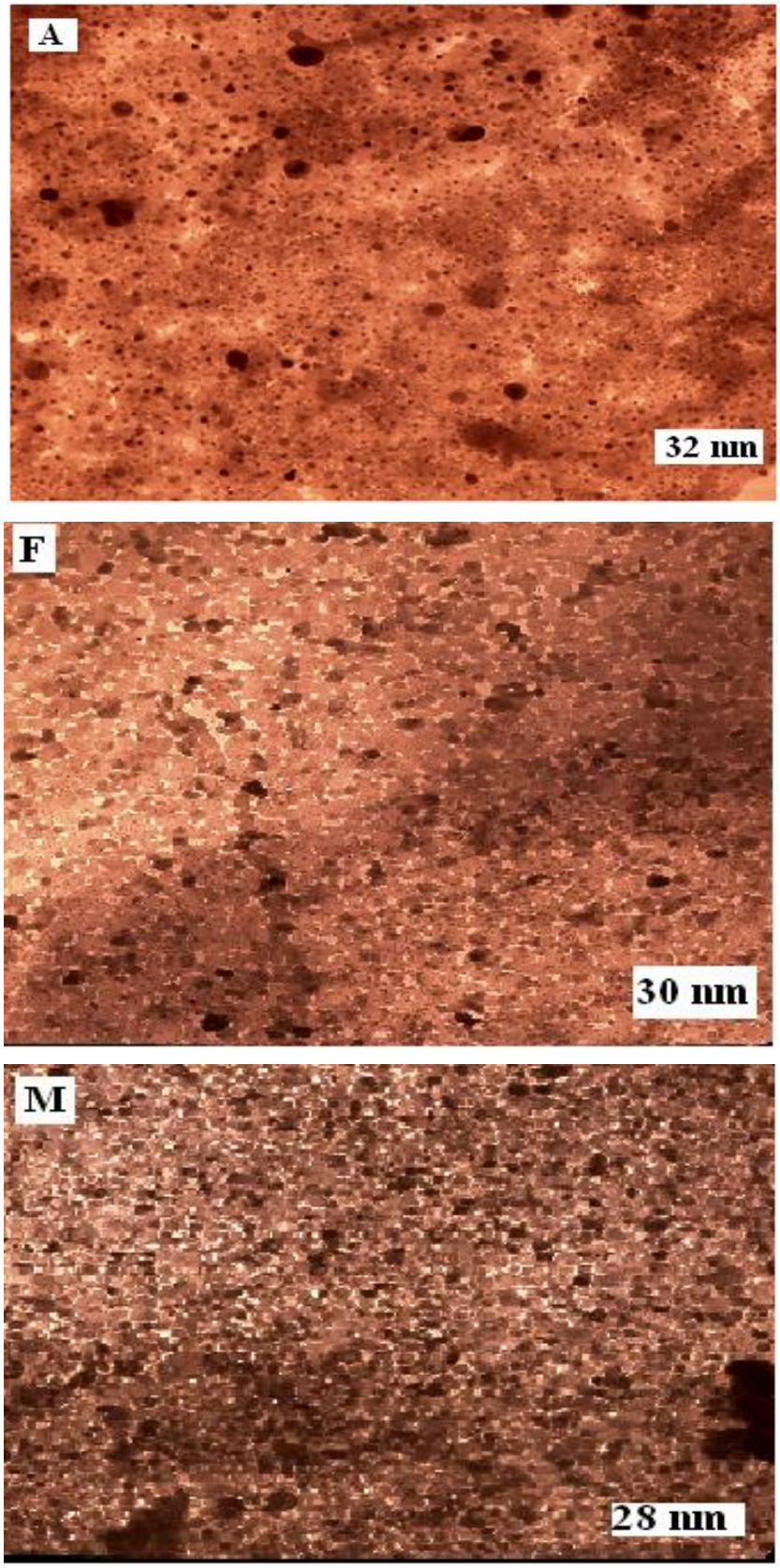

Figure (64):Transmission electron microscopy (TEM) for A=0.01, F=0.05 and M=0.10 mole of Co^{2+} systems at 1100ºC by using oxalyl dihydrazide as fuel.

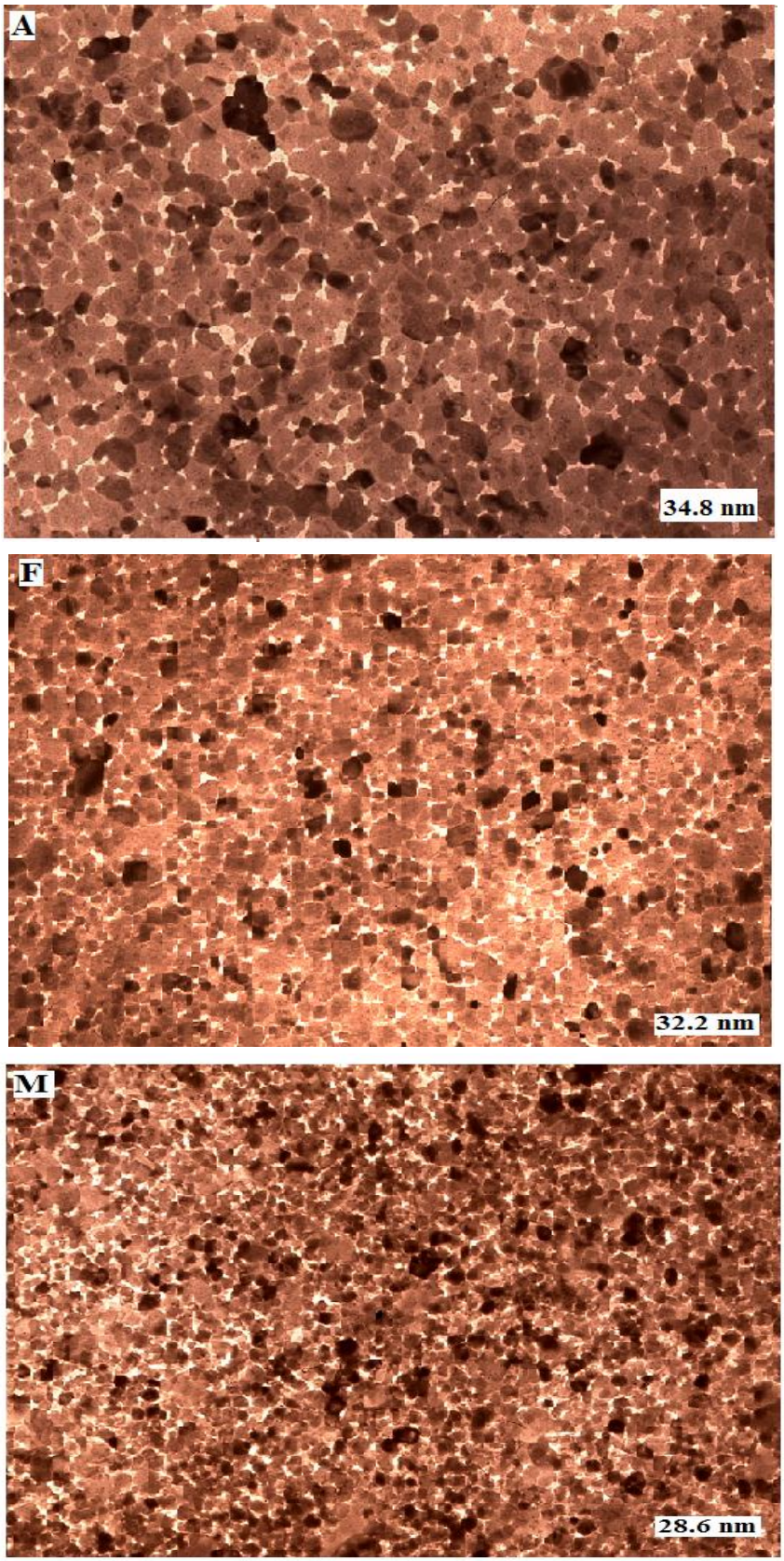

Figure (65):Transmission electron microscopy (TEM) for A=0.01, F=0.05 and M=0.10 mole of Co^{2+} systems at 1100ºC by using 3-methyl pyrozole-5-one as fuel.

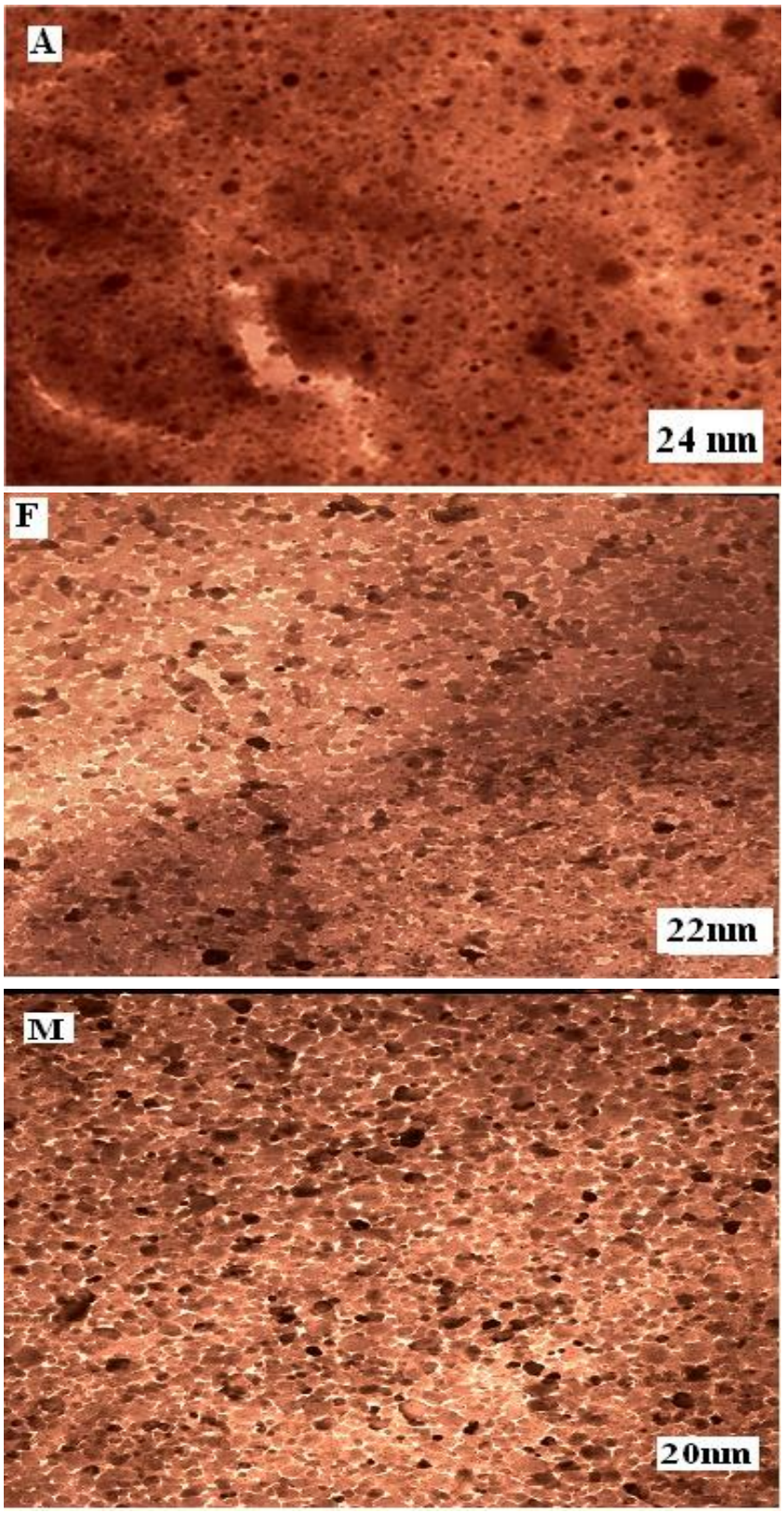

Figure (66):Transmission electron microscopy (TEM) for A=0.01, F=0.05 and M=0.10 mole of Co^{2+} systems at 1100ºC by using N, N-bis-(3-amino-propyl) oxalamide as fuel.

3.4. The crystal structure characterization for $Ni_xMg_{1-x}Al_2O_4$ system.

3.4.1. The thermal analysis.

3.4.1.1. Thermal analysis for 0.50 mole of Ni^{2+} system using urea as fuel.

The thermalgravimetric analysis for 0.50 mole of Ni^{2+} system using urea as fuel give a weight losing of urea system changes in three steps as shown in TGA curve for ash material as present in Figure (67). The losing of 10% (calc. 9%) by weight in the first step within the range 50-100 ºC occurs for elimination of the humidity water in sample. The losing of 9.5% (calc. 9.5%) in the second in the range100-300ºC and the third steps 300-550ºC occur due to evolution of CO_2 gas from sample. Three endothermic steps in DTG curve that shown at 100, 300 and 550 ºC. DTA shows two endothermic steps at 100 and 700 ºC and one exothermic reaction at 350 ºC. The first endothermic step occurs for elimination of the water and the second exothermic step for elimination of t he residual organic material in sample as carbon dioxide. The third endothermic reaction step shows phase formation and appearance of phase under study. The activation energy is calculated from TG-curves by using Coats-Redfern[117] method. The activation energy of this system equals to13.86 kJ/mol. The calcination steps for this system can be represented as the following:

$$(NiO)_{0.5}.\ (Mg\ CO_3)_{0.5}\ .\ Al_2O_3.\ H_2O \xrightarrow{\text{50-100 ºC}} Ni_{0.5}O.Mg_{0.5}\ CO_3.Al_2O_3 + H_2O$$

$$Ni_{0.5}.\ Mg_{0.5}\ CO_3\ .Al_2O_3 \xrightarrow{\text{100-550 º C}} Ni_{0.5}Mg_{0.5}Al_2O_4 + 0.5CO_2$$

3.4.2. Thermal analysis for 0.50 mole of Ni^{2+} system using urea as fuel.

The thermalgravimetric curve in Figure (68) for 0.50 mole of Ni^{2+} system using 3-methyl pyrozole-5-one (3MP5O) as fuel shows that the weight loss percentages were 10% (calc. 9.6%) in range 50–200ºC, this lose can be attributed to elimination of the humidity water in sample. The weight loss of 34% (calc.35%), in range 200–300 ºC, represents the removal of the organic molecule. The masses remaining at 550 °C were 15% (calc. 15%) corresponding to the removal of CO,CO_2, and NH_3 gases from the sample then the solid solution of Nickel aluminates and magnesium aluminates began to be formed at 550°C. DTG shows three endothermic steps at 100, 300 and 550 ºC. Also, DTA shows three endothermic steps at 100, 250 and 650 ºC and one exothermic reaction at 400 ºC. The first and second endothermic steps occurred for elimination of the humidity water and the third exothermic step for elimination of the residual organic material in sample. The fourth endothermic reaction step shows phase formation and appearance of phase under study. The activation energy is calculated from TG-curves by using Coats-Redfern[117] method. The activation energy of this system equals to16.628 kJ/mol. The calcination steps for this system can be represented as the following:

$$Ni_{0.5}.\ Mg_{0.5}\ O + Al_2\ (CO_3)_3.\ 0.5(C_4H_6N_2O).\ 2H_2O \xrightarrow{\text{50-200 º C}} Ni_{0.5}O.\ Mg_{0.5}\ Al_2(O)(CO_3)_3\ .\ 0.5(C_4H_6N_2O) + 2H_2O$$

$$Ni_{0.5}O.\ Mg_{0.5}\ Al_2(O)_2(CO_3)_3\ .\ 0.5(C_4H_6N_2O) \xrightarrow{\text{200-300 º C}} Ni_{0.5}O.\ Mg_{0.5}\ Al_2(O)_2\ (CO_3)_2 + 2\ CO_2 + CO + NH_3$$

$$Ni_{0.5}O.\ Mg_{0.5}\ Al_2(O)_2(CO_3)_2 \xrightarrow{\text{300-500 ºC}} Ni_{0.5}\ Mg_{0.5}\ Al_2O_4 + 2CO$$

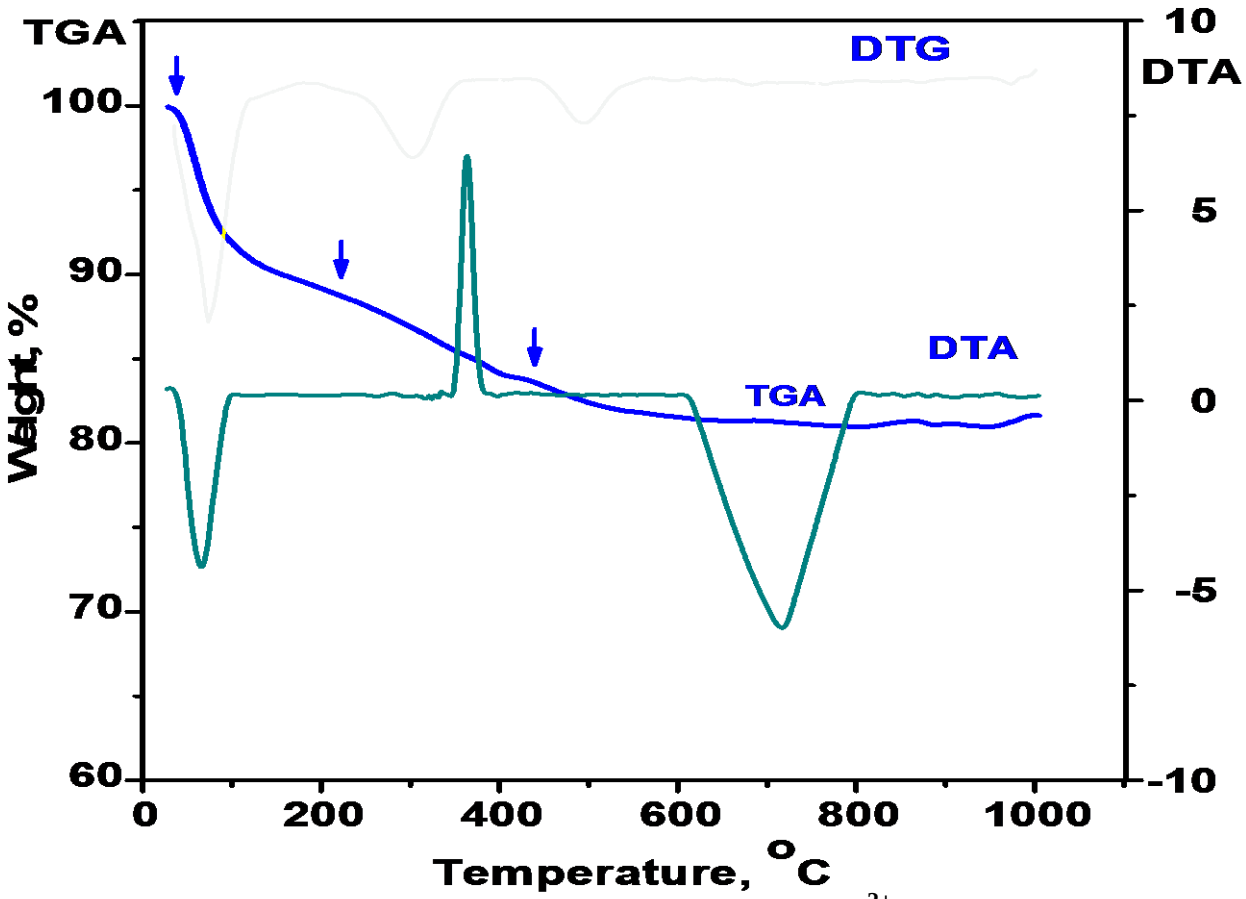

Figure (٦7): Thermal analysis for F=0.05 mole of Ni^{2+} system using urea as fuel.

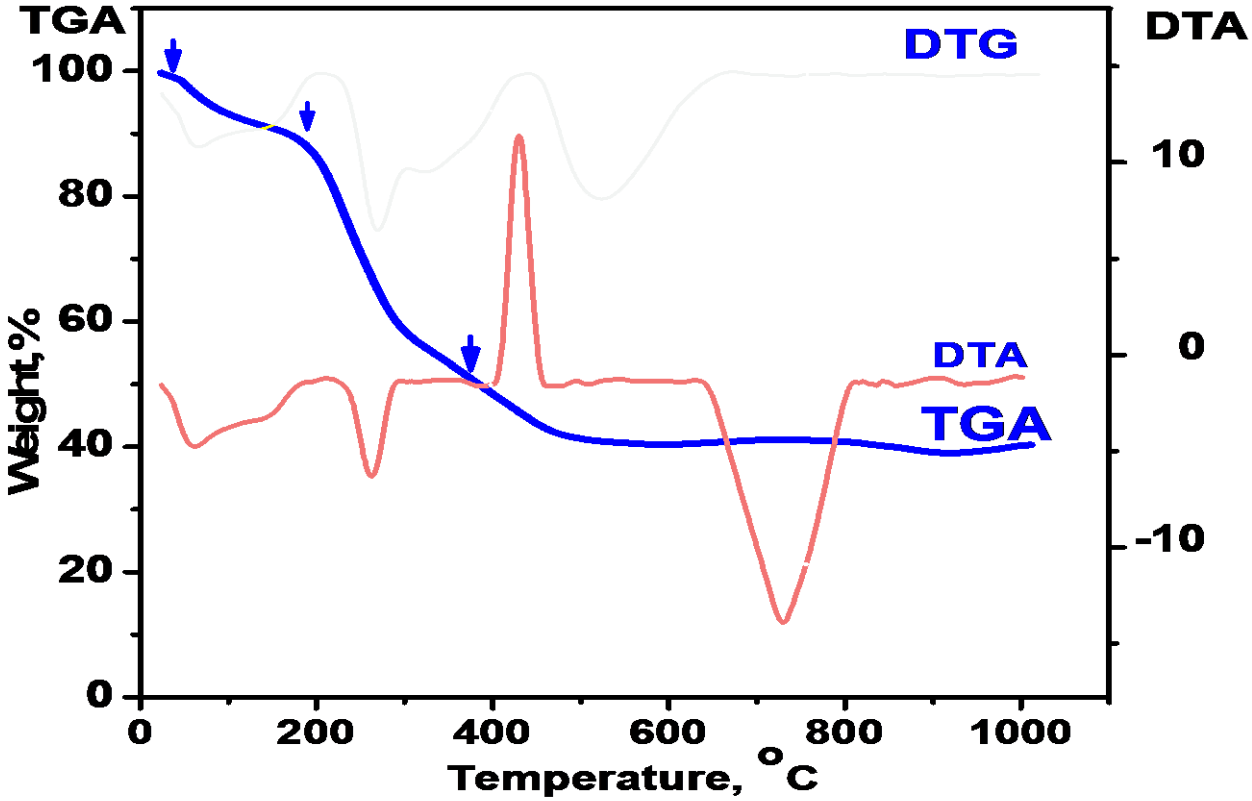

Figure (68): Thermal analysis for F=0.05 mole of Ni^{2+} system using 3-methyl pyrozole-5-one (3MP5O) as fuel.

3.4.2. X-ray diffraction analysis (XRD) for $Ni_xMg_{1-x}Al_2O_4$ systems.

3.4.2.1. X-ray diffraction of $Ni_xMg_{1-x}Al_2O_4$ system using urea as fuel.

The x-ray diffraction of calcinated powders at different firing temperatures using urea as fuel is shown in Figures (69). Up to 800º C, the powders remained X-ray amorphous or contained only small crystallites lines with small Al_2O_3 peaks. Up to 900º C, the calcinated powders begin to show the spinel crystalline with disappear Al_2O_3 phase. With an increasing temperature above 900º C, the intensities of peaks increase gradually until sharpen peaks are observed at 1100 C and 1200ºC [124-125].

The average crystallite sizes are calculated from the X-ray diffraction peaks by using scherrer equation [120-121]

$D=0.9\lambda/\beta\cos\theta)$, where

λ is wavelength,

θ is the diffraction angle

and β is the corrected halfwidth.

The crystalline spinel phase content and also the particles size increase with increasing calcination temperatures that shown in Figure (70). The particles sizes of different systems of Ni^{2+} using urea calculated from XRD data are shown in Table (19). The density of 0.10, 0.50 and 0.80 mole of Ni^{2+} systems calculated from x-ray are compared with experimental that obtained present in Table (21).

3.4.2.2. X-ray diffraction of $Ni_xMg_{1-x}Al_2O_4$ system using 3-methyl pyrozole-5-one as fuel.

The X-ray diffraction of calcinated powders at different firing temperatures using 3-methyl pyrozole-5-one (3MP5O) as fuel is shown in Figures (71). Up to 800º C, the powders remained X-ray amorphous or

contained only small crystallites that indicated by the broadening lines of XRD peaks that agree well with data of thermal analysis for the formation of the stable phase. At 900ºC the calcinated powders begin to exhibit the spinel crystalline with small Al_2O_3 peaks. By increasing the temperature above 900 ºC, the intensities of the peaks increase gradually until sharpen peaks are observed [124-125] at 1100º C and 1200º C and disappearance of Al_2O_3 phase. The average crystallite sizes are calculated from the data of X-ray diffraction peaks by using scherrer equation. The crystalline spinel phase content [8] and also the particles size increase with increasing calcination temperature that shown in Figure (72). The particles sizes of different systems of Ni^{2+} using of 3-methyl pyrozole-5-one (3MP5O) as fuel calculated from XRD that shown in Table (20). The density of 0.10, 0.50 and 0.80 mole of Ni^{2+} systems calculated from x-ray data are compared with that obtained experimentally and present in Table (22).

The particle sizes for Ni^{2+} systems using 3-methyl pyrozole-5-one (3MP5O) is smaller compared with urea as fuel as shown in Figure (73). This means that the number of carbon atoms in each fuel effect on the particle sizes as result of the different the amount of energy from each fuel.

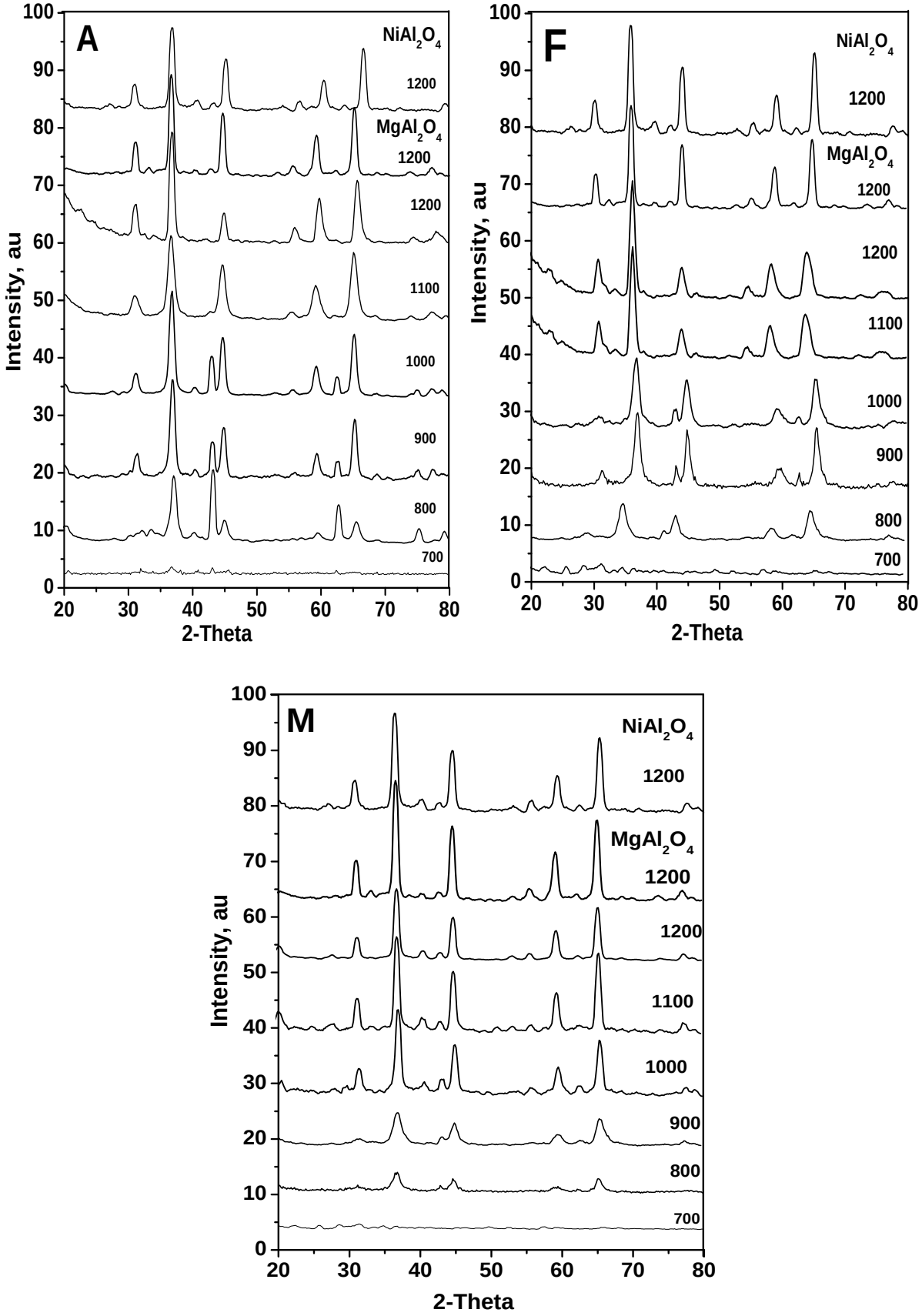

Figure (69): X-ray diffraction for 0.10 (A), 0.50 (F) and 0.80 (M) mole of Ni^{2+} systems at different calcination temperatures using urea as fuel.

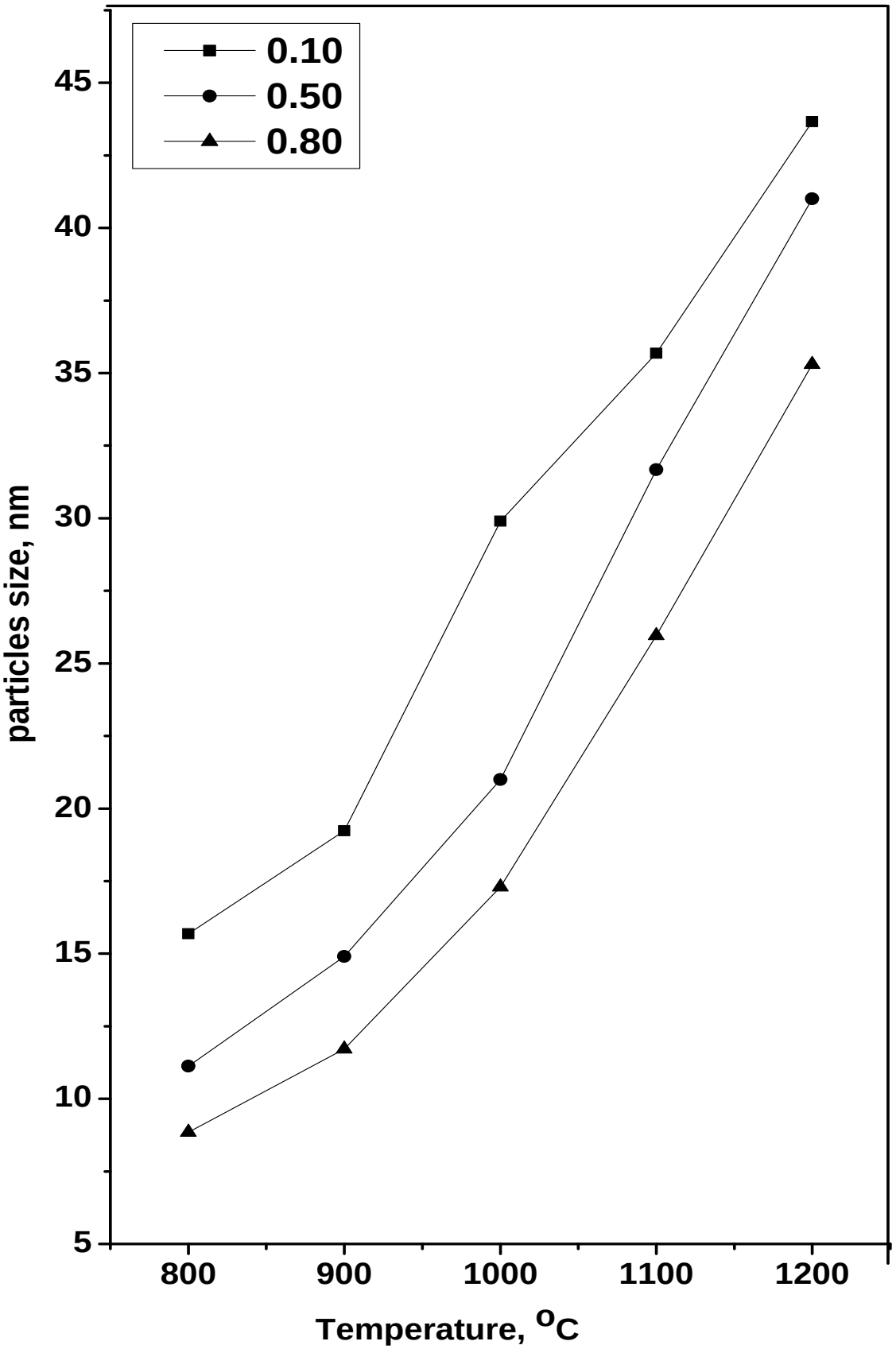

Figure (70): The relation between particle size from X-ray diffraction for A=0.10, F=0.50 and M=0.80 mole of Ni^{2+} systems at different calcination temperatures using urea as fuel.

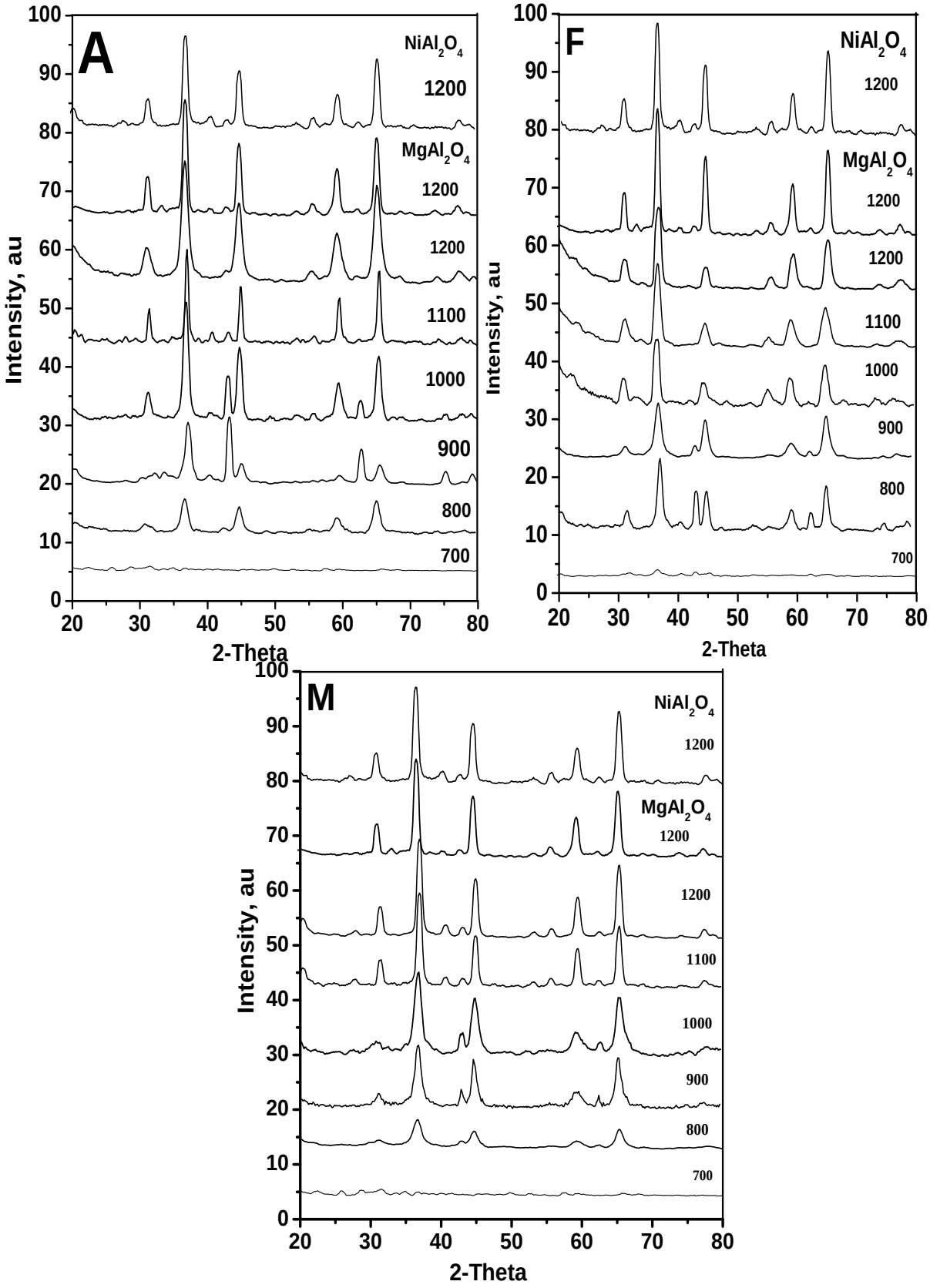

Figure (71): X-ray diffraction for 0.10(A) , 0.50 (F) and 0.80 (M) mole of Ni^{2+} systems at different calcination temperatures using 3-methyl pyrozole-5-one as fuel.

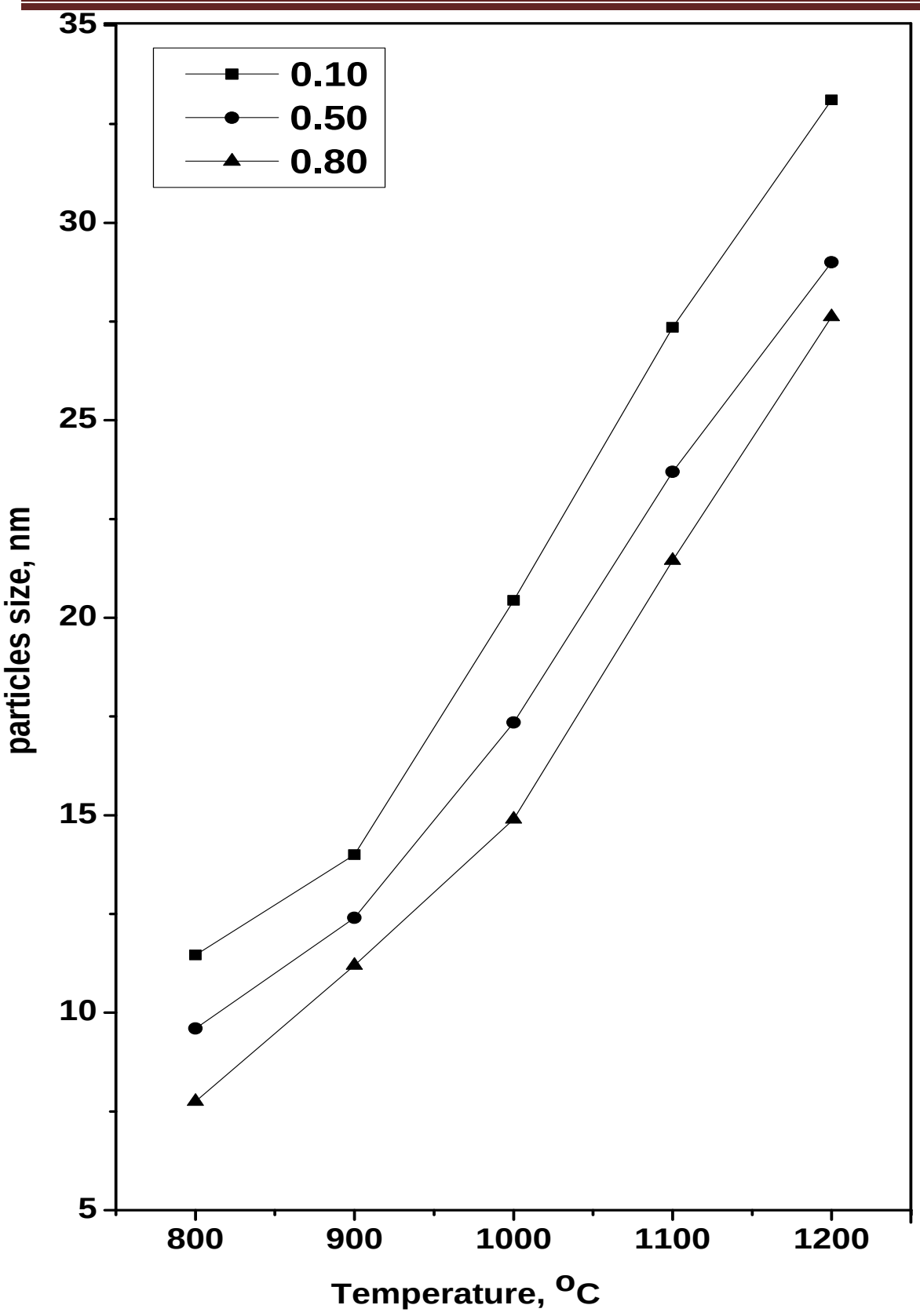

Figure (72): The relation between particle size from X-ray diffraction for A=0.10, F=0.50 and M=0.80 mole of Ni^{2+} systems at different calcination temperatures using 3-methyl pyrozole-5-one as fuel.

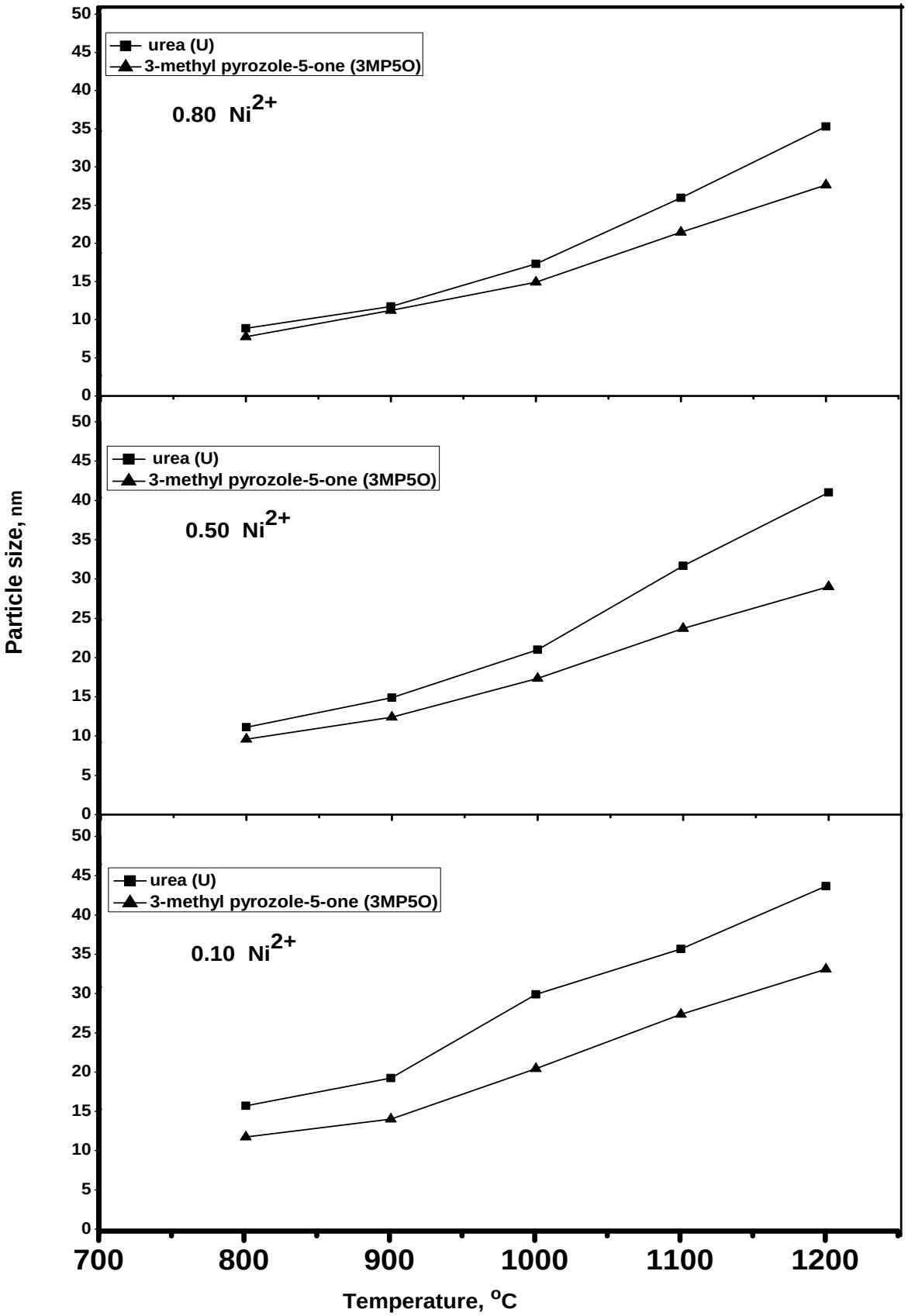

Figure (73): The relation between particle size from X-ray diffraction for A=0.10, F=0.50 and M=0.80 mole of Ni^{2+} systems at different calcination temperatures using different fuels.

Table(١٩):Particles size (nm) from X-ray diffraction for different Ni^{2+} systems at different Calcination temperatures using different fuels.

fuel	Calcination temperatures, ^{o}C						
	System	٧٠٠	٨٠٠	٩٠٠	١٠٠٠	١١٠٠	١٢٠٠
Urea	٠,١٠	Am	١٥,٦٩	١٩,٢٣	٢٩,٩	٣٥,٦٨	٤٣,٦٦
	٠,٥٠	Am	١١,١٢	١٤,٩٠	٢١,٠٠	٣١,٦٧	٤١,٠٠
	٠,٨٠	Am	٨,٨٥	١١,٧٢	١٧,٣٠	٢٥,٩٦	٣٥,٣٠
3MP5O	٠,١٠	Am	١١,٤٦	١٤,٠٠	٢٠,٤٤	٢٧,٣٥	٣٣,١١
	٠,٥٠	Am	٩,٦٠	١٢,٤٠	١٧,٣٥	٢٣,٦٩	٢٩,٠٠
	٠,٨٠	Am	٧,٧٥	١١,٢٠	١٤,٩٠	٢١,٤٥	٢٧,٦٢

3MP5O=3-methyl pyrozole-5-one, Am=Amorphous

Table(٢٠): XRD crystallite and TEM particle sizes for different nickel systems at 1100^{o}C using different fuels.

3MP5O=3-methyl pyrozole-5-one

Fuel	System	Particle size, nm	
		X-ray	TEM
Urea	٠,١٠	٣٥,٦٨	٣٦
	٠,٥٠	٣١,٦٧	٣٣
	٠,٨٠	٢٥,٩٦	٢٧
3MP5O	٠,١٠	٢٧,٣٥	٢٩,٥
	٠,٥٠	٢٣,٦٩	٢٤
	٠,٨٠	٢١,٤٥	٢٢

Table(21) Lattice parameters and densities of different Ni^{2+} doping using urea as fuel.

system	Lattice parameters	Calcinations temperature, ^oC				
		٨٠٠	٩٠٠	١٠٠٠	١١٠٠	١٢٠٠
٠,١٠	a	٨,٠٨٦	٨,٠٨٥	٨,٠٨٨٧	٨,٠٩٤٨	٨,١٣٩٣
	a^3	٥٢٧,٦٣	٥٢٨,٤٩	٥٢٩,٢٢	٥٣٠,٤٢	٥٣٩,٢١
	d_{theo}g\ml	٣,٦٦٢	٣,٦٥٦	٣,٦٥١	٣,٦٤٣	٣,٥٨٤
	d_{exp}g\ml	٣,٦٥٥	٣,٦٥٠	٣,٦٤٥	٣,٦٣٠	٣,٥٩٠
٠,٥٠	a	٨,٠٨٠٦	٨,٠٨٨٧	٨,٠٩٤٨	٨,١٠٦٦	٨,١٢٣١
	a^3	٥٢٧,٦٣	٥٢٩,٢٢	٥٣٠,٤٢	٥٣٢,٧٥	٥٣٦
	d_{theo} g\ml	٤,٠٢٠	٤,٠٠٤	٣,٩٩٩	٣,٩٨٣	٣,٩٥٧
	d_{exp}g\ml	٤,٠٠٠	٣,٩٥٠	٣,٩٠٠	٣,٨٨٠	٣,٨٥٠
٠,٨٠	a	٨,٠٧٥	٨,٠٨٠٦	٨,٠٨٥	٨,٠٩٤٨	٨,١٠٦٦
	a^3	٥٢٦,٥٤	٥٢٧,٦٣	٥٢٨,٤٩	٥٣٠,٤٢	٥٣٢,٧٥
	g\ml d_{theo}	٤,٢٨٤	٤,٢٧٦	٤,٢٦٩	٤,٢٥٣	٤,٢٣٦
	d_{exp} g\ml	٤,٢٦٥	٤,٢٥٥	٤,١٥٥	٤,١٠٠	٤,٠٠٠

a= Lattice parameters, d_{theo}= theoretical density and d_{exp}=experimental density

Table(22) Lattice parameters and densities of different Ni^{2+} doping using 3MP5O as fuel

system	Lattice parameters	Calcinations temperature, ^oC				
		٨٠٠	٩٠٠	١٠٠٠	١١٠٠	١٢٠٠
٠,١٠	a	٨,٠٨٠٦	٨,٠٨٥	٨,٠٨٨٧	٨,٠٩٤٨	٨,١٠٦٦
	a^3	٥٢٧,٦٣	٥٢٨,٤٩	٥٢٩,٢٢	٥٣٠,٤٢	٥٣٢,٧٥
	d_{theo}g\ml	٣,٦٦٢	٣,٦٥٦	٣,٦٥١	٣,٦٤٣	٣,٦٢٨
	d_{exp}g\ml	٣,٦٥٣	٣,٦٥٠	٣,٦٤٥	٣,٦٣٧	٣,٦٢٠
٠,٥٠	a	٨,٠٧٠	٨,٠٧٥	٨,٠٨٥	٨,٠٨٨٧	٨,٠٩٤٨
	a^3	٥٢٥,٥٦	٥٢٦,٥٤	٥٢٨,٤٩	٥٢٩,٢٢	٥٣٠,٤٢
	d_{theo} g\ml	٤,٠٢٩	٤,٠٢٢	٤,٠٠٦	٤,٠٠١	٣,٩٩٢
	d_{exp}g\ml	٤,٠٠٠	٣,٩٨٠	٣,٩٥٤	٣,٩٣٥	٣,٩٢٠
٠,٨٠	a	٨,٠٧٠	٨,٠٧٥	٨,٠٨٠٦	٨,٠٨٥	٨,٠٨٨٧
	a^3	٥٢٥,٥٦	٥٢٦,٥٤	٥٢٧,٦٣	٥٢٨,٤٩	٥٢٩,٢٢
	g\ml d_{theo}	٤,٢٩٢	٤,٢٨٤	٤,٢٧٦	٤,٢٦٩	٤,٢٦٢
	d_{exp} g\ml	٤,٢٦٦	٤,٢٥٣	٤,٢٤٥	٤,٢٣٣	٤,٢١٥

a= Lattice parameters, d_{theo}= theoretical density and d_{exp}=experimental density

3.4.3. Microstructure characterizations for $Ni_yMg_{1-y}Al_2O_4$ systems.

3.4.3.1. Microstructure characterizations for $Ni_yMg_{1-y}Al_2O_4$ system using urea as fuel.

Transmission electron microscopy (TEM) photographs of powder samples show the spherical particles for 0.10, 0.50 and 0.80 mole of Ni^{2+} systems as shown in Figure (74). The particles sizes observed by XRD are in the range that observed by TEM as present in Table (20). The morphology and particle size decrease with increasing the amount of doping Ni^{2+} ion. The particle sizes are calculated using ultrastructure size calculator or quantitative electron microscopy using an areal analysis. Measurements of at least 20 particles were required to characterize each size distribution from TEM photographs.

3.4.3.2. Microstructure characterizations for $Ni_yMg_{1-y}Al_2O_4$ using 3-methyl pyrozole-5-one as fuel.

Transmission electron microscopy (TEM) photographs of powder samples show the spherical particles for 0.10, 0.50 and 0.80 mole of Ni^{2+} systems as shown in Figure (75). The particles sizes observed by XRD are in the range that observed by TEM as present in Table (20). The morphology and particle size decrease with increasing the amount of Ni^{2+} in ceramic pigment.

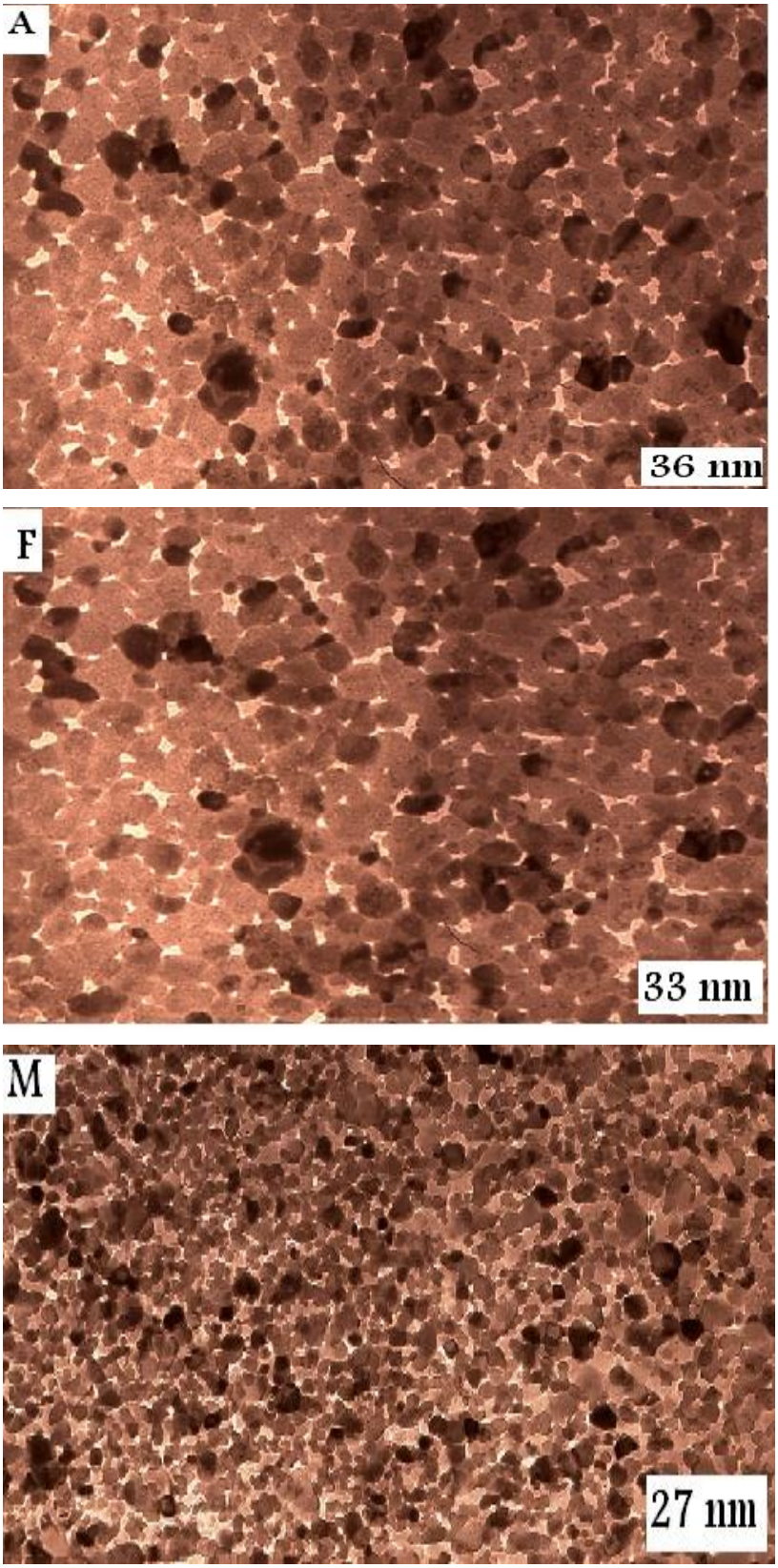

Figure (٧٤): TEM of A=0.10, F=0.50 and M=0.80 of Ni^{2+} systems at 1100°C temperature by using urea as fuel.

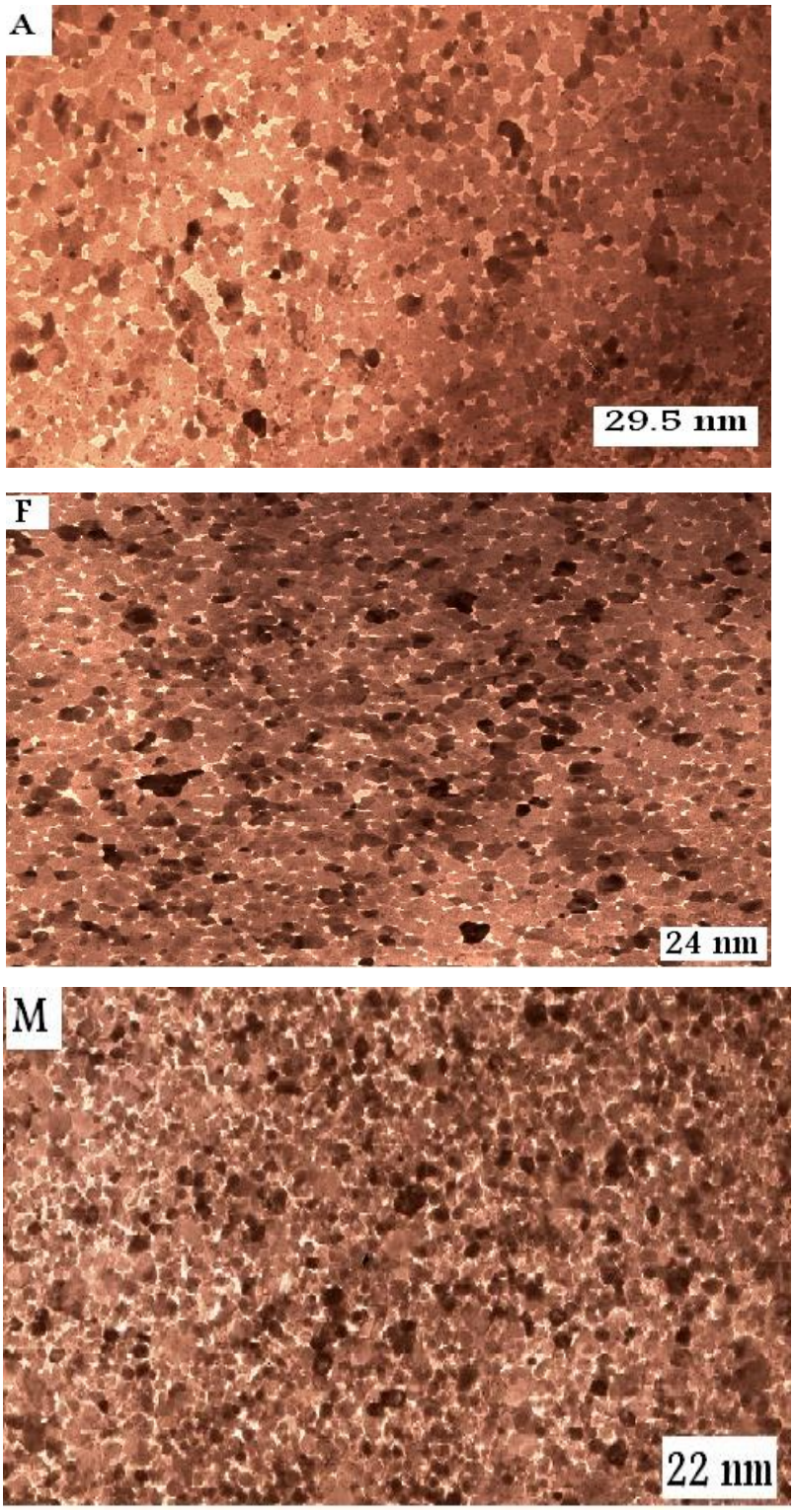

Figure (٧٥): TEM of A=0.10, F=0.50 and M=0.80 of Ni^{2+} systems at 1100°C temperature by using 3-methyl pyrozole-5-one as fuel.

CHAPTER (IV)

Application of nano ceramic pigment

4. Glaze:

Glaze is thin, hard, shiny and finally transparent layer in ceramic field. Glaze has different composition depending on the using field. Glazes are thin layers of glass fused on to the surface of the body. They are applied to bodies to make them impervious, mechanically stronger and resistant to scratching, chemically more inert and more pleasing touch and eye.

4.1. Composition of Glaze:

Glaze contains frit and chain clay. The example for glaze and its composition present in Table (23) as the following

No.	Glaze	Raw material	Formula	Percentage in glaze, %
1	Frit	1.Whiting	1.$CaCO_3$	12
		2.Borax	2.$Na_2B_4O_7.10H_2O$	19
		3.Broic acid	3.H_3PO_3	4
		4.Feldspar	4.$K_2O.Al_2O_3.6SiO_2$	57
		5.Flint	5.SiO_2	8
				100
				88
2	China clay	China clay	$Al_2O_3.2SiO_2.2H_2O$	12
				١٢

4.2. The preparation of colored glazed:

The colored glaze is prepared by mixing pigment (colored material) with glaze 10% (wt/wt). The mixture is good grinding in mill for distribution of pigment in glaze. The mixture painted over the body of ceramic and calcinated at 1100-1150 ^{o}C.

4.3. Diffuse reflectance spectra for cobalt systems using 3-methyl pyrozole-5-one (3MP5O) and N, N-bis-(3-amino-propyl) oxalamide as fuel:

Diffuse reflectance spectra for A, F and M systems of 0.01, 0.05 and 0.10 mole of Co^{2+} respectively on glaze for 15 and 30 minute using 3-methyl pyrozole-5-one (3MP5O) and N, N-bis-(3-amino-propyl) oxalamide as fuel comparing with spectra of pigment powder as present in Figures (120-123). The colorimetric data for cobalt systems are present in Table (24). The values of a* are random while L* values decrease and b* values increases in negative direction as result of increasing calcinations times. The intensity of blue color on glaze is more than pigment powder as shown in Figure (124).

4.4. Diffuse reflectance spectra for nickel systems using urea and 3-methyl pyrozole-5-one (3MP5O) as fuel:

Diffuse reflectance spectra for A, F and M systems of 0.10, 0.50 and 0.80 mole of Ni^{2+} respectively on glaze using urea and 3-methyl pyrozole-5-one (3MP5O) as fuel comparing with pigment powder are given in Figures (125-128). From colorimetric data present in Table (24), the values of b* are increase in positive direction while L* values decreases and a* values increases in negative direction as result of increasing calcinations time. The a* values are increasing in negative direction leading to the higher intensity of

green color. The b* values are increasing in the positive direction leading to the appearance of yellow color as shown in Figures (129). The increasing of b* in positive direction is more than the increasing values of a*in negative direction. This means that the present of two mixed color yellow and green and yellow is more than green color intensity. The decreasing in L* parameter value corresponds to reduce the lightness of sample.

4.5. The effect of time on the colored glaze:

The effect of calcinations time on colored glaze is studied at 1200 ^{o}C for 15 and 30 minutes. The intensity of blue pigment color on glaze at 30 minute is more than 15 minute for cobalt systems as shown in Figure (120-123).

The intensity of cyan pigment color on glaze at 30 and 15 minutes for nickel systems is changed to green-yellow direction as shown in Figure (125-128). This means that the type of glaze is effect on the stability of the pigment color.

4.6. The effect of mineral acids and base:

Concentrated and diluted mineral acids such as sulphuric, hydrochloric, nitric acids are not effect on the pigment powder and colored glaze. But, hydrogen fluoride acid is effect on pigment after 14 days. Pigment is not effect by sodium and ammonium hydroxide.

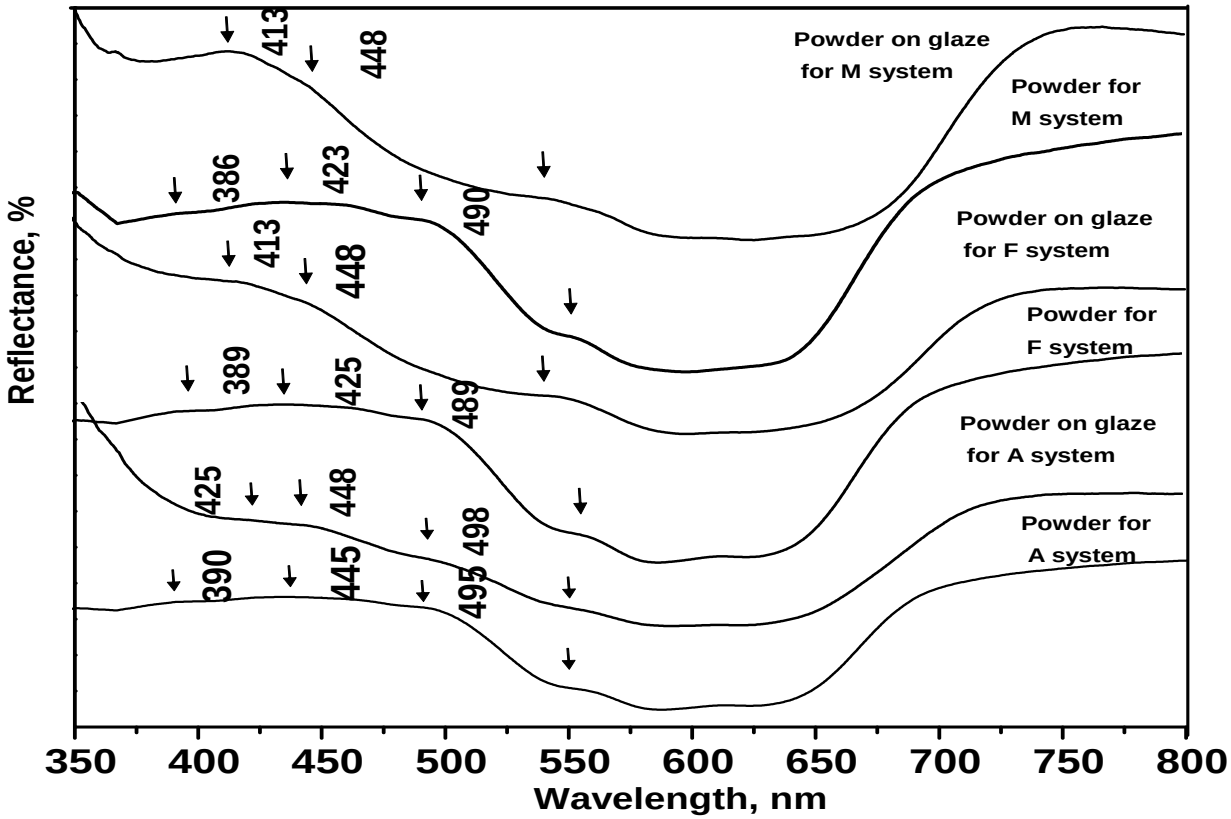

Figure (76): Diffuse reflectance spectra for 0.01 (A), 0.05 (F) and 0.10 (M) mole of Co^{2+} systems at 1100°C by using 3-methyl pyrozole-5-one as fuel for 15 minute.

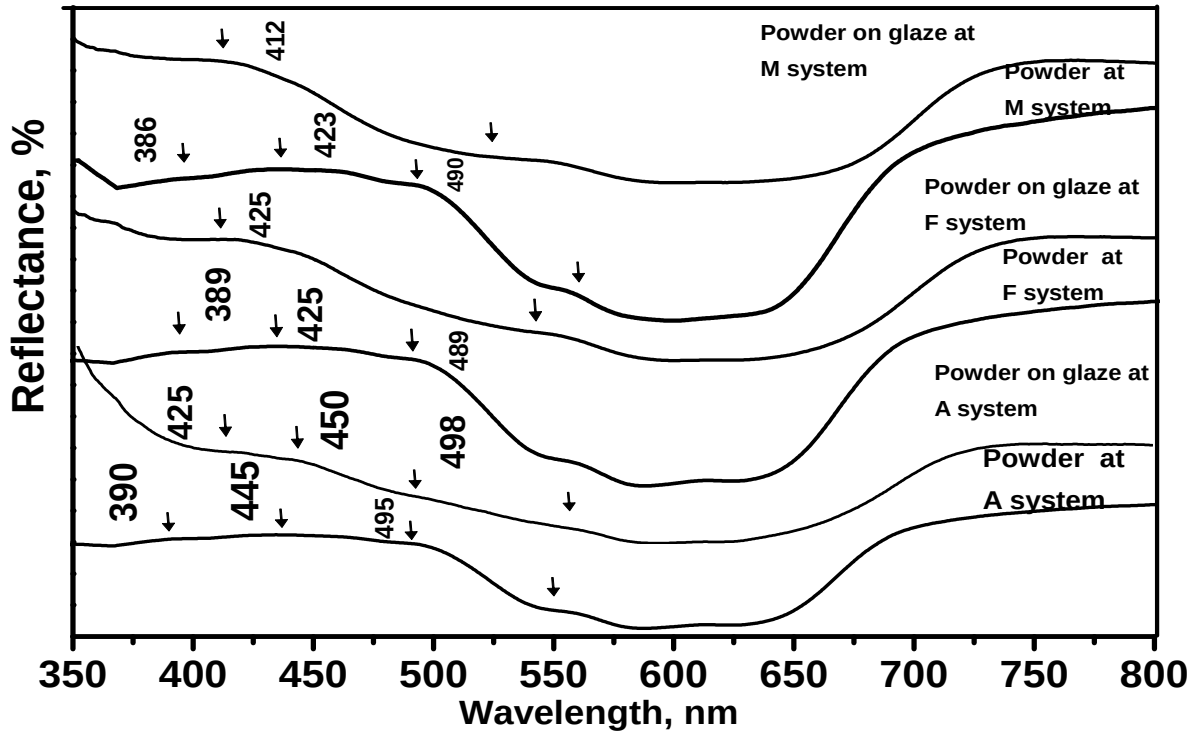

Figure (77): Diffuse reflectance spectra for 0.01 (A), 0.05 (F) and 0.10 (M) mole of Co^{2+} systems at 1100°C by using 3-methyl pyrozole-5-one as fuel for 30 minute.

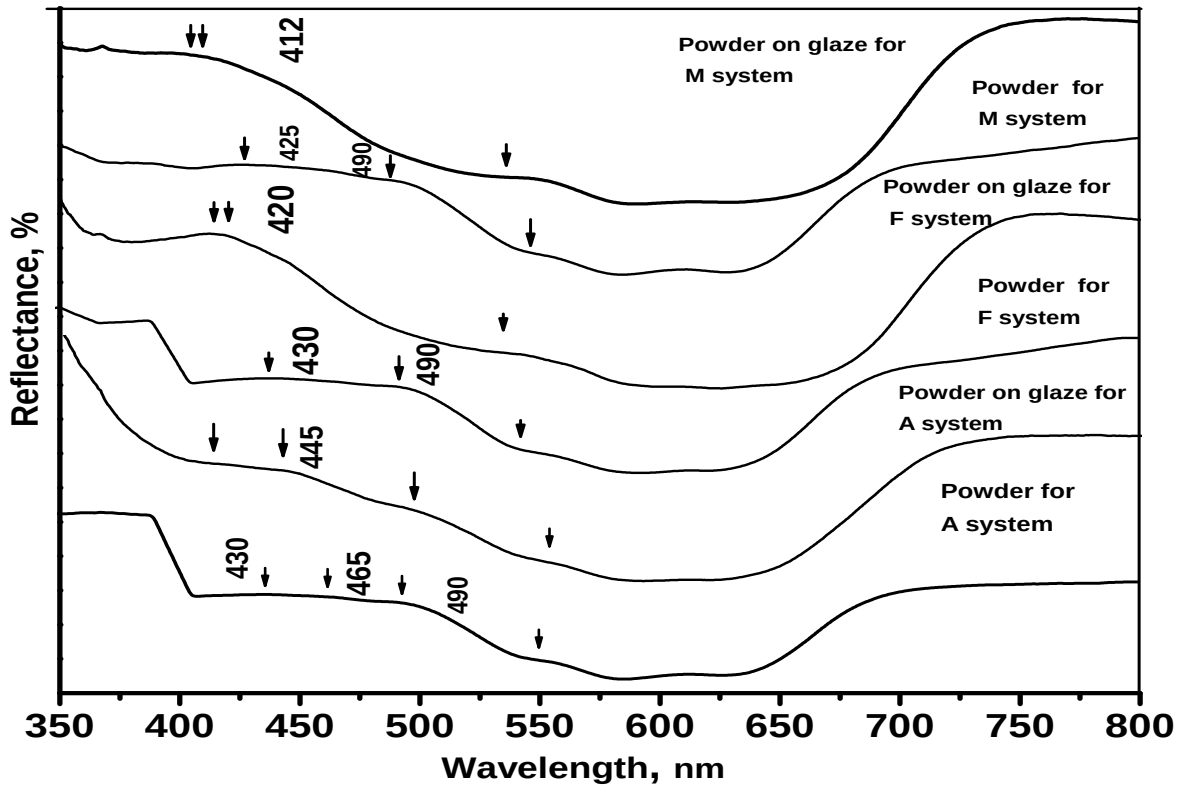

Figure (78): Diffuse reflectance spectra for 0.01 (A), 0.05 (F) and 0.10 (M) mole of Co^{2+} systems at 1100°C by using N, N-bis-(3-amino-propyl) oxalamide as fuel for 15 minute.

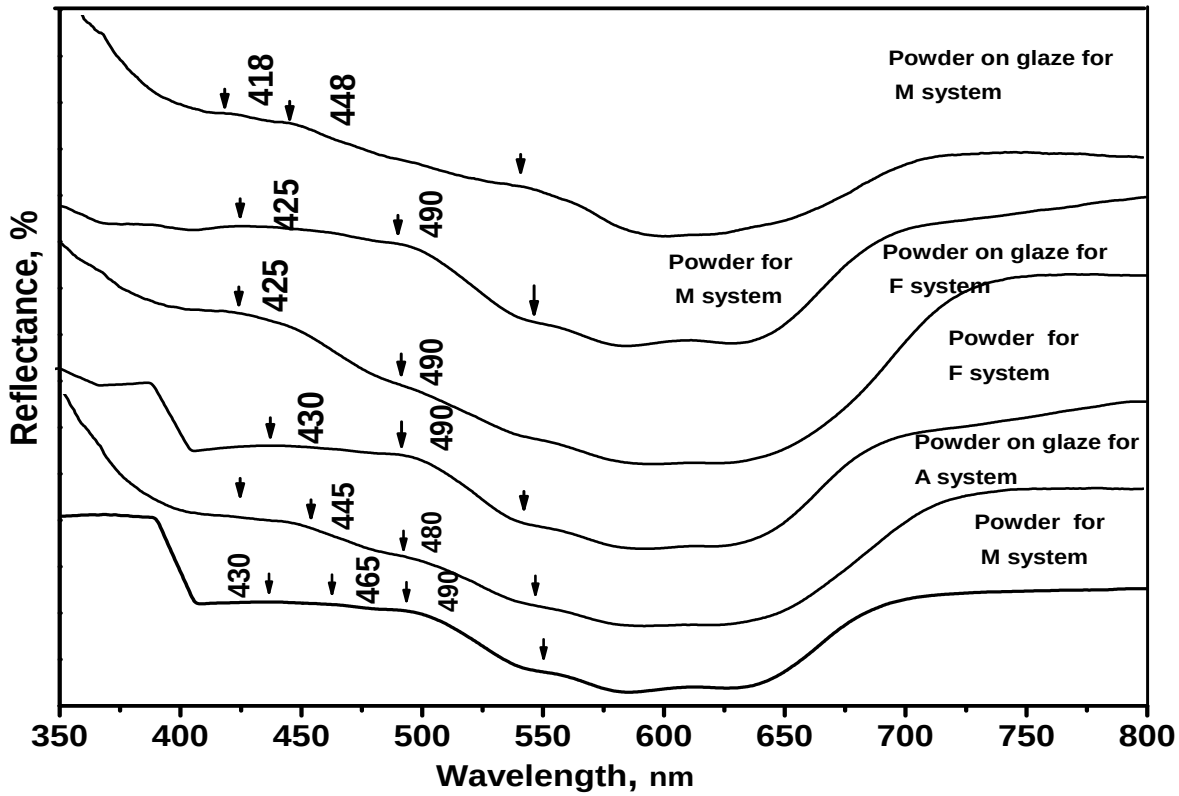

Figure (79): Diffuse reflectance spectra for 0.01 (A), 0.05 (F) and 0.10 (M) mole of Co^{2+} systems at 1100°C by using N, N-bis-(3-amino-propyl) oxalamide as fuel for 30 minute.

Table (24): Colorimetric data for 0.01, 0.05 and 0.10 mole of Co^{2+} systems for powder pigment and pigment on glaze at different time using 3-methyl pyrozole-5-one and N, N-bis-(3-amino-propyl) oxalamide as fuel at 1100 °C.

Fuel	Materials	system											
		٠,٠١ mole of Co^{2+}				٠,٠5 mole of Co^{2+}				٠,10 mole of Co^{2+}			
	parameter	L*	a*	b*	ΔE	L*	a*	b*	ΔE	L*	a*	b*	ΔE
3MP5O	Pigment powder	95.02	-2.35	-6.17	95.18	92.66	-10.72	-2.56	92.00	93.26	-4.01	-16.84	87.44
	Pigment on glaze after 15 min.	74.55	-2.27	-12.91	75.70	67.95	0.43	-18.08	70.32	66.29	3.02	-22.29	70.00
	Pigment on glaze after 30 min.	65.97	- 0.14	-13.90	67.42	63.68	2.75	-22.71	67.66	61.04	-1.27	-24.49	65.78
3APOA	Pigment powder	٩١,٣٣	-٢,٧٠	-١١,٠١	٩٢,٠٣	٨٤,٤٨	-٣,٤٨	-١٥,٥١	٨٥,٩٦	٨٥,٥٥	-١٠,٠٠	-١٧,٠٠	٨٧,٨٠
	Pigment on glaze after 15 min.	75.16	-0.15	-11.49	76.03	71.03	-2.40	-24.54	75.15	63.18	6.32	-29.06	69.83
	Pigment on glaze after 30 min.	70.73	-1.23	-15.50	72.42	69.06	0.70	-26.58	74.00	57.77	4.75	-31.44	65.94

Fuel	Materials	system		
		٠,٠١ mole of Co^{2+}	٠,٠5 mole of Co^{2+}	٠,10 mole of Co^{2+}
3MP5O	Pigment powder	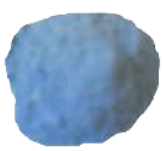		
	Pigment on glaze after 15 min.			
	Pigment on glaze after 30 min.			
3APOA	Pigment powder	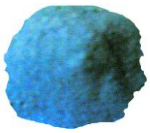		
	Pigment on glaze after 15 min.	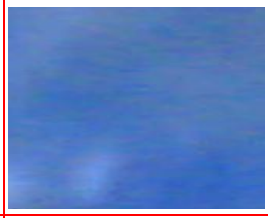		
	Pigment on glaze after 30 min.			

3MP5O=3-methyl pyrozole-5-one, 3APOA= N, N-bis-(3-amino-propyl) oxalamide

Figure(80): The color of ceramic powder for 0.01, 0.05 and 0.10 mole of Co^{2+} systems for powder pigment and pigment on glaze at different time using 3-methyl pyrozole-5-one and N, N-bis-(3-amino-propyl) oxalamide as fuel at 1100 ^{o}C.

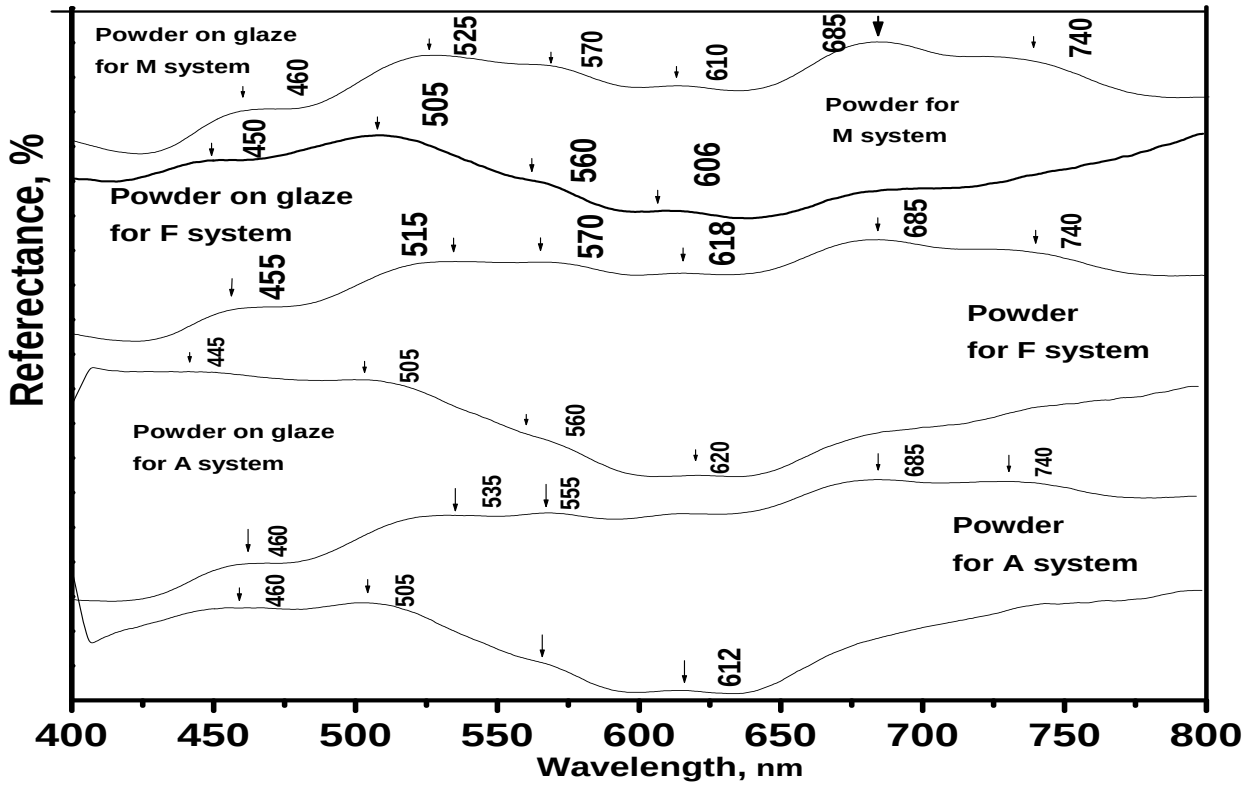

Figure (81): Diffuse reflectance spectra for 0.10 (A), 0.50 (F) and 0.80 (M) mole of Ni^{2+} systems at 1100°C by using urea as fuel for 15 minute.

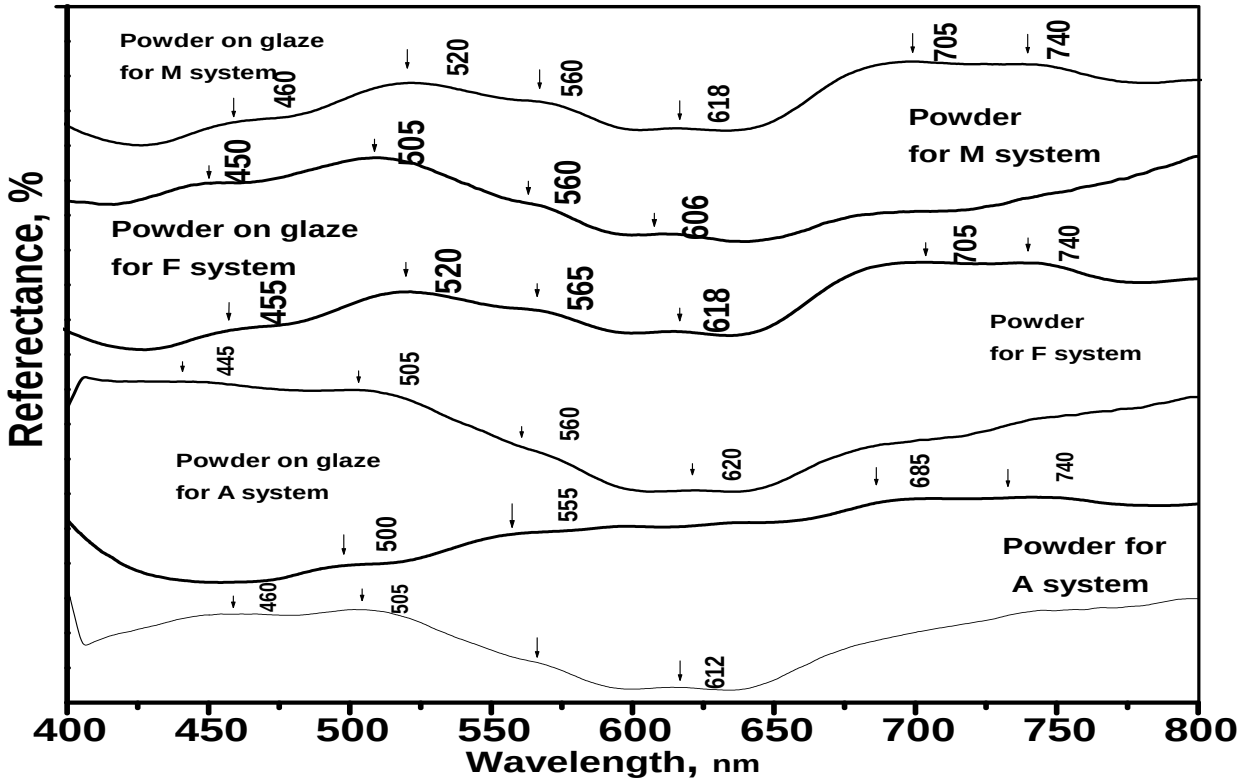

Figure (82): Diffuse reflectance spectra for 0.10 (A), 0.50 (F) and 0.80 (M) mole of Ni^{2+} systems at 1100°C by using urea as a fuel for 30 minute.

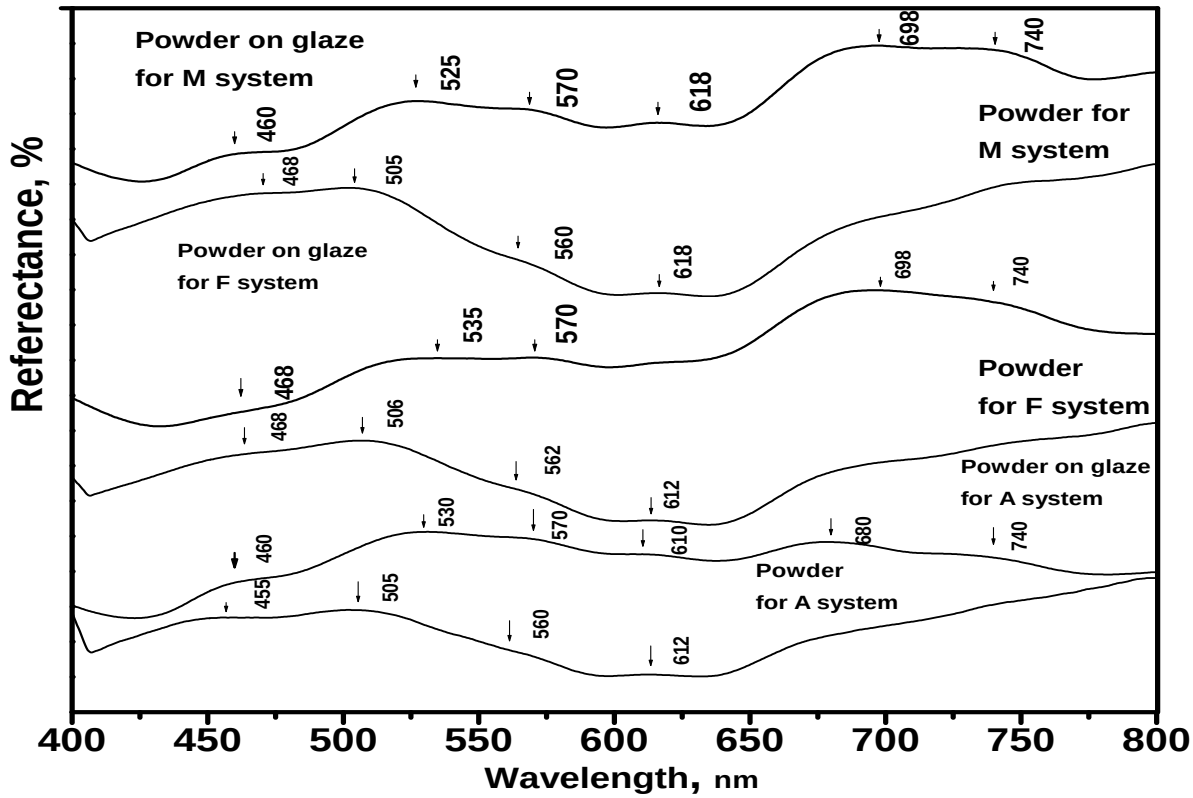

Figure (83): Diffuse reflectance spectra for 0.10 (A), 0.50 (F) and 0.80 (M) mole of Ni^{2+} systems at 1100°C by using 3-methyl pyrozole-5-one as fuel for 15 minute.

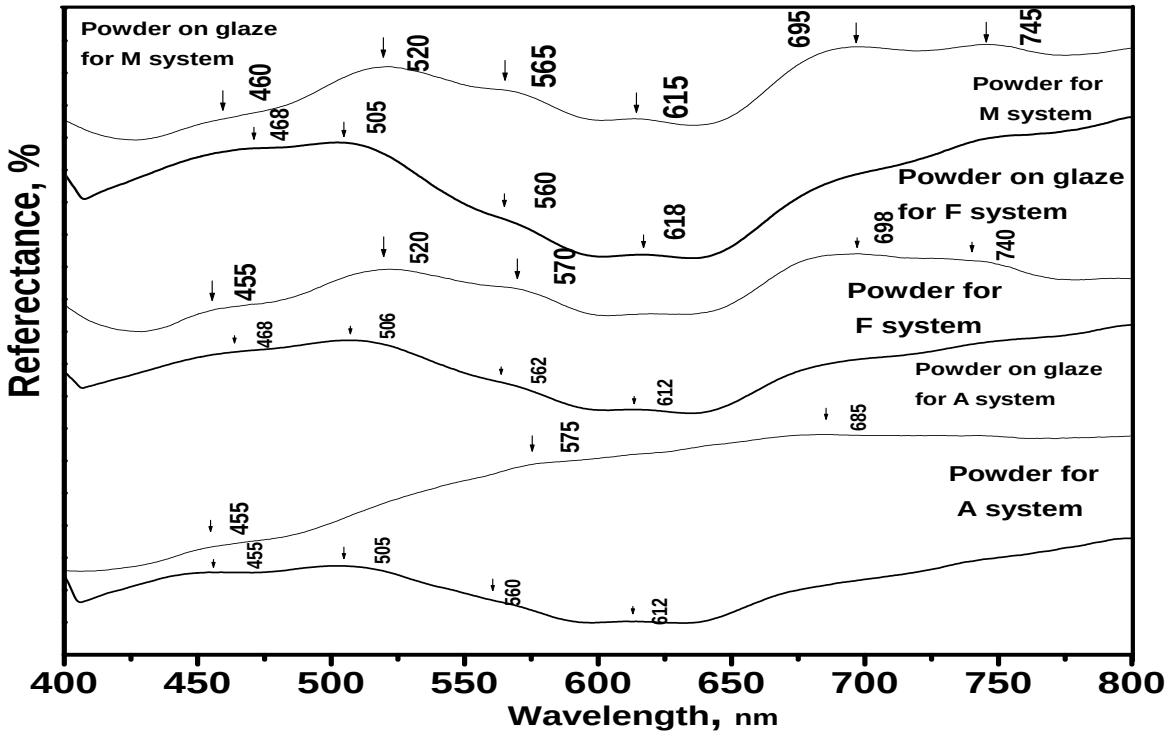

Figure (84): Diffuse reflectance spectra for 0.10 (A), 0.50 (F) and 0.80 (M) mole of Ni^{2+} systems at 1100°C by using 3-methyl pyrozole-5-one as fuel for 30 minute.

Table (25):Colorimetric data for 0.10, 0.50 and 0.80 mole of Ni^{2+} systems for powder pigment and pigment on glaze at different time using urea and 3-methyl pyrozole-5-one as fuel at 1100 ^{o}C.

Fuel	Materials	system											
		٠,١٠ mole of Ni^{2+}				٠,50 mole of Ni^{2+}				٠,80 mole of Ni^{2+}			
	parameter	L*	a*	b*	ΔE	L*	a*	b*	ΔE	L*	a*	b*	ΔE
urea	Pigment powder	٩٥,١١	-٥,٧١	-٢,٧٧	٩٥,٣٢	٩٢,٤٨	-٨,٨٨	-٥,١٤	٩٣,١٠	٩٣,٥٤	-١٠,٦٥	-٧,٨٣	٩٤,٤٧
	Pigment on glaze after 15 min.	96.08	-9.58	17.23	98.08	88.90	-10.87	20.10	91.79	82.17	-9.13	15.47	84.11
	Pigment on glaze after 30 min.	90.06	-2.47	14.96	91.33	84.83	-5.60	6.74	85.28	78.26	-6.17	10.29	79.17
3MP5O	Pigment powder	٩١,٥٦	-٢,٤٧	-١,٨٥	٩١,٦١	٨٥,٩٢	-٧,٥٨	-٣,٠٠	٨٦,٣١	٨٨,٦٠	-٩,٩٦	-٥,٧٧	٨٩,٣٥
	Pigment on glaze after 15 min.	85.49	-4.74	13.55	86.69	76.70	-6.53	11.77	77.87	69.08	-9.22	6.95	70.04
	Pigment on glaze after 30 min.	86.92	-3.41	14.25	88.15	72.48	-6.98	5.00	72.99	63.22	-9.75	11.11	64.94

Fuel	Materials	system		
		٠,١٠ mole of Ni^{2+}	٠,50 mole of Ni^{2+}	٠,80 mole of Ni^{2+}
urea	Pigment powder			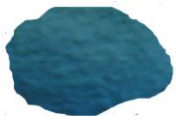
	Pigment on glaze after ١٥ min.			
	Pigment on glaze after 30 min.			
3MP5O	Pigment powder		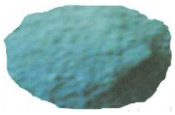	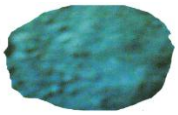
	Pigment on glaze after15 min.			
	Pigment on glaze after 30 min.			

Figure(85): The color of ceramic powder for 0.10, 0.50 and 0.80 mole of Ni^{2+} systems for powder pigment and pigment on glaze at different time using urea and 3-methyl pyrozole-5-one as fuel at 1100 ^{o}C.